

**Characterisation of the Role of LysM Receptor-Like
Kinases and the CHIA Chitinase in the Perception of
Peptidoglycan and in the Innate Immunity of
*Arabidopsis thaliana***

Dissertation

der Mathematisch-Naturwissenschaftlichen Fakultät

der Eberhard Karls Universität Tübingen

zur Erlangung des Grades eines

Doktors der Naturwissenschaften

(Dr. rer. nat.)

vorgelegt von

Heini Marjatta Grabherr

geb. Lajunen

aus Helsinki

Tübingen

2011

Tag der mündlichen Qualifikation:

26.10.2011

Dekan:

Prof. Dr. Wolfgang Rosenstiel

1. Berichterstatter:

Prof. Dr. Thorsten Nürnberger

2. Berichterstatter:

Prof. Dr. Georg Felix

Table of contents

1	Introduction.....	1
1.1	Host-pathogen interaction	1
1.2	Plant innate immunity	1
1.2.1	PAMP-triggered immunity	1
1.2.2	Effector-triggered immunity	4
1.2.3	Chitinases in plant pathogen defense	5
1.3	Peptidoglycan - A bacterial cell wall constituent	6
1.4	PGN processing and perception in animals.....	9
1.5	Lysin motif (LysM) as mediator in carbohydrate signaling in plants.....	14
1.6	Aims of the thesis	15
2	Materials and methods.....	16
2.1	Materials.....	16
2.1.1	Chemicals	16
2.1.2	Media	16
2.1.3	Vectors.....	18
2.1.4	Primers	18
2.2	Organisms	19
2.2.1	Bacteria and fungi.....	19
2.2.2	<i>Arabidopsis thaliana</i> lines	19
2.3	Cultivation conditions of the organisms	20
2.3.1	Growth of <i>Escherichia coli</i>	20
2.3.2	Growth of <i>Pseudomonas syringae</i>	21
2.3.3	Growth of <i>Agrobacterium tumefaciens</i>	21
2.3.4	Growth of <i>Pichia pastoris</i>	21
2.3.5	Growth of <i>Alternaria brassicicola</i> and <i>Botrytis cinerea</i>	21
2.3.6	Growth of <i>Arabidopsis thaliana</i> and <i>Nicotiana benthamiana</i>	21
2.4	Methods.....	22
2.4.1	Isolation of peptidoglycan from Gram-negative bacteria	22
2.4.2	Isolation of peptidoglycan from Gram-positive bacteria	23
2.4.3	General molecular biology methods.....	23
2.4.4	Cloning.....	23
2.4.5	DNA isolation	24
2.4.6	RNA isolation	24
2.4.7	Semi-quantitative RT-PCR.....	24
2.4.8	Quantitative Real-time PCR.....	24
2.4.9	Isolation of mesophyll protoplasts from Arabidopsis	25
2.4.10	Stable transformation of <i>Arabidopsis thaliana</i>	25
2.4.11	Transient transformation of <i>Nicotiana benthamiana</i>	25
2.4.12	Crossing <i>Arabidopsis thaliana</i> plants	26
2.4.13	Generation of knock-down lines.....	26

2.4.14	Generation of overexpression lines.....	27
2.4.15	Generation of <i>pCHIA::GUS</i> lines.....	27
2.4.16	Generation of constructs for expression in <i>E.coli</i>	28
2.4.17	Generation of constructs for expression in <i>P.pastoris</i>	28
2.4.18	Generation of constructs for the yeast two-hybrid system	28
2.4.19	Genotyping analysis of T-DNA insertion lines	28
2.5	Biochemical methods	29
2.5.1	Protein expression in <i>E.coli</i>	29
2.5.2	Ni ²⁺ -NTA affinity purification.....	30
2.5.3	Protein expression in <i>P.pastoris</i>	30
2.5.4	Protein extraction from plant tissue.....	30
2.5.5	Immunoprecipitation.....	31
2.5.6	Determination of protein concentration	31
2.5.7	SDS-PAGE	31
2.5.8	Western blot analysis.....	31
2.5.9	Coomassie blue stain.....	32
2.5.10	Silver stain	32
2.5.11	Turbidity assay (PGN-hydrolysis assay)	33
2.5.12	4-MUCT assay (Chitin-hydrolysis assay).....	33
2.5.13	Colloidal chitin hydrolysis assay.....	33
2.5.14	Yeast two-hybrid	34
2.6	Bioassays	34
2.6.1	Infection with <i>Pseudomonas syringae</i>	34
2.6.2	Infection with <i>Alternaria brassicicola</i>	34
2.6.3	Infection with <i>Botrytis cinerea</i>	35
2.6.4	Elicitation assays in leaves or seedlings	35
2.6.5	Microarray analysis	35
2.6.6	pH assay.....	36
2.7	Microscopy and Histochemistry.....	36
2.7.1	Confocal microscopy.....	36
2.7.2	Aniline blue stain.....	36
2.7.3	Trypan blue stain	36
2.7.4	GUS stain.....	37
2.8	Statistical analysis	37
3	Results.....	38
3.1	Isolation and analysis of PGN from <i>P.syringae</i> and other bacteria.....	38
3.2	Identification of putative PGN receptor(s) among the LysM-RLKs.....	41
3.2.1	Analysis of the <i>LYK</i> T-DNA insertion lines	43
3.2.1.1	Phenotypic analysis of <i>lyk3</i> and <i>lyk5</i> single and double mutants ...	45
3.2.2	Role of LYKs in fungal resistance	47
3.2.3	Influence of LYKs on bacterial resistance	49
3.2.4	Analysis of peptidoglycan responsiveness in <i>lyk</i> mutants.....	51
3.2.4.1	The LysM-receptor kinase CERK1 mediates sensitivity to PGN	52

3.2.5	Analysis of potential redundancy among <i>LYK</i> genes	55
3.3	The role of PGN hydrolysis in the PGN sensing process	56
3.4	Identification of a putative PGN hydrolase in <i>Arabidopsis thaliana</i>	57
3.4.1	Analysis of the class III chitinase CHIA	58
3.4.2	Expression pattern of the <i>CHIA</i> gene upon biotic stress	60
3.4.3	Analysis of the transgenic <i>CHIA</i> lines	64
3.4.3.1	Phenotypic analysis of the <i>CHIA</i> overexpression and knock-down lines	66
3.4.4	Subcellular localisation of CHIA	67
3.4.5	Detection of CHIA protein in the transgenic <i>CHIA</i> lines	71
3.4.6	Posttranslational modification of the CHIA protein	72
3.4.7	Expression of CHIA protein using heterologous expression systems ...	73
3.4.8	Analysis of homo-oligomerisation properties of CHIA	76
3.4.9	Assessment of the chitin- and PGN-hydrolase activity of CHIA	77
3.4.10	Role of <i>CHIA</i> in fungal resistance	82
3.4.10.1	Infection of the transgenic <i>CHIA</i> lines with <i>Botrytis cinerea</i>	82
3.4.10.2	Infection of the transgenic <i>CHIA</i> lines with <i>Alternaria brassicicola</i> .	83
3.4.11	Impact of CHIA on bacterial resistance	86
4	Discussion	88
4.1	LYKs contribute to plant innate immunity	88
4.1.1	Effects of LYK gene deletions in plant fungal and bacterial resistance .	88
4.1.2	CERK1 serves together with LYM3 peptidoglycan recognition	90
4.2	CHIA chitinase is involved in plant innate immunity	93
4.2.1	Chitinolytic activity of CHIA and its impact on fungal immunity	94
4.2.2	PGN-lytic activity of CHIA and its importance to bacterial immunity	95
4.3	Peptidoglycan perception systems have arisen through convergent evolution in metazoans and plants	97
5	Summary	99
6	Zusammenfassung	101
7	References	103
8	Appendix	i

Abbreviations

aa	Amino acid
amiRNA	Artificial microRNA
<i>At</i>	<i>Arabidopsis thaliana</i>
Avr	Avirulence factor
bp	Base pair
cDNA	Complementary DNA
cfu	Colony forming unit
Col-0/Col-2	Columbia-0/Columbia-2, ecotypes
DAMP	Danger-associated molecular pattern
DNA	Deoxyribonucleid acid
EF-Tu	Elongation factor Tu
Elf18	Peptide from EF-Tu with the sequence SKEKFERTKPHVNVGTIG
ETI	Effector-triggered immunity
ETS	Effector-triggered susceptibility
Flg22	Peptide from flagellin with the sequence QRLSTGSRINSAKDDAAGLQIA
FLS2	Flagellin-sensitive 2
GFP	Green fluorescent protein
HEWL	Hen egg-white lysozyme
HR	Hypersensitive reaction
kb	Kilobase
kDa	KiloDalton
KO	Knock-out
Ler	Landsberg erecta, ecotype
LRR	Leucine-rich repeat
LPS	Lipopolysaccharide
LysM	Lysin motif
MAMP	Microbe-associated molecular pattern
MAPK/MPK	Mitogen-activated protein kinase
<i>Os</i>	<i>Oryza sativa</i>
PAMP	Pathogen-associated molecular pattern
PCD	Programmed cell-death
PCR	Polymerase chain reaction
PGN	Peptidoglycan
PGRP	Peptidoglycan recognition protein
PR	Pathogenesis-related
PRR	Pattern recognition receptor
PTI	PAMP-triggered immunity
<i>Pto</i>	<i>Pseudomonas syringae</i> pv. <i>tomato</i>
pv.	Pathovar
R-Gene	Resistance gene
RNA	Ribonucleic acid
R-Protein	Resistance protein
RLK	Receptor-like kinase
ROS	Reactive oxygen species
SA	Salicylic acid
SAR	Systemic acquired resistance
T-DNA	Transfer-DNA
TLR	Toll-like receptor
UTR	Untranslated region
WT	Wild type

List of Figures

Figure 1-1: Plant pattern-recognition receptors and their signaling adapters.....	3
Figure 1-2: The schematic structure of peptidoglycan	7
Figure 1-3: Gram-positive and Gram-negative cell walls	8
Figure 1-4: Peptidoglycan sensing in animals	11
Figure 1-5: Metazoan PGN hydrolytic activities	13
Figure 2-1: Working mode of amiRNA-mediated gene silencing	27
Figure 2-2: Genotyping analysis of T-DNA lines by gene- and insertion-specific primer	29
Figure 3-1: Peptidoglycan induces defense responses in <i>Arabidopsis thaliana</i>	40
Figure 3-2: <i>Arabidopsis</i> LysM receptor-like kinase family	42
Figure 3-3: Characterisation of <i>CERK1</i> , <i>LYK3</i> and <i>LYK5</i> and their mutants	44
Figure 3-4: Characterisation of <i>LYK2</i> and <i>LYK4</i> and their mutants	45
Figure 3-5: Phenotypes of <i>lyk3</i> and <i>lyk5</i> single and double mutants	46
Figure 3-6: Infection of <i>lyk</i> mutants with <i>Botrytis cinerea</i>	48
Figure 3-7: Infection of <i>lyk</i> mutants with <i>Pseudomonas syringae</i> strains.....	50
Figure 3-8: Analysis of PGN responsiveness in <i>lyk</i> mutants.....	52
Figure 3-9: Functional characterisation of PGN-induced genes by GO analysis	53
Figure 3-10: <i>CERK1</i> mediates PGN sensitivity	54
Figure 3-11: Generation of triple <i>lyk</i> knock-out mutants.....	55
Figure 3-12: Muropeptide-induced gene expression requires <i>LYM3</i> and <i>CERK1</i>	57
Figure 3-13: Sequence alignment of the <i>Arabidopsis</i> chitinases	58
Figure 3-14: <i>CHIA</i> protein sequence and annotated features.....	59
Figure 3-15: <i>CHIA</i> expression profile upon biotic stress	61
Figure 3-16: <i>CHIA</i> expression analysis using a <i>pCHIA::GUS</i> reporter line	63
Figure 3-17: Characterisation of <i>CHIA</i> T-DNA insertion lines	64
Figure 3-18: Characterisation of <i>CHIA</i> knock-down and overexpression lines	66
Figure 3-19: Phenotypes of <i>CHIA</i> overexpression and knock-down lines	67
Figure 3-20: Localisation of <i>CHIA</i> -GFP in <i>Arabidopsis</i>	68
Figure 3-21: Localisation of <i>CHIA</i> -GFP and <i>CHIA</i> ΔSP-GFP in tobacco	70
Figure 3-22: Detection of <i>CHIA</i> protein in <i>Arabidopsis</i>	72
Figure 3-23: Deglycosylation of <i>CHIA</i> -GFP and <i>CHIA</i> ΔSP-GFP	73
Figure 3-24: Expression of His ₆ - <i>CHIA</i> in <i>Escherichia coli</i>	75
Figure 3-25: Expression of <i>CHIA</i> in <i>Pichia pastoris</i>	76
Figure 3-26: Yeast two-hybrid analysis	77
Figure 3-27: Chitin- and PGN-hydrolysis activity of <i>CHIA</i> leaf protein	79
Figure 3-28: Chitin- and PGN-hydrolysis activity of <i>CHIA</i> protoplast samples.....	81

Figure 3-29: Infection of the transgenic <i>CHIA</i> lines with <i>Botrytis cinerea</i>	83
Figure 3-30: Infection of the transgenic <i>CHIA</i> lines with <i>Alternaria brassicicola</i>	85
Figure 3-31: Infection of the transgenic <i>CHIA</i> lines with <i>Pseudomonas syringae</i>	87
Figure 4-1: Plant perception and signaling of carbohydrate PAMPs/MAMPs	92
Figure 8-1: ClustalW2 protein sequence alignment of CHIA (<i>At5g24090</i>) and selected plant class chitinases	iv

List of Tables

Table 2-1: Used media	17
Table 2-2: Used antibiotics	17
Table 2-3: Used vectors	18
Table 2-4: Used bacterial strains.....	19
Table 2-5: Knock-out and complementation lines used in this work	20
Table 8-1: Used oligonucleotides	iii

1 Introduction

1.1 Host-pathogen interaction

Plants, animals and other organisms are continuously confronted with potential disease-causing pathogens. Host organisms provide the successful invaders nutrients, protection, convenient transmission routes or a platform for propagation. Luckily, the host barriers are seldomly overcome by the pathogenic microbes due to effective defense mechanisms. Animals rely on two types of surveillance and defense systems. The innate immunity renders animals a first line of protection against many pathogens due to the recognition of conserved microbial signatures by pattern recognition receptors (PRRs) mediating host inflammatory responses. The second line of defense is brought about by the adaptive immune system, which is comprised of specialised immune cells and immunoglobulins with immense diversity and specificity for macromolecules derived from invading pathogens. Invertebrates like *Drosophila* and *Caenorhabditis* are solely dependent on the innate immunity, suggesting this immune system to be more ancient than that of jawed vertebrates, which rely on both adaptive and innate immunity (Medzhitov and Janeway, 2000).

1.2 Plant innate immunity

Although plants lack the recombinatorial adaptive immunity known from the animal kingdom, also they possess an effective immune system. The basis of the plant innate immunity is the ability to differentiate between self and non-self or modified self. Furthermore, the plant innate immune system is branched into two forms of immunity, termed pathogen-associated molecular pattern (PAMP)-triggered immunity (PTI) and effector-triggered immunity (ETI), formerly also known as basal disease resistance and resistance (R) gene-based disease resistance, both aiming at a successful restriction of pathogen growth to defeat pathogenic attack (Abramovitch et al., 2006; Chisholm et al., 2006; Jones and Dangl, 2006).

1.2.1 PAMP-triggered immunity

PAMPs or MAMPs (microbe-associated molecular patterns) are highly conserved molecules and often essential for the fitness and survival of the microbial organisms (Nürnberg and Brunner, 2002). They include for instance proteinaceous signatures such as bacterial flagellin, elongation factor Tu (EF-Tu), a 13 aa-fragment of a *Phytophthora* transglutaminase (Pep-13) and cell wall components like fungal chitin, oomycete heptaglucan and bacterial lipopolysaccharides and peptidoglycan (Cosio et al., 1990; Dow et al., 2000; Erbs et al.,

2008; Felix et al., 1999; Felix et al., 1993; Gust et al., 2007; Kunze et al., 2004; Nürnberger et al., 1994). The perception of such non-self structures is mediated by cell surface PRRs (Figure 1-1), which transduce the signal into the plant cell ultimately triggering a generic, broad-range defense response leading to PTI. Many of the PRRs identified so far belong to the large receptor-like kinase (RLK)/Pelle gene family (Shiu and Bleecker, 2001). They typically harbour an extracellular domain dedicated for ligand perception and possibly protein-protein interaction, a transmembrane domain and a cytoplasmic protein kinase domain. Motifs found within the extracellular domain vary, a prominent example is the leucine-rich repeat (LRR) domain present in two well-studied receptor proteins, FLS2 (FLAGELLIN-SENSING 2) and EFR (EF-Tu receptor) (Gómez-Gómez and Boller, 2000; Zipfel et al., 2006). The LRR domain is also a feature of some of the animal PRRs, the *Drosophila* Toll and the mammalian Toll-like receptors (TLRs) (Imler and Hoffmann, 2001; Medzhitov et al., 1997). Intriguingly, the perception of bacterial flagellin is mediated through LRR domain-containing receptors both in plants and in animals by FLS2 and TLR5, respectively (Gómez-Gómez and Boller, 2000; Hayashi et al., 2001). However, the extracellular LRR domains of the two proteins and also the flagellin epitopes recognised by these receptors differ greatly suggesting that the perception systems are the product of convergent evolution. The PRR-dependent activation of the basal immune reactions truly contributes to resistance towards pathogens. For instance, the depletion of *FLS2* was shown to lead to enhanced bacterial susceptibility and the mutant line lacking the gene encoding the chitin elicitor receptor kinase 1 (CERK1) was less resistant towards fungal pathogens than wild type plants (Miya et al., 2007; Wan et al., 2008; Zipfel et al., 2004).

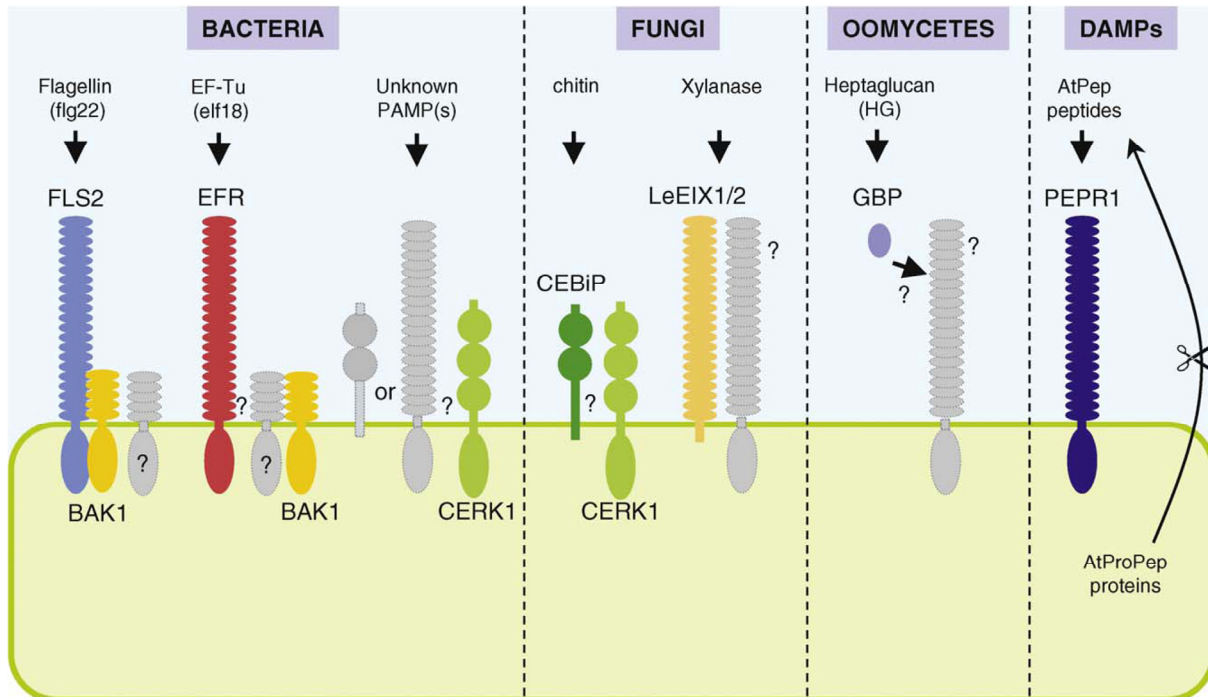


Figure 1-1: Plant pattern-recognition receptors and their signaling adapters

The bacterial PAMPs flagellin (flg22) and elongation factor Tu (EF-Tu) are perceived by the Arabidopsis LRR receptor kinases FLS2 and EFR, respectively. FLS2 and EFR form hetero-oligomers with the coreceptor BAK1 (the BRI1-associated kinase 1) in a ligand-dependent manner. AtCERK1 mediates the recognition of an so far unknown bacterial PAMP and is also essential for chitin perception and fungal resistance. In rice, OsCERK1 acts together with the CEBiP protein in the chitin detection. In tomato, xylanase is detected by the RLPs LeEIX1 and LeEIX2. In leguminous plants, oomycete heptaglucon (HG) is bound by the glucan-binding protein (GBP), which subsequently activates the plant immune responses in a receptor-dependent manner. The AtPep peptides act as danger-associated molecular patterns (DAMPs) and are recognised by the LRR-RLK PEPR1. From Zipfel (2009).

The PRR-based recognition of microbial signatures generates a battery of basal defense reactions in plants. One of the very early responses is the change of ion fluxes across the plasma membrane. Thereby, the influx of Ca^{2+} and H^+ and the efflux of K^+ and anions like chloride and nitrate are increased (Boller, 1995; Nürnberger et al., 2004; Wendehenne et al., 2002). Experimental proof for the role of Ca^{2+} as an intracellular second messenger activating calcium-dependent protein kinases (CDPKs) and membrane channels has been provided (Blume et al., 2000; Brunner et al., 2002; Lecourieux et al., 2002; Ranf et al., 2008). Additional early responses are the generation of reactive oxygen species (ROS) and the activation of mitogen-activated protein kinases (MAPKs) (Apel and Hirt, 2004; Asai et al., 2002; Rodriguez Suarez et al., 2010). The MAPK signaling cascade culminates in the activation of transcription factors, such as members of the WRKY family, leading ultimately to induction of defense-responsive genes. Among these genes are for instance camalexin biosynthesis genes and genes encoding antimicrobial enzymes or receptor proteins (Boudsocq et al., 2010; Gust et al., 2007; Miya et al., 2007; Zipfel et al., 2006; Zipfel et al., 2004). The changes in the transcriptome induced by different PAMPs strongly overlap

indicating that the PRR pathways are at some point merging thereby giving rise to a generic plant immune response. An additional defense response is the accumulation of β -1,3-glucan (callose) deposits at the plant cell periphery (Flors et al., 2005; Luna et al., 2011). Callose deposition is detectable only after several hours upon infection and thus belongs to the so-called late immune responses.

In addition to non-self signals also signals resulting from altered host molecules can induce the primary plant defense response. Such danger-associated molecular patterns (DAMPs) are released and sensed upon pathogen attack (Hückelhoven, 2007). Among active DAMPs are polysaccharides like oligogalacturonides (OGAs) (D'Ovidio et al., 2004) and cutin monomers (Schweizer et al., 1996), which are released from the plant cell wall, but also endogenous peptides. The *Arabidopsis* peptide *AtPep1* acts as a DAMP molecule and induces upon perception by the PEPR1 and PEPR2 receptors defense gene expression and also the induction of the *AtPep1* precursor protein (Huffaker and Ryan, 2007; Krol et al., 2010; Ryan et al., 2007; Yamaguchi et al., 2006).

Up to date, many more PTI-triggering structures, such as peptidoglycans (see chapter 1.3), have been characterised than corresponding plant receptors, leaving intriguing gaps in the knowledge of PAMP perception and PTI.

1.2.2 Effector-triggered immunity

Virulent pathogens have found ways to overcome the first inducible layer of defense, the PTI, in the plant. Phytopathogenic Gram-negative bacteria, for instance, use a sophisticated secretion system to smuggle a complete battery of proteins, called effectors, into the host cell. One of the best studied bacterial protein-secretion systems is the type III secretion system (T3SS). The T3SS forms a macromolecular infection apparatus with more than 20 subunits, that is able to rupture the plant cell surface (Büttner and Bonas, 2006). Once in the host cytoplasm the effectors start to disable the defense mechanisms and manipulate the host metabolism resulting in profit for the pathogen (Abramovitch et al., 2006; Chisholm et al., 2006). The *P. syringae* effector proteins *AvrPto*, *AvrPtoB* and *AvrRpt2* suppress responses induced by PAMPs or MAMPs by inhibiting proteins involved in the PTI pathway, such as PRR receptors (Hauck et al., 2003; He et al., 2006; Kim et al., 2005). The toxin coronatine mimicks the plant hormone jasmonate and can reverse the MAMP-induced stomatal closure thus allowing pathogenic bacteria to gain entry into the host (Melotto et al., 2006). As a result of the effector activities the plant resistance mechanisms are impaired, and the pathogen can proliferate. This phenomenon is termed effector-triggered susceptibility (ETS) (Jones and Dangl, 2006). The effectors and more importantly their action in the host

cell served, however, as a new and more pathogen-specific surveillance platform mediated by specific host disease resistance (R) proteins. Most of these R proteins are cytoplasmic and contain a nucleotide binding (NB) and an LRR domain (NB-LRR proteins) (Caplan et al., 2008). The recognition of an effector or its activity by a NB-LRR protein triggers an efficient, prolonged defense response accompanied by a programmed cell death leading renewed to immunity (effector-triggered immunity, ETI) (Jones and Dangl, 2006). In tomato, the host Pto kinase mediates the association between the effector AvrPto and the host NB-LBB receptor protein Prf leading to successful defense (Mucyn et al., 2006). Also AvrPtoB can be recognised by the tomato Pto, which upon phosphorylation inactivates its E3 ligase activity needed for virulence, and subsequently signals ETI through Prf (Ntoukakis et al., 2009). Due to natural selection pathogens able to evade the ETI are favored and so the arms race between plants and pathogenic microbes continues.

1.2.3 Chitinases in plant pathogen defense

Bacterial and fungal chitinases often have housekeeping functions in nutrition processes or within morphogenesis of the cell wall (Cohen-Kupiec and Chet, 1998). In contrary, the plant and animal chitinases mainly play a role in the host self-defense against pathogen attack (Cohen-Kupiec and Chet, 1998; Kasprzewska, 2003; Patil et al., 2000). Therefore, plant chitinases are grouped among other defense-related enzymes and proteins into the large family of pathogenesis-related (PR) proteins (van Loon et al., 2006). Pathogens often try to enter the plants via natural openings, like stomata and hydathodes, hence the apoplastic space is an ancient battleground for plant-pathogen interactions. In addition to other host PR proteins also the acidic chitinase forms are secreted into the apoplast (Sahai and Manocha, 1993). The basic chitinases accumulate mainly in the vacuole. The role of chitinases as antimicrobial proteins is supported by experimental data showing that the expression of many chitinases is induced upon infection with fungal pathogens (Majeau et al., 1990; Samac and Shah, 1991). Moreover, chitinases have been reported to degrade fungal cell walls and inhibit fungal growth *in vitro*, especially when combined with β -1,3 glucanases (Arlorio et al., 1992; Mauch et al., 1988; Schlumbaum et al., 1986). The first chitinase gene isolated in *Arabidopsis* encodes the basic chitinase ATHCHIB (At3g12500), which could inhibit growth of *Trichoderma reesei* *in vitro* (Samac et al., 1990). The pathogen-induced expression of ATHCHIB was shown to be ethylene-dependent (Thomma et al., 1999a). Interestingly, pathogens have evolved counter attack mechanisms to evade the antimicrobial activity of plant chitinases and so promote virulence. One example for such a mechanism is the production of chitinase-specific inhibitors (Misas-Villamil and van der Hoorn, 2008). Moreover, the *Cladosporium fulvum* effector Avr4 was reported to protect the fungal cell wall

against chitinolytic degradation by masking the cell wall chitin, suggesting that the chitin-binding properties of Avr4 are also part of a counter-defensive arsenal of the fungi (van den Burg et al., 2006). Another fungal effector, Ecp6, inhibits as scavenger the release of free chitin fragments needed for PTI-activation (de Jonge et al., 2010). Chitinases (EC.3.2.1.14) cleave the glycosidic $\beta(1\rightarrow4)$ bond in biopolymers of N-acetylglucosamine, present mainly in chitin. Chitin is the major building block of fungal cell walls and also of the exoskeleton of insects and crustaceans. According to sequence similarity of the catalytic glycosyl hydrolase domains, chitinases are divided in families 18 and 19 (Henrissat, 1991). Family 18 chitinases are widely distributed across the kingdoms and are present in bacteria, fungi, viruses, plants and animals, whereas family 19 chitinases are almost exclusively found in plants. The chitinases of both families differ in their biochemical features; family 18 chitinases employ a retention mechanism (catalysis product has the same configuration as the substrate) and family 19 chitinases use an inversion mechanism changing the configuration form of the catalysis product (Brameld and Goddard, 1998; van Aalten et al., 2001). The protein structure of chitinases contains a signal sequence for secretion, a glycosyl hydrolase domain and sometimes an additional chitin-binding domain (Passarinho and De Vries, 2002). Chitinases can be further divided into two different categories: endochitinases hydrolyse internal $\beta(1\rightarrow4)$ bonds and exochitinases, which catalyse the hydrolysis only in the reducing end of the chitin chain. Many plant endochitinases with a high isoelectric point exhibit an additional lysozyme-like activity (Collinge et al., 1993; Heitz et al., 1994; Majeau et al., 1990).

1.3 Peptidoglycan - A bacterial cell wall constituent

Virtually all bacteria have a cell wall, which upholds the cell shape and provides a rigid exoskeleton, a so-called sacculus, protecting the bacterial cell against mechanical and osmotic lysis (Nanninga, 1998; Navarre and Schneewind, 1999). Besides its protective function and shape formation, the cell wall also provides an interface for interactions with the surrounding environment and possible hosts. The most important component of the bacterial cell wall conferring strength and rigidity is the heteropolymeric macromolecule peptidoglycan (PGN). It consists of firm glycan chains that are interlinked either directly or via short peptide bridges (Glauner et al., 1988; Schleifer and Kandler, 1972). The disaccharide building block establishing the glycan chains is made up of N-acetylglucosamine (GlcNAc) and N-acetyl muramic acid (MurNAc) in $\beta(1\rightarrow4)$ linkage (Figure 1-2). The D-lactyl group of MurNAc provides a possibility for the attachment of the stem peptides via amide linkage. Whereas the glycan chain displays surprisingly little divergence among different bacterial species, the amino acid composition of the peptide bridges can vary. Depending on the presence of L-lysine (Lys) or meso-diaminopimelic acid (Dap) at the third position in the stem peptide

(Figure 1-2) the peptidoglycan is termed either Lys-type or Dap-type. Lys-type PGN peptides are usually interconnected by a peptide bridge and the Dap-type PGN peptides are directly crosslinked (Navarre and Schneewind, 1999; Schleifer and Kandler, 1972).

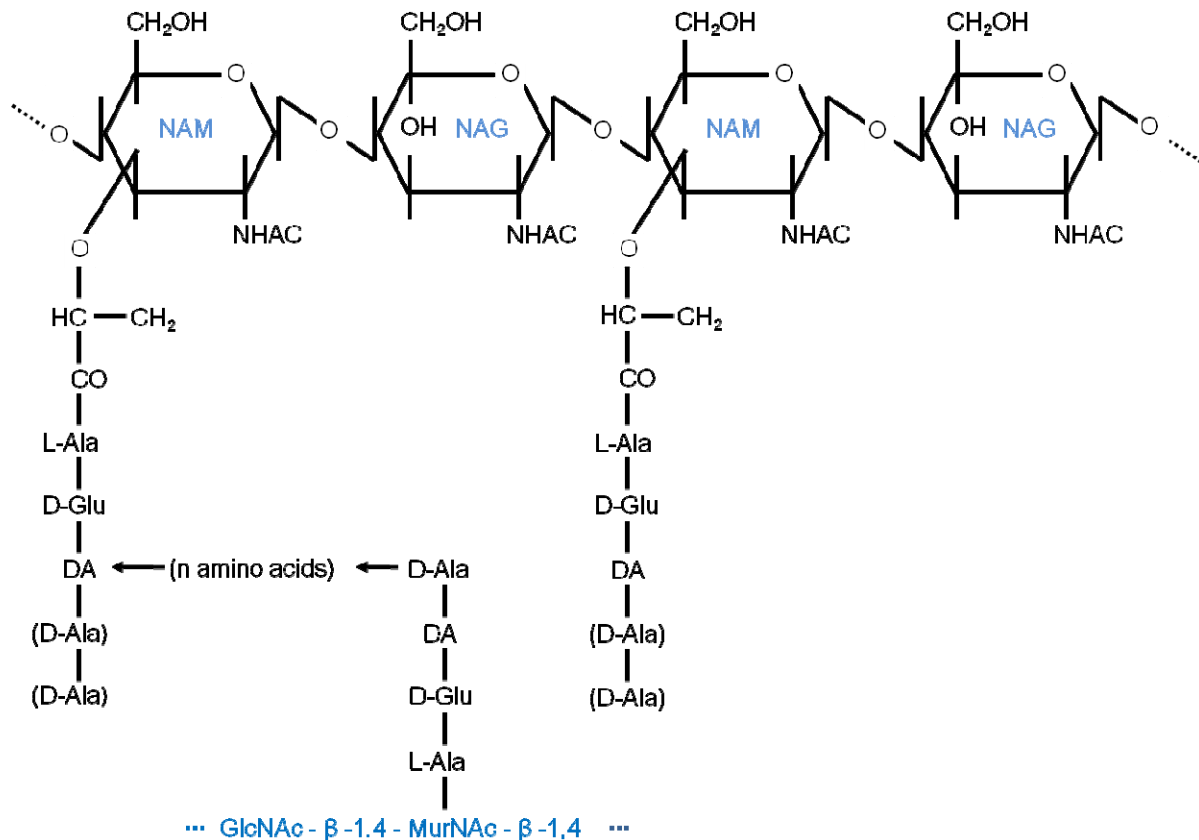


Figure 1-2: The schematic structure of peptidoglycan

Bacterial peptidoglycan is composed of alternating N-acetylglucosamine (NAG, GlcNAc) and N-acetylmuramic acid (NAM, MurNAc) molecules, which form the glycan strands, and stem peptide units which connect neighboring glycan strands in some bacteria, via a peptide crossbridge, with each other. The NAG and NAM sugars are linked with each other by β -1,4 linkage. DA stands for diamino acid (generally diaminopimelic acid or L-lysine) and n for the number of amino acids in the cross-bridge ($n=0$ to 5 depending on the bacteria). Based on van Heijenoort (2001).

Most Gram-positive bacteria contain the Lys-type peptidoglycan, whereas the Dap-type peptidoglycan is typical for Gram-negative bacteria like *Pseudomonas syringae* and *Escherichia coli*. Gram-positive and Gram-negative bacteria differ not only in the type of peptidoglycan they harbor, but also in the PGN amount. Gram-positive cell walls contain a thick multilayered PGN coat (20 - 80 nm), which is embedded with teichoic and lipoteichoic acids and proteins (see Figure 1-3). Instead, Gram-negative cell walls consist of only few layers of peptidoglycan (1-7 nm) and an additional membrane, the outer membrane (Cabeen

and Jacobs-Wagner, 2005). These two cell wall components are connected with each other via lipoproteins and contain also lipopolysaccharide (LPS) molecules (Figure 1-3).

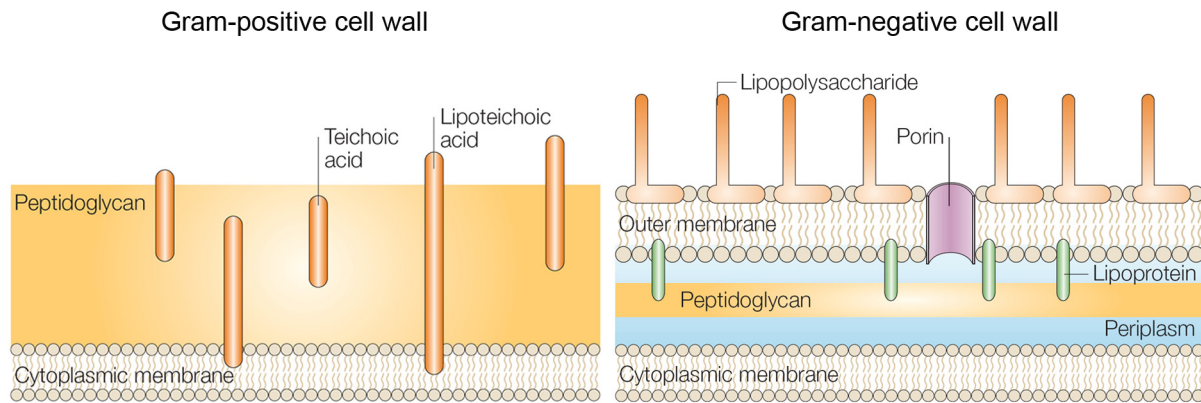


Figure 1-3: Gram-positive and Gram-negative cell walls

A schematic picture shows the components of the cell wall of Gram-positive (left) and Gram-negative (right) bacteria. Left: The Gram-positive cell wall is composed of a thick PGN layer outside of the cytoplasmic membrane. Teichoic and lipoteichoic acids are embedded into the peptidoglycan. Right: The cell wall of Gram-negative bacteria consists of an outer membrane linked by lipoproteins to thin, mostly single-layered PGN in the periplasmic space. In addition to lipoproteins, also porins and lipopolysaccharides are present in the cell wall. Modified after Cabeen and Jacobs-Wagner (2005).

The growth of the bacterial peptidoglycan sacculus takes place by insertion of disaccharide pentapeptide subunits into the existent peptidoglycan and is mediated by the penicillin-binding proteins (PBPs) (Höltje, 1998; Macheboeuf et al., 2006; Nanninga, 1998). To allow the extension of this covalent structure peptidoglycan hydrolase activity is required. This is accomplished by peptidoglycan (murein) hydrolases, which are divided into groups according to their enzymatic properties (Shockman and Höltje, 1994). N-acetylmuramidases (EC 3.2.1.17) and N-acetylglucosamidases (EC 3.2.1.96) cleave the glycosidic bond behind either the MurNAc or GlcNAc sugar, respectively (Tipper et al., 1964). N-Acetylmuramoyl-L-Ala amidases (amidases, EC 3.5.1.28) are specialised in the hydrolysis of the peptide bond between the polysaccharide chain and the stem peptide and glycyl-glycine endopeptidases (e.g. lysostaphin, EC 3.4.24.75) cleave the attachment site of the peptidoglycan cross-bridges (Jayaswal et al., 1990; Schindler and Schuhardt, 1964). The peptidoglycan hydrolysis by bacterial enzymes is essential not only during bacterial growth but also for cell division, peptidoglycan turnover and other biological processes, hence being highly controlled to avoid autolysis of the cells. During the reconstruction of the cell wall peptidoglycan fragments are released from the murein sacculus and despite an effective recycling system a portion of these turnover products is lost in the surroundings (Boothby et

al., 1973; Goodell, 1985). Other microorganisms, animals and plants also contain peptidoglycan degrading activities. However, these enzymes are a part of the antibacterial defense machinery (see chapters 1.2.3 and 1.4).

Due to its essential function within the bacterial cell wall peptidoglycan is strongly conserved. In addition, PGN is exposed at the cell surface, hence fulfilling important requirements for an optimal PAMP.

1.4 PGN processing and perception in animals

The bacterial peptidoglycan acts immunostimulatory in metazoans and several components of the PGN detection machinery have been elucidated in the past years both in insects and mammals (Dziarski and Gupta, 2010; Girardin and Philpott, 2004; Royet and Dziarski, 2007).

In the fruit fly, *Drosophila melanogaster*, two distinct systems of peptidoglycan detection exist. The Toll pathway senses preferentially Lys-type peptidoglycan derived from Gram-positive bacteria, whereas the IMD (immune deficiency) pathway recognises mainly Gram-negative bacteria and their Dap-type PGN (Leulier et al., 2003). Interestingly, the LRR-domain containing cell surface receptor Toll is not directly activated by peptidoglycan, but by the cytokine Spätzle (Figure 1-4), a signaling intermediate, of which proteolytic cleavage is triggered by infection with Gram-positive bacteria (Weber et al., 2003). The intracellular domain of the Toll receptor, the TIR (Toll/Interleukin-1 receptor) domain is then mediating the signal transduction via the TIR-containing adapter protein dMyD88 (Belvin and Anderson, 1996; Horng and Medzhitov, 2001; Kopp and Medzhitov, 1999).

The genuine PGN receptors belong to the Peptidoglycan Recognition Protein (PGRP) family. In total, 19 PGRP proteins are present in *Drosophila*, some of them being differential splicing products of a single PGRP gene (Werner et al., 2000). The PGRP domain resembles the N-acetylmuramoyl-L-alanine amidase domain of bacterial enzymes and indeed some of the PGRPs have amidase activity and are able to digest PGN (Mellroth et al., 2003). The PGN receptor PGRP-SA binds specifically to Lys-type PGN and thereby triggers the Toll pathway culminating in the nuclear factor κ B (NF- κ B)-dependent induction of the antimicrobial peptide (AMP) gene *Drosomycin* (Michel et al., 2001). In addition, The Gram-negative binding protein 1 (GNBP1) is needed for the PGRP-SA-mediated activation of the Toll pathway (Figure 1-4). Experimental data suggest that both the degradation of polymeric PGN into smaller fragments and the generation of reducing MurNAc ends by GNBP1, and the physical interaction of GNBP1 with the receptor protein PGRP-SA in a PGN-dependent manner are crucial steps for the perception (Filipe et al., 2005; Wang et al., 2006). Whereas *M. luteus*

PGN is strictly recognized by PGRP-SA, some other Lys-type PGNs can be sensed by the partially redundant receptors PGRP-SA and PGRP-SD (Bischoff et al., 2004). PGRPs with amidase activity have been suggested to have either immunostimulatory or scavenger properties (Garver et al., 2006; Mellroth et al., 2003). The paradigm of receptors and scavengers belonging to the same family is logic; the scavenger PGRP cleaves in the middle of the binding site of the PGRP receptor dampening thereby the immune response (Mellroth et al., 2003).

The IMD pathway is named after the signaling intermediate protein IMD (a Death Domain protein), which upon stimulation of the PGN receptors activates several downstream pathways resulting in the activation of genes encoding for antimicrobial peptides and other defense responses. In contrast to the Toll pathway, the IMD pathway preferentially induces the expression of *Diptericin*, *Attacin* and *Drosocin* genes (Royet and Dziarski, 2007). The main PGN receptor stimulating the IMD pathway upon infection with Gram-negative bacteria is the membrane-bound PGRP-LC (Choe et al., 2002; Gottar et al., 2002; Ramet et al., 2002). However, also the soluble receptor protein PGRP-LE can activate the IMD pathway and for instance upon *E.coli* infection both PGRP-LC and PGRP-LE are required to effectively produce resistance (Takehana et al., 2004). The minimal motif of the Dap-type PGN stimulating PGRP-LC is a GlcNAc-MurNAc monomer attached to a tetrapeptide containing m-DAP, the so-called tracheal cytotoxin (TCT) (Stenbak et al., 2004). TCT is perceived by a heterodimeric complex containing the isomers PGRP-LCx (which has affinity to PGN) and PGRP-LCa (an isomer with no PGN affinity), and the PGRP-LCx homodimer complex acts as a receptor for the polymeric Dap-type PGN *in vitro* (Kaneko et al., 2004; Lim et al., 2006; Mellroth et al., 2005; Stenbak et al., 2004). Also the dimerisation of PGRP-LE upon ligand binding has been suggested (Lim et al., 2006). Additionally to the extracellular role described above, PGRP-LE has an additional role within the cytosol. The *Drosophila* PGRP-LE mutant is susceptible to infection by the intracellular bacterium *Listeria monocytogenes* with Dap-type PGN (Yano et al., 2008). The finding suggests that a specific sensing system depending on PGRP-LE is present detecting invading pathogenic bacteria able to escape the cell-surface receptors. Beside the PGRP receptors, also enzymatically active PGRPs are involved in the regulation of the IMD pathway. For example, PGRP-LB, PGRP-SC1 and PGRP-SC2 have all been implicated as negative regulators of the IMD pathway by cleaving peptides from the glycan chains (Figure 1-5), thus reducing or eliminating the biological activity of PGN (Bischoff et al., 2006; Zaidman-Rémy et al., 2006). These proteins are mainly expressed in the gut and maintain the fine balance of the immune response to commensal and pathogenic bacteria (Royet and Dziarski, 2007). A recent publication added the PGRP-LF protein to the list of negative regulators of the IMD pathway

(Basbous et al., 2011). However, unlike the other PGRPs PGRP-LF contains no PGN-docking groove and thus cannot bind PGN. The downregulation of the IMD pathway is taking place via interaction with the PGN receptor PGRP-LC (Basbous et al., 2011).

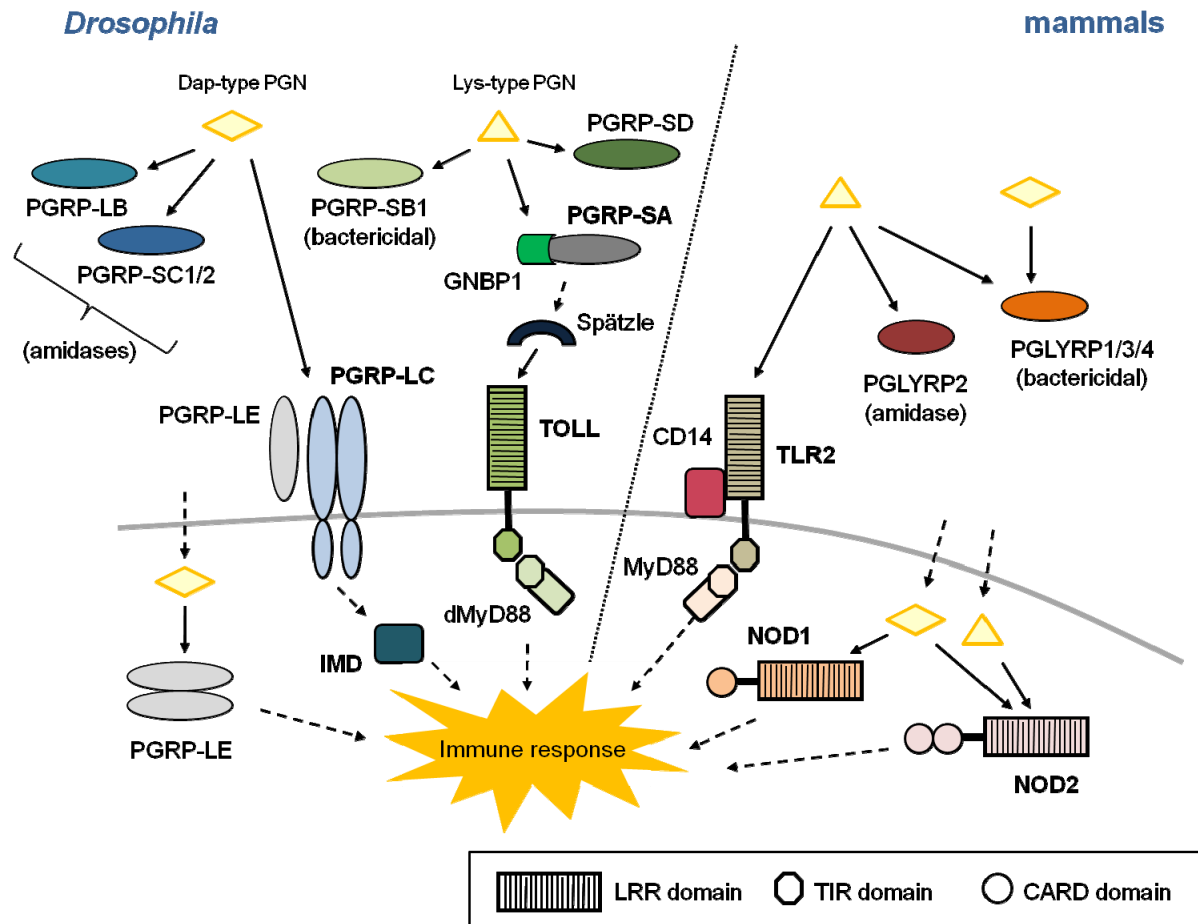


Figure 1-4: Peptidoglycan sensing in animals

Recognition of peptidoglycan in *Drosophila* (left) and mammals (right) by the innate immune system relies on specific detection of Dap-type or Lys-type peptidoglycan (PGN). In *Drosophila*, Dap-type PGN is sensed by PGRP-LC and PGRP-LE leading to the stimulation of the IMD pathway and finally production of antimicrobial peptides. PGRP-LB and PGRP-SC1/2 act via their amidase activity as modulators of PGN-induced inflammatory responses. Lys-type PGN is mainly recognised by the PGRP-SA, whereas it's complexed to GNBP1, leading to Spätzle-dependent activation of the Toll receptor. The signal transduction is mediated via TIR domain-containing dMyD88 resulting in immune responses, including gene expression of antimicrobial peptides. Additionally, also PGRP-SD mediates the perception of certain types of Gram-positive PGN and PGRP-SB1 acts bactericidal. In mammals, the intracellular LRR-domain containing proteins Nod1 and Nod2 recognise Dap- and/or Lys-type PGN. The TLR2/CD14 receptor complex mediates perception of Lys-type PGN. The mammalian PGRPs, PGLYRPs, function either directly bactericidal or harbor amidase activity. PGRP, peptidoglycan recognition protein; GNBP1, Gram-negative binding protein 1; IMD, Immune deficiency; TLR, Toll-like receptor; Nod, nucleotide oligomerisation domain; LRR, leucine-rich repeat; TIR, Toll/Interleukin 1 receptor; CARD, caspase recruitment domain. Based on Girardin and Philpott (2004).

In mammals, both extracellular and intracellular receptors detecting peptidoglycan are present. The membrane-bound Toll-like receptor 2 (TLR2) contains an extracellular LRR-domain similar to its *Drosophila* homologue Toll. TLR2 has been shown to colocalise with

peptidoglycan and mediate together with another cell-surface receptor protein, CD14, the extracellular recognition of PGN (Dziarski et al., 1998; Gupta et al., 1996; Müller-Anstett et al., 2010; Schwandner et al., 1999; Takeuchi et al., 1999; Yoshimura et al., 1999). The role of TLR2 as a specific PGN receptor has been heavily debated though (Dziarski and Gupta, 2005b; Travassos et al., 2004; Zähringer et al., 2008), and experimental data have also suggested other agonists for the TLR2-CD14 receptor complex, such as lipoproteins and chitin (Bubeck Wardenburg et al., 2006; Da Silva et al., 2008; Müller et al., 2010). The intracellular PGN sensing system containing members of the Nod-like receptor (NLR) family is widely accepted. The two main receptors, Nod1 and Nod2, contain a C-terminal LRR-domain for ligand sensing, an N-terminal caspase recruitment domain (CARD) and a central nucleotide oligomerisation domain (NOD) (Figure 1-4) (Inohara et al., 2005; Tanabe et al., 2004). Interestingly, these mammalian cytosolic receptors have striking structural similarities to the plant NBS-LRR-type resistance proteins (Ausubel, 2005; Nürnberger et al., 2004). However, the mammalian Nod proteins and plant NBS-LRR resistance proteins perceive different pathogenic signatures and activate completely different downstream signaling cascades giving little evidence for a common evolutionary origin (Ausubel, 2005). The PGN binding specificities of Nod1 and Nod2 vary greatly. Nod1 is a specific receptor for Dap-type PGN and its minimal motif is L-Ala-D-Glu-DAP (iE-DAP) (Chamaillard et al., 2003; Girardin et al., 2003a). In contrast, the Nod2 is a more universal PGN receptor recognising muramyl dipeptide (MurNAc-L-Ala-D-Glu; MDP), which is present in all peptidoglycans (Girardin et al., 2003b; Inohara et al., 2003). Upon PGN-dependent stimulation Nod1 and Nod2 activate a NF- κ B-mediated pro-inflammatory response (Strober et al., 2006). The TLR- and Nod-dependent defense pathways also crosstalk with each other and can act in a synergistic manner (Pettersson et al., 2011; Tada et al., 2005).

In addition to the receptor-based surveillance systems, mammals also possess PGRPs orthologous to the insect PGRPs. Whereas the *Drosophila* PGRPs carry out various tasks (recognition of PGN and activation of defense pathways, negative regulation of PGN-triggered inflammation or direct antimicrobial activity), the mammalian PGRPs have somewhat limited functions (Figure 1-4). The four Peptidoglycan Recognition Proteins (PGLYRP1-4) present in mammals are all secreted proteins, three of them (PGLYRP1, PGLYRP3 and PGLYRP4) are bactericidal and PGLYRP2 is an amidase (Figure 1-5) (Royet and Dziarski, 2007). The mammalian PGRP domain binds similar to the insect PGRP with high affinity to muramyl-tripeptide, but it does not bind muramyl-dipeptide or a peptide without MurNAc (Guan et al., 2004; Kumar et al., 2005; Swaminathan et al., 2006). Mammalian PGRPs bind both Dap- and Lys-type PGN (Liu et al., 2000; Lu et al., 2006) and thus do not display the same specificity and differential PGN-mediated responses as *D.*

melanogaster PGRPs (Royet and Dziarski, 2007). Furthermore, it has been reported that some PGRPs also bind to other polymeric structures, like lipoteichoic acid (LTA) and LPS and to some fungi (Liu et al., 2000; Lu et al., 2006; Tydell et al., 2002). In the case of human and mouse PGRPs the highest affinity is for peptidoglycan (Liu et al., 2000; Lu et al., 2006). The preferred substrates for PGLYRP2 are soluble PGN fragments, which may be generated either by bacterial PGN hydrolases or other host enzymes, like lysozyme (Gelius et al., 2003; Wang et al., 2003). The minimal PGN fragment hydrolysed by PGLYRP2 is muramyl tripeptide, which is also the minimal binding motif for PGRPs (Wang et al., 2003). It has been suggested that PGLYRP2 acts as a scavenger dampening PGN-triggered pro-inflammatory responses similar to the amidase-active fruit fly PGRPs (Hojjer et al., 1997). Interaction with the bacterial cell wall peptidoglycan is essential for the bactericidal activity of PGLYRP1, PGLYRP3 and PGLYRP4, and they also require N-glycosylation and divalent cations for their antimicrobial properties (Wang et al., 2007). Although the bactericidal activity of PGLYRPs differs from the activity of other antimicrobial peptides, they are present in the same sites in the body and combat bacteria synergistically with each other (Wang et al., 2007).

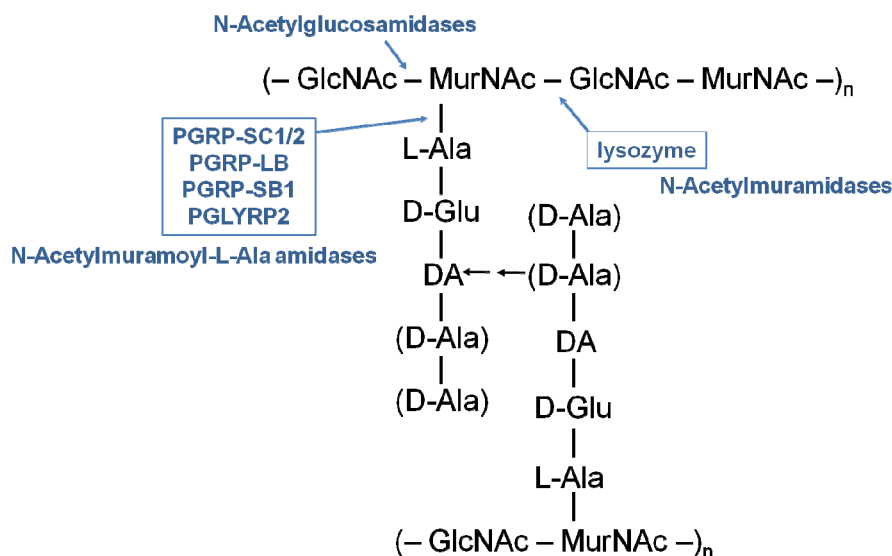


Figure 1-5: Metazoan PGN hydrolytic activities

The cleavage of glycan and peptide bonds of bacterial peptidoglycan by *Drosophila* and mammalian PGRPs and lysozyme with N-Acetylmuramoyl-L-alanine amidase or N-Acetylmuramidase activities are shown. Lysozyme and other N-Acetylmuramidases hydrolyse the glycosidic bond between MurNAc and GlcNAc, whereas the N-Acetylglucosamidases cleave between GlcNAc and MurNAc. PGRP, peptidoglycan recognition protein.

Lysozymes also belong to the antimicrobial defense armory in metazoans. They are divided into three subgroups: c-type (chicken or conventional type), g-type (goose-type) and i-type (invertebrate type) lysozymes (Callewaert and Michiels, 2010). Lysozymes are present in tissues and body secretions that are in contact with the environment or involved in bacterial

neutralization. The muramidase activity of lysozyme hydrolyses the glycosidic bond between MurNAc and GlcNAc (Figure 1-5) resulting in loss of peptidoglycan integrity and bacterial lysis (Jollès, 1996). Thereby soluble immunoactive PGN fragments are released (Zaidman-Rémy et al., 2006). Some pathogenic bacteria have found ways to acquire lysozyme resistance. For instance, peptidoglycan modification by O-acetylation and N-glycolylation or production of lysozyme inhibitors can ward off the PGN-hydrolytic activity of lysozyme (Clarke and Dupont, 1992; Monchois et al., 2001; Raymond et al., 2005).

The detection of bacterial PGN in animals is a highly complex system involving PGN sensing, binding and hydrolysing molecules. Similarities but also many differences occur between the surveillance systems of insects and higher animals.

1.5 Lysin motif (LysM) as mediator in carbohydrate signaling in plants

The lysin motif (LysM), usually about 40 amino acids in length, is a ubiquitous protein domain found in all living organisms except for Archaea (Bateman and Bycroft, 2000; Zhang et al., 2007). The three dimensional $\beta\alpha\alpha\beta$ structure of the LysM contains two α -helices stacking onto one side of a two-stranded antiparallel β -sheet (Bateman and Bycroft, 2000; Bielnicki et al., 2006; Mulder et al., 2006). In prokaryotes, many LysM-containing proteins are bacterial lysins or chitinases, which hydrolyse glycosidic bonds present in peptidoglycan and chitin, a homopolymer of N-acetylglucosamine, respectively (Buist et al., 2008; Ponting et al., 1999). Thus, the LysM is generally thought to mediate (peptido)glycan binding. In fact, also the plant LysM-domain containing proteins characterised so far are implicated in recognition of carbohydrates, like chitin and lipochitooligosaccharides, containing N-Acetylglucosamine moieties. The plant LysM proteins are divided into several subgroups depending on their domain architecture (Zhang et al., 2007). The Nodulation factor receptor 1 and 5 (NFR1 and NFR5) from *Lotus japonicus* and *Glycine max* (Indrasumunar et al., 2010; Madsen et al., 2003; Radutoiu et al., 2003) and the LysM-type receptor-like kinase 3 (LYK3) and LYK4 from *Medicago truncatula* (Limpens et al., 2003) belong to the LysM receptor-like kinase (LYK) subgroup. These legume receptor proteins have been shown to be essential for sensing lipochitooligosaccharides (Nod factors) derived from rhizobacteria and hence for the formation of nitrogen-fixing nodules and the establishment of endosymbiosis (Indrasumunar et al., 2010; Limpens et al., 2003; Madsen et al., 2003; Radutoiu et al., 2003). The perception of the fungal PAMP chitin in rice is mediated by two LysM-containing PRRs, a LysM receptor-like protein (LYP) called CEBiP (Chitin elicitor binding protein) and a LysM receptor kinase, OsCERK1 (Kaku et al., 2006; Shimizu et al., 2010). In *Arabidopsis*, the receptor kinase CERK1, which contains three extracellular LysM motifs, has been reported to play an

important role in chitin perception and basal fungal resistance (Miya et al., 2007; Wan et al., 2008). The combination of LysM and kinase domains is a unique feature of plant LysM proteins (Bateman and Bycroft, 2000). Likewise, the presence of a specific intervening sequence between LysM domains containing a conserved CxC motif is exclusively present in the plant lineage (Arrighi et al., 2006; Madsen et al., 2003; Radutoiu et al., 2003). Although the plant LysM motifs display similarities, they are evolutionarily specialised in the perception of distinct oligosaccharide structures. Accordingly, *Lotus japonicus* NFR1 and NFR5 did not participate in the activation of chitin-induced responses (Wan et al., 2008). Not only alterations within the LysM domain, but also adaptations of the kinase domain renders specificity for the LysM receptor kinases as demonstrated by Shimizu et al. (2010).

1.6 Aims of the thesis

The main goal of this work was to gain insights into the plant perception mechanism for the bacterial PAMP peptidoglycan. The activation of the immune response by peptidoglycan in *Arabidopsis thaliana* was only recently revealed and experimental data suggested a receptor-dependent mode of action (Erbs et al., 2008; Gust et al., 2007). Reverse genetic approaches, bacterial infection assays and peptidoglycan elicitation assays were employed to find possible peptidoglycan receptor proteins in *Arabidopsis*.

Moreover, the possible degradation of the large biopolymeric structure of PGN by plant enzymes prior to the recognition process was analysed. Such processing of complex microbial surface molecules into more accessible fragments has been reported to take place *in planta* (Fliegmann et al., 2004; Mithöfer et al., 2000). The role of a putative *Arabidopsis* PGN hydrolase in bacterial cell wall degradation and bacterial resistance was studied both *in vitro* and *in vivo*.

2 Materials and methods

2.1 Materials

2.1.1 Chemicals

All used standard chemicals were of standard purity and purchased from Sigma-Aldrich (Taufkirchen), Carl Roth (Karlsruhe), Merck (Darmstadt), Qiagen (Hilden), Invitrogen (Karlsruhe), Duchefa (Haarlem, Niederlande), Molecular Probes (Leiden, Niederlande), Fluka (Buchs, Schweiz) und BD (Sparks, USA), unless noted otherwise in the text. Restriction enzymes, ligase and DNA modification enzymes were purchased from Fermentas (St. Leon-Rot) and New England Biolabs (Beverly, USA). Oligonucleotides were received from Eurofins MWG Operon (Ebersberg) and antibodies from the companies Sigma-Aldrich (Taufkirchen), New England Biolabs (Beverly, USA) and Acris Antibodies GmbH (Herford). The antibody against tobacco class III chitinases from rabbit and the antibody against YFP from rabbit were kind gifts from Frédéric Brunner and Sara Mazzotta, respectively.

Xanthomonas campestris pv. *campestris* PGN and muro-peptides derived thereof were kindly provided by Mari-Anne Newman. The synthetically generated Flg22 peptide was a kind gift from Georg Felix. *Pto* DC3000 PGN was prepared as described in 2.4.1. *Staphylococcus aureus* PGN was obtained from Fritz Götz (Microbiology Department, University of Tübingen) or prepared as described in 2.4.2. *Bacillus subtilis*, *Escherichia coli* and *Micrococcus luteus* PGN and chitin were commercially available (Invivogen, Sigma). All described PGNs and chitin were dissolved in water at a concentration of 10mg/ml and stored at -20°C.

2.1.2 Media

Table 2-1 summarizes the media used in this work. All media were prepared using deionized water and sterilized by autoclaving for 20 minutes at 121°C. For solid media 15g/l Bacto-agar (BD) or 8g/l Select-Agar for MS plates (Sigma-Aldrich) was added to the medium. If necessary, antibiotics were added to the sterilized medium in appropriate final concentrations as listed in Table 2-2.

Medium	Ingredients per 1 liter	Species
LB	10 g Bacto-Tryptone, 5 g NaCl, 5 g Yeast extract (YE)	<i>Escherichia coli</i>
King's B	20 g glycerol, 40 g Proteose Pepton 3, after autoclaving addition of 0.1 % (v/v) MgSO ₄ and KH ₂ PO ₄	<i>Pseudomonas syringae</i>
MD	1.34 % (w/v) YNB, 4x10 ⁻⁵ % (w/v) Biotin, 2 % (w/v) Glucose	<i>Pichia pastoris</i>
YPD	20 g Peptone, 20 g Glucose, 10 g YE	<i>Pichia pastoris</i>
BMGY and BMMY	1 % (w/v) YE, 2 % (w/v) Peptone, 1.34 % (w/v) YNB, 100 mM potassium phosphate, pH 6.0, 4x10 ⁻⁵ % (w/v) Biotin, 1 % (v/v) glycerol or 2 % (v/v) MeOH	<i>Pichia pastoris</i>
CSM-LT	6.7 g YNB, 20 g glucose, 1546 mg -Leu, -Trp Kaiser-dropout (20 g Oxoid agar for plates)	<i>Saccharomyces cerevisiae</i>
CSM-LTA	6.7 g YNB, 20 g glucose, 1546 mg -Ade, -His, -Leu, -Trp Kaiser-dropout, 76 mg L-Histidin (20 g Oxoid agar for plates)	<i>Saccharomyces cerevisiae</i>
½ PDB	12 g PDB (Potato Dextrose Broth, Duchefa), pH 5.8 (NaOH)	<i>Botrytis cinerea</i>
½ MS	2.2 g MS (Duchefa), pH 5.7 (KOH)	<i>Arabidopsis thaliana</i>

Table 2-1: Used media

Antibiotics	c (µg/µl)	Solvent
Carbenicillin	100	Water
Cycloheximid	50	Water
Kanamycin	50	Water
Rifampicin	50	Methanol
Spectinomycin	100	Water
Tetracyclin	50	Ethanol

Table 2-2: Used antibiotics

2.1.3 Vectors

All used vectors are listed in Table 2-3.

Vector	Characteristics	Reference
pDONR201	Ori Puc, rrnB, T2, rrnB,T1, attP1, attP2, ccdB,Cm ^r , Kan ^r	Invitrogen
pDONR207	Ori Puc, rrnB, T2, rrnB,T1, attP1, attP2, ccdB,Cm ^r , Gent ^r	Invitrogen
pK7FWG2.0	P _{35S} , T _{35S} , eGFP, attR1, attR2, ccdB, Cm ^r , Kan ^r	VIB
pK7WGF2.0	P _{35S} , T _{35S} , eGFP, attR1, attR2, ccdB, Cm ^r , Kan ^r	VIB
pDEST17	PT7, RBS, His ₆ -tag, attR1, attR2, ccdB, Cm ^r , PT7, bla, Promotor, Amp ^r , pBR322 origin, ROP, orf	Invitrogen
pBGWFS7	attR1, attR2, ccdB, Ba ^r , Sm/Sp ^r , GUS, eGFP	Karimi et al. 2005
pBGW	attR1, attR2, ccdB, Cm ^r ,Sm/Sp ^r , Ba ^r	Karimi et al. 2005
miR319a pBSK (pRS300)	B reverse, T3 promotor, miR319a, T7 promotor, forward, Amp ^r A	Weigelworld.org
pBluescript	pUCori, P Lac, MCS, lac Z', f1+ori, Amp ^r	Stratagene
pGREEN0229	pSa-ORI, ColEI ori, MCS, lac Z', Kan ^r , Ba ^r	Hellens et al. 2000
pSOUP	ColEI ori, oriV, RepA, trfA, MCS, Tet ^r	Hellens et al. 2000
pPIC9K	5'AOX1, Ampr, pBR322, 3'AOX1, Kan ^r , HIS4 ORF, TT, secretion signal	Invitrogen
pPICZαC	5'AOX1, Ori Puc, CYC1 TT, Zeocin ^r , P _{EM7} , P _{TEF1} , AOX1 TT, α-Factor, cmyc-epitope, His ₆ -tag	Invitrogen
pGADT7-GW	MCS, Amp ^r , GAL4-AD, HA-tag, T7 promoter, gateway cassette (attR1, attR2, ccdB, Cm ^r) introduced into MCS-site	Clontech Laboratories (modified by Sandra Postel)
pGBKT7-GW	MCS, Amp ^r , GAL4-DNABD, Myc-tag, T7 promoter, gateway cassette (attR1, attR2, ccdB, Cm ^r) introduced into MCS-site	Clontech Laboratories (modified by Sandra Postel)

Table 2-3: Used vectors

2.1.4 Primers

The primers used in this work for cloning, genotyping, transcript analysis and sequencing are listed in the Appendix Table 8-1.

2.2 Organisms

2.2.1 Bacteria and fungi

The bacterial strains used in the frame of this work are listed in Table 2-4.

Species	Strain	Genotype
<i>Escherichia coli</i>	DH5 α	<i>supE44 ΔlacU169 (Φ80 lacZM15) hsdR17 recA1 endA1 gyrA96 thi-1 relA1</i>
	TOP10	<i>mcrA, delta (mrr-hsdRMS-mcrBC), phi 80delta lac delta M15, delta lacX74, deoR, recA1, araD139 delta (ara, leu), 7697, galU, galK, lambda⁻, rpsL, endA1, mupG</i>
	DB3.1	<i>RR1 gyrA endA recA Spec^r</i>
	BL21AI	<i>F-ompT hsdSb(rb-mb-) gal dcm araB::T7RNAP-tetA</i>
<i>Pseudomonas syringae</i>	<i>Pto</i> DC3000	Rif ^r
	<i>Pto</i> DC3000 Δ avrPto/PtoB	Rif ^r , Kan ^r , Δ avrPto, Δ avrPtoB
	<i>Pto</i> DC3000 <i>hrcC</i> ⁻	Rif ^r Kan ^r (nptII)
	<i>Pph</i>	Rif ^r
<i>Agrobacterium tumefaciens</i>	GV3103::pMP90	T-DNA ⁻ vir ⁺ rif ^r , pMP90 gen ^r

Table 2-4: Used bacterial strains

Additionally, the necrotrophic fungi *Alternaria brassicicola* (MUCL 20297) and *Botrytis cinerea* (B05-10) were used for fungal infections, the yeast *Pichia pastoris* (GS115) for protein expression and *Saccharomyces cerevisiae* strain AH109 for yeast two-hybrid experiments.

2.2.2 *Arabidopsis thaliana* lines

All experiments were conducted using the *Arabidopsis thaliana* ecotypes *Columbia-0* (Col-0), *Columbia-2* (Col-2) or Landsberg *erecta* (Ler) and transgenic lines generated in these ecotypes. The knock-out (KO) lines mainly used in this work are listed in Table 2-5 and were purchased from the Nottingham Arabidopsis Stock Centre (NASC) or received from other

research groups. The transgenic *p35S::secGFP* (*secGFP*) line has been described previously (Teh and Moore, 2007).

Stock number	T-DNA/KO line	AGI	Position of the T-DNA	Reference
	<i>chia-kd</i>	<i>At5g24090</i>	amiRNA line	this work
WiscDsLox387C11	<i>chia-1</i>	<i>At5g24090</i>	promoter	this work
SALK_095362	<i>chia-2</i>	<i>At5g24090</i>	3. exon	this work
CSHL_ET14179	<i>chia-3</i>	<i>At5g24090</i>	1. intron	this work
GABI_096F09	<i>cerk1-2</i>	<i>At3g21630</i>	10. exon	Miya et al. 2007
SALK_012441	<i>lyk2-1</i>	<i>At3g01840</i>	1. intron	Volker Lipka
SALK_140374	<i>lyk3-1</i>	<i>At1g51940</i>	10. exon	Volker Lipka
SALK_030271	<i>lyk3-2</i>	<i>At1g51940</i>	10. exon	Volker Lipka
GABI_857A10	<i>lyk4-1</i>	<i>At2g23770</i>	exon at 1615 bp	
CSHL_GT7089	<i>lyk5-1</i>	<i>At2g33580</i>	exon at 1280 bp	Volker Lipka
SALK_131911	<i>lyk5-2</i>	<i>At2g33580</i>	exon at 870 bp	
SALK_140374/ CSHL_GT7089	<i>lyk3-1/lyk5-1</i> (<i>LGK2-6-1-2</i>)	<i>At1g51940/At2g33580</i>		Volker Lipka
GABI_096F09/ SALK_140374	<i>cerk1-2/lyk3-1</i>	<i>At3g21630/At1g51940</i>		this work
GABI_096F09/ SALK_140374 CSHL_GT7089	<i>cerk1-2/lyk3-1/lyk5-1</i>	<i>At3g21630/At1g51940/ At2g33580</i>		this work
SALK_111212	<i>lym3-1</i>	<i>At1g77630</i>	1. intron	Roland Willmann 2011

Table 2-5: Knock-out and complementation lines used in this work

2.3 Cultivation conditions of the organisms

2.3.1 Growth of *Escherichia coli*

E.coli strains were cultivated overnight at 37°C either on LB-plates or in liquid LB medium at 230 rpm. Antibiotics were added into the media according to the resistance cassettes the strains were harboring.

2.3.2 Growth of *Pseudomonas syringae*

P.syringae strains were grown for 24-48 hours at 28°C either on King's B-plates or in liquid King's B medium at 180 rpm. For the determination of bacterial growth in infection assays the *Pseudomonas* strains were re-isolated from plant material (see 2.6.1) and plated on LB-plates containing cycloheximide in addition to other antibiotics.

2.3.3 Growth of *Agrobacterium tumefaciens*

A.tumefaciens strains were cultivated for 48 hours at 28°C on LB-plates or liquid LB medium at 230 rpm. Additional antibiotics were added into the media according to the plasmid-DNA the strains were carrying.

2.3.4 Growth of *Pichia pastoris*

P.pastoris strains were grown in liquid BMGY medium overnight at 30°C and 230 rpm to an OD600 of 2-6. The cells were harvested and resuspended in BMMY medium (OD600~1) to induce expression. To maintain the expression the yeast cells were fed with 0.5% (v/v) MeOH every 24 hours.

2.3.5 Growth of *Alternaria brassicicola* and *Botrytis cinerea*

The cultivation of *A.Brassicicola* and *B.cinerea* and the preparation of the spores for the infection assays were performed as published previously (Kemmerling et al., 2007).

2.3.6 Growth of *Arabidopsis thaliana* and *Nicotiana benthamiana*

A.thaliana seeds were sown on steam-sterilized GS90-soil (Gebr. Patzer GmbH) mixed with vermiculite or after surface-sterilization with chlorine gas on sterile ½ MS plates. After stratification of the seeds for two days at 4°C and in the dark the plants were grown in environmental chambers either in long-day (16 h light, 8 h darkness) or short-day (8 h light, 16 h darkness) under standard conditions (150µmol/cm²s light, 40-60 % humidity, 22°C). *N.benthamiana* plants were cultivated in a mixture of soil and sand containing 0.1 % (v/v) Confidor in the greenhouse (13 h light, 11 h darkness).

2.4 Methods

2.4.1 Isolation of peptidoglycan from Gram-negative bacteria

Peptidoglycan was isolated from the Gram-negative phytopathogenic bacteria *Pseudomonas syringae* (Pto DC3000) using a modified protocol of Glauner (1988). The fermentation of the bacteria was performed in the fermentation unit of the Microbiology department by Andreas Kulik (RG Fiedler). The preparation of the 10L fermentation culture was done in two steps. First, a small preculture (10 ml) was inoculated with bacteria freshly grown on King's B agar plate and grown at 28°C overnight. Secondly, a large preculture (1L) was inoculated with the small preculture and cultivated at 28°C for 8 hours up to a density of 3 - 3.5 (OD_{600nm}). The 1 liter culture was used for the inoculation of the 10 liter fermenter of the type Biostat E. The fermentation was performed at 28°C for 16 hours using free pH and pO₂ conditions. The bacteria were harvested by flow-through centrifugation (45 minutes at 5500 x g and 4°C) and immediately frozen in liquid nitrogen. After lyophilization the dry bacterial pellet (25 - 30 g) was homogenized by grinding and resuspended in ice-cold water in small portions (~5 g in 40 ml water). Immediately after resuspension the bacteria were added dropwise into boiling 4 % (w/s) SDS solution (~1g dry bacteria/10 ml SDS). The bacterial suspension was boiled for 1 hour under continuous stirring and then cooled down overnight at RT. The heat-stable peptidoglycan was harvested by ultracentrifugation for 1 hour at 43000 x g and at RT (Sorvall WX Ultra 80, Thermo Scientific). The PGN pellet was washed until it was free of SDS. For detection of residual SDS 335 µl washing supernatant was mixed with 170 µl 0.7 M sodium phosphate buffer, pH 7.2, 7µl 0.5 % (w/v) methylene blue and 1 ml chloroform. An SDS-free solution appeared light red, whereas a SDS-containing sample showed a light blue colour. The SDS-free peptidoglycan sample was then treated with several enzymes for degradation and removal of PGN-associated molecules. Degradation of high molecular weight glycogen was facilitated using 100µg/ml α-amylase (Fluka) in 10 mM Tris-HCl buffer pH 7 (2 hours at 37°C). In a subsequent second step the peptidoglycan was treated with 10 µg/ml DNaseI (Sigma) and 50 µg/ml RNase A (Qiagen) for additional two hours at 37°C, following an overnight digestion with 100 µg/ml Trypsin (Sigma) at 37°C (degradation and removal of RNA and DNA and covalently bound lipoproteins). Afterwards the PGN pellet was resuspended in Proteinase K buffer (50 mM Tris pH 7.5, 5 mM CaCl₂, 0.5 % (w/v) SDS) and digested for one hour at 65°C with 50 µg/ml Proteinase K (Carl Roth) for removal of residual proteinous impurities. After the digestion Proteinase K was inactivated for 15 minutes at 75°C. After washing the PGN pellet with water and harvesting by ultracentrifugation it was incubated at RT for one hour with shaking in 8 M LiCl solution. After washing the pellet for two times, it was further incubated in 100 mM EDTA, pH 8 for one hour. Then the PGN pellet was washed again and finally treated with 100 % (v/v) acetone at RT for two hours (removal

of lipoteichoic acids and traces of LPS). After final washing steps (3 times with water) the PGN pellet was lyophilized and stored either as powder or resuspended in water at -20°C. In the case of the presence of residual impurities in the PGN preparation after the isolation procedure, the Proteinase K digestion was repeated.

2.4.2 Isolation of peptidoglycan from Gram-positive bacteria

The isolation procedure for peptidoglycan from Gram-positive bacteria, such as *Staphylococcus aureus*, was performed as published previously (Bera et al., 2005). In comparison to the isolation protocol of PGN from Gram-negative bacteria, some steps of the basic scheme are either added or removed. The starting material was less (0.5 - 2 liter) and the bacterial cells were disrupted after boiling in SDS by vigorous homogenization. The digestion step with Proteinase K was omitted, but instead the PGN pellet was treated with hydrofluoric acid (HFA) before the LiCl incubation step to remove residual covalently bound polysaccharides, e.g. teichoic acids.

2.4.3 General molecular biology methods

Standard protocols were used for PCR, agarose gel electrophoresis, restriction digestion, ligation, transformation of bacteria and yeast and plasmid isolation (Ausubel, 1993; Sambrook and Russell, 2001). The transformation of TOP10 cells was performed according to the manufacturer's protocols (Invitrogen). The enzymes were used according to the manufacturer's protocols (Fermentas and NEB). Deglycosylation of proteins was carried out using the deglycosylation Kit and according to manufacturer's recommendations (NEB). For the generation of PCR fragments either the *Taq* DNA-Polymerase or the *Pfu* DNA-polymerase (cloning purposes; Fermentas) were used. GeneRuler™ DNA Ladder Mix (Fermentas) was used as size marker for the agarose gel electrophoresis. DNA fragments were extracted out of agarose gels or purified out of PCR reactions by using the Qiagen Gel Extraction Kit and Qiagen PCR Purification Kit (Qiagen).

2.4.4 Cloning

The constructs were generated either by traditional cloning techniques (via introduced restriction sites) or by the Gateway™ Technology (Invitrogen). For the traditional cloning the digested vector was treated with the antarctic phosphatase (NEB) prior ligation to inhibit self-ligation. Gateway™-cloning was performed according to the manufacturer's recommendations (Invitrogen). To obtain Gateway-compatible inserts gene-specific adaptor

primers were used in the first PCR. The essential recombination sites were then completed in a second PCR using the Gateway-primers attB1 and attB2 (see Appendix Table 8-1). The resulting inserts were then subcloned into pDONR201 or pDONR207 (Invitrogen) by using the BP clonase reaction and afterwards inserted into the expression vectors by using the LR clonase reaction following the manufacturer's specifications (Invitrogen).

2.4.5 DNA isolation

Genomic DNA from plant tissue for genotyping purposes was isolated as outlined in Edwards et al. (1991). For sequencing purposes plasmid-DNA were isolated and column-purified using the QIAprep Spin MiniPrep Kit (Qiagen). Sequencing of the generated constructs was performed by the companies Eurofins MWG Operon (Ebersberg) and GATC Biotech AG (Konstanz). The sequence analysis was performed using the Lasergene DNA*STAR software.

2.4.6 RNA isolation

Total RNA from leaves or seedlings was isolated using the Trizol method according to the standard protocol (Chomczynski and Sacchi, 1987). For seedling samples the standard volumes were reduced up to one-third. In the end of the isolation procedure the RNA pellet was eluted in ddH₂O (leaf RNA in 20-40 µL and seedling RNA in 10 µL) and stored at -20°C.

2.4.7 Semi-quantitative RT-PCR

1 µg of total leaf RNA was used for the first strand cDNA synthesis using RevertAid™ M-MuLV Reverse Transcriptase according to manufacturer's recommendations (Fermentas). The analysis of residual transcript in KO lines was performed using semi-quantitative RT-PCR. 1 µL cDNA was used for a standard PCR reaction with primers specific for the analyzed transcript. In a control PCR primers specific for the house-keeping gene *elongation factor 1α* (*EF1α*) were used (Table 8-1).

2.4.8 Quantitative Real-time PCR

2.5 µL seedling RNA (amounts not adjusted) or 1 µg leaf RNA was used for the cDNA synthesis (in 5µl total reaction volume). Leaf cDNA was diluted 3 to 5 fold for RT-qPCR experiments, whereas seedling cDNA was used undiluted. RT-qPCR amplifications and measurements were performed with the iQ5 Multicolour Real Time PCR detection system

from Bio-Rad. RT-qPCR amplifications were monitored using the ABsolute SYBR Green Fluorescein Mix (Thermo Scientific). The gene expression data was quantified using the 2- $\Delta\Delta$ CT method (Livak and Schmittgen, 2001). The normalization of the expression levels was done using the CT values obtained for the *EF-1 α* gene. The presence of a single PCR product was further verified by dissociation analysis in all amplifications. All quantifications were made in duplicate on RNA samples obtained from three independent experiments, each performed with a pool of two leaves or 4-6 seedlings.

2.4.9 Isolation of mesophyll protoplasts from *Arabidopsis*

Isolation of mesophyll protoplasts from leaves of 4-5 week-old *Arabidopsis* plants was performed according to the protocol of Yoo et. al (2007). After the isolation procedure protoplasts were resuspended in W5 solution and incubated overnight at RT and in the dark (2×10^5 protoplasts in 1ml W5 solution).

2.4.10 Stable transformation of *Arabidopsis thaliana*

A.thaliana plants were stably transformed by the floral dip-method (Clough and Bent, 1998). 500 ml liquid LB medium containing appropriate antibiotics was inoculated with a preculture of selected agrobacteria and cultivated for further 18 – 24 hours. The cells were pelleted for 20 minutes at 4500 x g and resuspended in fresh 5 % (w/v) saccharose solution at a density of 0.8 (OD_{600nm}). After addition of 0.02 % (v/v) Silwet young *Arabidopsis* inflorescences were dipped for one minute into the bacterial suspension. Afterward the plants were incubated at 100 % humidity for 24 hours. Seeds from floral-dipped plants were then screened for resistance against Basta (glufosinate-ammonium) or kanamycin.

2.4.11 Transient transformation of *Nicotiana benthamiana*

Agrobacterium tumefaciens-mediated transient transformation was used for the transient expression of proteins in tobacco. The bacterial strain carrying the appropriate expression vector was cultured as described in 2.3.3. After harvesting the cells at 4°C for 10 minutes at 2000 x g they were washed for two times with 10mM MgCl₂. The density of the culture was diluted to 5×10^4 cfu/ml and 150 μ M acetosyringone is added. The bacterial suspension was then incubated shaking at RT for 3-6 hours. Afterwards the suspension was mixed 1:1 with a suspension of bacteria carrying an expression construct of p19 (Voinnet et al., 2003) and the mixture was then infiltrated into the leaves of 3 week-old tobacco leaves. The leaf tissue was analyzed 2-4 days post infection for the presence of the protein.

2.4.12 Crossing *Arabidopsis thaliana* plants

The sepals, petals and anthers of the young flowers of the mother plant were carefully removed. Then a mature flower from the father plant was gently opened by pinching with the forceps and rubbed onto the stigma of the emasculated mother plant until some pollen were visible on the surface of the stigma. The procedure was repeated with 4 to 6 flowers per inflorescence and after labeling of the crossed flowers they were kept at 100 % humidity under a glass bell for two days to increase the chance of fertilisation. After a day or two a successful fertilisation was observable by obvious elongation of the stigma to generate a silique. The siliques were harvested before the seeds fell out and let ripen in a reaction tube. Fully ripened seeds were sown on soil and the offspring seedlings were analysed by genotyping as described in 2.4.19.

2.4.13 Generation of knock-down lines

Artificial microRNA-mediated gene silencing was used to specifically knock-down *CHIA* in Col-0 background. The Web microRNA Designer (WMD; <http://wmd.weigelworld.org>) was used to select the primers (see Appendix Table 8-1) for the generation of an artificial 21mer microRNA (Schwab et al., 2005). The insert was generated in four PCR-steps (see Figure 2-1). In PCR 1 the template pRS300 and the primers A and At5g24090miR*a were used. In PCR 2 the primers At5g24090miR*-s and At5g24090miR-a were used to amplify the second product from the same template. The third product was generated using the same template and the primer pair At5g24090miR-s and B. In the fourth PCR the final insert was generated using the overlapping products from the PCRs 1- 3 as template. The *CHIA*-specific amiRNA was introduced into the EcoRV site of pBSK⁽⁻⁾ (Stratagene) via T/A cloning and subsequently cloned into the EcoRI/XbaI site of pGREEN0229 (Hellens et al., 2000). Additionally, the p35S from pK7FWG2.0 (VIB) was introduced into the HindIII/EcoRI site and the 35S-terminator from pAeq-Hyg (a kind gift from Magdalena Krzymowska) into XbaI/SacI site of the binary vector pGREEN0229. The transformation of the resulting vector into agrobacteria was mediated using the accessory plasmid pSOUP (Hellens et al., 2000). The stable transformation of the construct into the *Arabidopsis* genome was performed using the floral-dip method (see 2.4.10). Analysis of the *CHIA* transcript level in the *CHIA* knock-down line (*chia-kd*) was performed by quantitative RT-PCR using primers listed in Table 8-1.

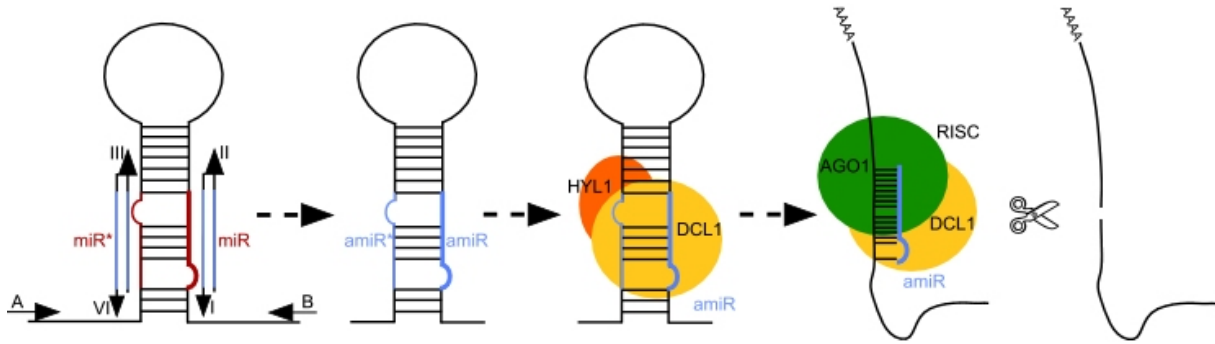


Figure 2-1: Working mode of amiRNA-mediated gene silencing

A schematic overview for the generation of artificial microRNA (amiRNA) and amiRNA-mediated gene silencing in plants (<http:wmd.weigelworld.org>). Primer I: microRNA-s; primer II: microRNA-a; primer III: miR*s; miR*a and primer A and B (plasmid specific).

2.4.14 Generation of overexpression lines

For the *p35S::CHIA-GFP* fusion construct, a 906bp fragment of the *CHIA* coding sequence was cloned using the primers At5g24090gatF and At5g24090gatR (Table 8-1). For the *p35S::CHIA Δ SP-GFP* fusion construct, which was lacking the predicted N-terminal signal peptide, a 849bp fragment of the *CHIA* coding sequence lacking amino acids 2-22 was cloned using the primers FP_5g24090d(2-22)gat and RP_5g24090-STOPgat (Table 8-1). In a second PCR the recombination sites of the inserts were completed using the Gateway adaptor primers (Invitrogen, see Table 8-1). The resulting inserts were first introduced into an entry vector pDONR201 and then finally into the binary expression vector pK7WGF2.0 (Karimi et al., 2005) as described in 2.4.4. The *p35S::CHIA-GFP* construct was stably transformed in WT *A.thaliana* plants (see 2.4.10) and offspring was screened for phosphinothricin (Basta) resistance.

2.4.15 Generation of *pCHIA::GUS* lines

For the *pCHIA::GUS* reporter construct, a 1948 bp fragment of the *CHIA* promoter sequence was cloned using the primers At5g24090_gatF and At5g24090_gatR (Table 8-1). In a second PCR the recombination sites of the inserts were completed using the Gateway adaptor primers (Invitrogen). The resulting insert was first introduced into an entry vector pDONR207 and then finally inserted into the binary expression vector pBGWFS7 (Karimi et al., 2005) by using the GatewayTM Technology (Invitrogen).

2.4.16 Generation of constructs for expression in *E.coli*

A 909 bp fragment of the coding sequence of *CHIA* gene was cloned using the primers At5g24090gatF and At5g24090gatR-STOP (Table 8-1). After completion of the recombination sites the resulting fragment was first introduced into an entry vector and afterwards into the *E. coli* expression vector pDEST17 (Invitrogen) using the Gateway™ Technology.

2.4.17 Generation of constructs for expression in *P.pastoris*

For the expression of the CHIA protein in the *Pichia* system both untagged and His₆-tagged versions were generated. The primers 5g24090EcoRIF and 5g24090NotI_mstopR were used to create a construct with the CHIA insert without the stop codon in pPICZαC (untagged), whereas the primers 5g24090EcoRIF and 5g24090NotI_ostopR enabled the generation of a CHIA construct with a C-terminal His₆-tag in pPICZαC. To generate an untagged version of CHIA in the pPIC9K vector the primers FP_EcoRI_pPIC9K and RP_20bp_tag_stop_NotI were taken. Each pair of used cloning primers (listed in Table 8-1) introduced the restriction sites EcoRI and NotI into the inserts, which then allowed the site-directed insertion of the inserts into the expression vectors pPICZαC and pPIC9K (both from Invitrogen).

2.4.18 Generation of constructs for the yeast two-hybrid system

The entry clone for *CHIA*ΔSP (lacking the sequence for signal peptide; see 2.4.14) was used for the generation of the Y2H-constructs. The insert was introduced into bait and prey vectors pBGKT7-GW and pGADT7-GW, respectively. The addition of the Gateway recombination cassette into the original vectors pBGKT7 and pGADT7 (Clontech Laboratories) enabled the usage of the Gateway™ Technology (Invitrogen) (the modified vectors were a kind gift from Sandra Postel).

2.4.19 Genotyping analysis of T-DNA insertion lines

The T-DNA lines used in the frame of this work were analyzed for their genotype. Since diploid plants contain two copies of each gene and are thus able to segregate it was necessary to confirm that the T-DNA insertion lines used for the experiments were homozygous. The discrimination between WT, heterozygous insertion and homozygous insertion lines was achieved by two sets of PCR reactions (see Figure 2-2). In the WT-PCR, primers were used, which bind a region flanking the T-DNA insertion (product amplified only in the WT plants, the large size of the T-DNA insertion inhibits the amplification in mutants).

In the second PCR a T-DNA specific left border primer (Lba primer) is used in a combination with a gene-specific primer allowing an amplification product only in plants carrying a T-DNA insertion. Thus, homozygous plants should show a product only in the Lba-PCR.

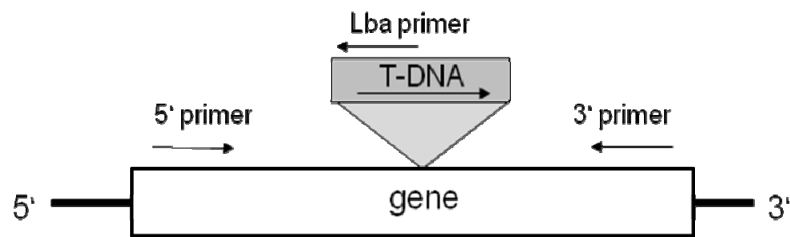


Figure 2-2: Genotyping analysis of T-DNA lines by gene- and insertion-specific primer

In the WT-PCR gene-specific primers (5' and 3' primer) amplify a product in WT plants, whereas in homozygous T-DNA insertion lines the large size of the T-DNA blocks the amplification. In the Lba-PCR reaction the usage of a gene-specific and a T-DNA-specific primer allows product amplification only in the T-DNA insertion lines. In heterozygous plants both PCR reactions produce an amplicon.

2.5 Biochemical methods

2.5.1 Protein expression in *E. coli*

BL21AI cells were used for expression of recombinant proteins. An overnight culture was used to inoculate a day culture with the density of 0.05 (OD_{600nm}), which was grown at 37°C up to an OD_{600nm} of 0.4-0.6. Then the culture was split in two; in the one culture flask the expression of the protein was induced by the addition of 0.01 % (w/v) L-arabinose and the other culture was left uninduced. Both cultures were further incubated at 18°C and harvested at different time points. The bacterial cells were pelleted at 2000 x g for 5 minutes and frozen in liquid N₂. The samples were afterwards treated with lysis buffer (500 mM potassium phosphate buffer, pH 7.8, 400 mM NaCl, 100 mM KCl, 10 % (v/v) glycerol, 0.5 % (v/v) Triton X-100, 10 mM Imidazole and freshly added 100 µg/ml lysozyme) and incubated for 30 minutes at 4°C on a stirrer. After 3 freeze-thaw cycles the samples were sonicated for 2 x 10 seconds (70% intensity, Bandelin UW 2070 sonicator) on ice. In a centrifugation step the insoluble proteins and cell fragments were pelleted and the soluble proteins were further characterized by SDS-PAGE (2.5.7) following Coomassie blue stain (2.5.9) or immunoblot (2.5.8).

2.5.2 Ni²⁺-NTA affinity purification

Ni²⁺-NTA agarose from Qiagen was used for the affinity purification of His₆-tagged *E.coli* proteins. Therefore, 1.5 ml column material was first washed 5 times with one column volume of water and then 5 times with lysis buffer (50 mM KH₂PO₄, 300 mM KCl, 10 mM imidazole, pH 8), elution buffer (50 mM KH₂PO₄, 300 mM KCl, 250 mM imidazole, pH 8) and washing buffer (50 mM KH₂PO₄, 300 mM KCl, 20 mM imidazole, pH 8) each. Then the crude supernatant (see 2.5.1) derived from a 500 ml bacterial culture was loaded on the column, the flow-through was collected and the column was washed two times with 6 ml washing buffer. Afterwards the His₆-tagged protein was eluted from the column with 750µl elution buffer in 6 elution steps. The protein content in the elution fractions was then analyzed by SDS-PAGE followed by Coomassie blue stain or immunoblotting.

2.5.3 Protein expression in *P.pastoris*

For protein expression in *Pichia pastoris* a clone carrying the desired construct was cultivated in BMGY medium while shaking at 30°C until the OD_{600nm} reached 2-6. Then the cells were pelleted for 5 minutes at 1500 x g, resuspended in BMMY to a density of 1 (OD_{600nm}) and further grown in the induction medium. Every 24 hours 0.5 % (v/v) MeOH was added to maintain induction conditions. After different time points 1 ml of culture was harvested, the cell pellet was concentrated using the sodium deoxycholate-trichloroacetic acid (DOC-TCA) precipitation method (Bensadoun and Weinstein, 1976) and then analysed for the presence of expressed protein.

2.5.4 Protein extraction from plant tissue

Total protein was extracted from plant tissue using either a protein extraction buffer specific for acidic chitinases (20mM sodium acetate, pH5.2/15mM β-mercaptoethanol supplemented with 1 proteinase inhibitor cocktail tablet/10ml from Roche) or an extraction buffer containing detergents for solubilization of membrane-bound proteins (50 mM Tris-HCl, pH 7.5, 150 mM NaCl, 1 % (v/v) Nonidet P40 and 1 protease inhibitor cocktail tablet/10 ml from Roche). The plant tissue was first homogenized in liquid N₂ and after addition of the extraction buffer the sample was incubated for 30 minutes at 4°C. Afterwards the soluble proteins were separated from the insoluble ones in a centrifugation step (15 minutes 20800 x g at 4°C) and used for further analysis.

For the extraction of protein from the protoplast samples the protoplast pellet was first separated from the medium by centrifugation (20sec 800rpm 4°C). The secreted protein in the medium was concentrated using Vivaspin 2 columns with a 10kD cut-off (GE

Healthcare). Protein from the harvested protoplast pellet was extracted using 20mM sodium acetate, pH5.2/15mM β -mercaptoethanol supplemented with 1x proteinase inhibitor cocktail (Roche).

2.5.5 Immunoprecipitation

Leaf protein was extracted from the *CHIA* overexpression plants (see 2.5.4) and approximately 200 μ g total protein was used for the immunoprecipitation of CHIA-GFP and therefore incubated for 90 minutes at 4°C with gentle rotation either with 15 μ l α -YFP rabbit or α -GFP goat antibody (Acris). In control protein samples no antibody was added. Meanwhile 400 μ l agarose A bead solution (Roche) was washed three times with 800 μ l water (1 min 2000 rpm 4°C), once with 800 μ l buffer A (50 mM Tris-HCl, pH 7.5, 5 mM EDTA, pH 8, 5 mM EGTA, pH 8, 2 mM DTT, 10 mM AEBSF, 2 μ g/ml Aprotinin, 2 μ g/ml Antipain). Finally, the agarose A beads were resuspended in buffer A (600 μ l) and 50 μ l bead solution was incubated with the protein/antibody mixture for further 30 minutes in a rotator at 4°C. Afterwards, the beads were washed two times with 500 μ l buffer A (1 min 1500 x g 4°C) and once with 500 μ l buffer A containing 1 M NaCl. The immunoprecipitated proteins were then further analysed by immunoblot or activity assay.

2.5.6 Determination of protein concentration

The protein concentration was measured using the Bradford method (Bradford, 1976) and Roti-Quant solution (Carl Roth). Standard curve was calculated using bovine serum albumin (BSA).

2.5.7 SDS-PAGE

SDS polyacrylamide gel electrophoresis was performed as described in Sambrook et. al (2001) using the gel chamber system of BioRad. 12 % SDS-PA gels were used as separating gels (with 5 % stacking gels) for the discontinuous SDS-PAGE by the method of Laemmli (1970) if not mentioned otherwise. The Prestained Protein Ladder Mix (Fermentas) was used as a protein marker.

2.5.8 Western blot analysis

For the western blot analysis the proteins were transferred after SDS-PAGE onto a Hybond nitrocellulose membrane (GE Healthcare) using a Mini Trans-Blot® Electrophoretic Transfer

Cell (BioRad) for one hour at 100 V. The protein transfer was controlled by Ponceau S red stain (0.1 % (w/v) Ponceau S red and 5 % (v/v) acetic acid). Unspecific binding sites were blocked by incubation of the membrane for 1 hour at RT with 5 % (w/v) milk in either 1 x TBST (150 mM NaCl, 20 mM Tris-HCl; pH 7.6 and 0.1 % (v/v) Tween 20) or 1 x PBST (140 mM NaCl, 2.7 mM KCl, 10 mM Na₂HPO₄, 1.8 mM KH₂PO₄, 0.1 % (v/v) Tween 20). Afterwards the membrane was incubated with a primary antibody overnight at 4°C. Then the membrane was washed for 3 x 5 minutes with 1 x TBST or 1 x PBST and incubated for 1.5 hours with a secondary antibody. The signal of a peroxidase-coupled secondary antibody was detected using the Enhanced Chemiluminescence Kit (GE Healthcare) according to the manufacturers' instructions. For the detection of an alkaline phosphatase-coupled secondary antibody the membrane was washed with 1 x TBST for 3 x 5 minutes and then equilibrated for 2 minutes with a Tris 9.5-buffer (150 mM Tris-HCl; pH 9.5, 5 mM MgCl₂ and 100 mM NaCl). The staining reaction was performed with 1 x BCIP/NBT in Tris 9.5-buffer (5-bromo-4-chloro-3-indolylphosphate; 200 x stock solution 50mg/ml in 70 % (v/v) dimethylformamide; Nitro-blue tetrazolium chloride; 200 x stock solution 50mg/ml in 100 % (v/v) dimethylformamide). After the staining the membrane was washed with water.

2.5.9 Coomassie blue stain

For non-specific staining of proteins after SDS-PAGE a Coomassie blue R-250 stain (0.125 % (w/v) Coomassie blue R-250, 50 % (v/v) MeOH, 10 % (v/v) acetic acid) was used. After incubation for 30 minutes at RT the superfluous stain was removed by 10 % (v/v) acetic acid.

2.5.10 Silver stain

Silver staining was used to control the purity of peptidoglycan preparations (higher sensitivity in comparison to a Coomassie blue stain). 100 µg PGN was loaded on a 15 % SDS-PA-gel and the proteinous impurities were separated by SDS-PAGE. Then the gel was incubated for at least one hour in a fixing solution (50 % (v/v) MeOH, 12 % (v/v) acetic acid and 0.0185 % (v/v) formaldehyde), washed with 50 % (v/v) EtOH for 3 x 20 minutes and treated with fresh 0.02 % (w/v) Na₂S₂O₃ solution for one minute. Subsequently, the gel was washed with water (3 x 20 seconds), incubated for one hour with an impregnation solution (0.2 % (w/v) AgNO₃ and 0.028 % (v/v) formaldehyde) and then repeatedly washed with water. In a final step the gel was treated for 10-15 minutes with a developer solution containing 6 % (w/v) Na₂CO₃, 0.0185 % (v/v) formaldehyde and 0.4 % (w/v) Na₂S₂O₃. The staining of the proteins was stopped with washing the gel with water for 2 x 2 min and then treating it with 50 % (v/v) MeOH and 12 % (v/v) acetic acid for 10 minutes.

2.5.11 Turbidity assay (PGN-hydrolysis assay)

The turbidity assay was performed as described in Park et al. (2002). Shortly, lytic activity towards *Micrococcus luteus* cell wall or *Bacillus subtilis* peptidoglycan (Sigma, Invivogen) was measured and compared to that of 1 µg hen egg-white lysozyme (HEWL, Sigma). 1ml 0.02% (w/v) *M. luteus* cells or PGN in 20 mM sodium acetate, pH 5.2 were incubated at 37°C together with the enzyme and the decrease in absorbance at 570nm of the suspension was measured with a spectrophotometer over time. Approximately 60µg total protein of the leaf extract (2.5.4) and 15µg total protein of the protoplast samples (2.4.9) were added to the reaction solutions.

2.5.12 4-MUCT assay (Chitin-hydrolysis assay)

The 4-MUCT assay was performed as described in Brunner et al. (Brunner et al., 1998). Shortly, the hydrolytic activity towards the substrate 4-methylumbelliferyl-β-D-N, N', N'' triacetylchitotriose (4-MUCT, Sigma) was measured and compared to that of 2 µg *Streptomyces griseus* chitinase (Sigma). After enzyme incubation in 250µl final volume of 0.05% (w/v) 4-MUCT in 20mM sodium acetate, pH5.2 at 37°C, 20µl of the reaction mixture were removed and added to 980µl 0.2M sodium carbonate solution. Free 4-MU (Sigma) was used for the generation of a standard curve. The intensity of the 4-MU fluorescence in the samples was monitored with an MWGt Sirius HT fluorescence microplate reader (absorbance at 360 nm and emission at 450 nm). Same protein amounts were used as for the turbidity assay (see 2.5.11).

2.5.13 Colloidal chitin hydrolysis assay

The chitinase activity (chitodextrinase, EC 3.2.1.14) was measured using a method published by Reissig et al. (1955). 500 µl suspension of colloidal chitin (10 mg/ml chitin in 100 mM Sodium acetate, pH 5.2) was incubated with approximately 60 µg total leaf protein (see 2.5.4) and incubated for 2 hours at 37°C. After centrifugation (20 min 10600 x g 4°C) the supernatant containing soluble hydrolyzed chitin fragments was collected and further incubated with a cytohellicase for 20 minutes at 37°C to further digest the chitin fragments into monomeric N-acetylglucosamines. Then 100 µl 0.6 M potassium tetraborate was added to the sample and incubated for 3 minutes at 100°C. After cooling down to RT 1 ml DMAB solution was added (1% (w/v) p-dimethylaminobenzaldehyde, 1 % (v/v) 12 M HCl in 100 ml acetic acid). After an incubation of 60 minutes at 60°C the absorbance was measured at 585 nm. An N-acetylglucosamine (GlcNAc, from Sigma) standard curve was used for the calculation of the chitinase activity.

2.5.14 Yeast two-hybrid

Yeast two-hybrid experiments were performed using the Matchmaker System (Clontech). *CHIA* cDNA fragment lacking the signal peptide sequence (849 bp) was cloned into pGBKT7 or pGADT7 (Clontech). Plasmids were transformed into *S. cerevisiae* using a lithium acetate/single-stranded carrier DNA/polyethylene glycol method (Gietz and Woods, 2002). The cultivation of the yeast cells was performed as described previously (Bergman, 2001; Kaiser, 1994). After 4 to 5 d of growth on vector-selective medium (CSM-LT), 12 independent clones in pools of four clones each were propagated in liquid vector selective medium and subsequently diluted to the same optical density. Of the three pooled cultures, 7.5 µl of a serial dilution was dropped on vector- and interaction-selective medium (CSM-LTA) and incubated at 28°C. At day 3, the growth of the clones was monitored.

2.6 Bioassays

2.6.1 Infection with *Pseudomonas syringae*

For the bacterial infection assay each *Pseudomonas* strain was diluted with 10mM MgCl₂ to a density of 1×10^4 cfu/ml ($OD_{600} \sim 2 \times 10^{-5}$) and was then infiltrated with a 1ml-needleless syringe into the leaf apoplast. Two leaves per plant and 8 plants were infected per plant genotype. The growth of bacteria was determined after 0, 2 and 4 days post infection. For the quantification infected leaves were harvested (2 leaves at 0 dpi and 3 leaves at 2 or 4 dpi) and washed for one minute in both 70 % (v/v) EtOH and water. Afterwards 2 leaf discs/leaf with a diameter of 5 mm were cut out and homogenized in 200 µl 10 mM MgCl₂. 10 µl of each homogenate were then plated undiluted and in different dilutions onto LB agar plates and incubated at 28°C for 24-48 hours. The growth of bacteria was determined by colony counting, and subsequently mean values and standard deviations were determined.

2.6.2 Infection with *Alternaria brassicicola*

Alternaria brassicicola spores used for the infection assays were obtained as published previously (Thomma et al., 1999b). Leaves to be tested were drop-inoculated with six 5µl droplets of aqueous spore solution (5×10^5 - 1×10^6 spores/ml) if not mentioned otherwise. Two leaves per plant and a minimum of 8 plants per line were infected. To avoid positional effects plants of different lines were randomly distributed in the tray and incubated at 100% relative humidity. Fungal growth was scored after 7-14 days by symptom classification: 1 (no symptoms), 2 (light necrotic lesions), 3 (severe necrotic lesions), 4 (spreading of lesions beyond infection site), 5 (whole leaf affected) and 6 (sporulation of the fungus) and a disease index (Kemmerling et al., 2007) was calculated.

2.6.3 Infection with *Botrytis cinerea*

Cultivation of *Botrytis* and the preparation of spores was performed as described in Thomma et al. (1999a). *Botrytis cinerea* spores were diluted with PDB medium to a final density of 5×10^5 spores/ml. The leaf surface was drop-inoculated with two 5 μ l droplets of spore solution if not mentioned otherwise. Two leaves per plant and a minimum of 8 plants per line were used for infection. The development of symptoms was monitored 2-3 days post infection.

2.6.4 Elicitation assays in leaves or seedlings

Leaves of 4-6 week old plants were infiltrated using a needle-less syringe with solutions of PAMPs and harvested after indicated time points. For the seedlings elicitation seedlings were first cultivated on sterile $\frac{1}{2}$ MS plates for 5-6 days in long-day. Then they were transferred into liquid MS medium supplemented with 1 % (w/v) saccharose (4-6 seedlings in 200 μ l medium/well, 48er well plate) and equilibrated overnight. After addition of the PAMPs, the seedlings were incubated with gentle shaking and harvested at indicated time points. The PAMPs were used in elicitation assays in following concentrations: 1 μ M flg22 and 100 μ g/ml chitin, PGNs and muropeptides derived from PGN.

2.6.5 Microarray analysis

Microarray experiments were performed on *Arabidopsis thaliana* Col-0 plants and on the T-DNA insertion line *cerk1-2*. Leaves of adult plants were infiltrated with 100 μ g/ml Xcc PGN or water as a control and analyzed after 6 h. RNA was extracted as described in 2.4.6 and profiled using the NimbleGen DNA microarray (*A. thaliana* Gene Expression 12x135K Array TAIR 9.0) according to the manufacturer's protocol (Roche). Three independent experiments (biological replicates) were performed. Probe signal values were subjected to the quantile normalization (Bolstad et al., 2003) using all the arrays. Normalized probe signal values were subjected to the robust multi-array average (RMA) summarization algorithm (Irizarry et al., 2003) to obtain the expression level values of the genes. Results were analyzed by the following linear model using the lmFit function in the limma package in the R environment:

$\log_2(\text{expression level value}) \sim \text{genotype:treatment} + \text{replicate}$

The eBayes function in the limma package was used for variance shrinkage in calculation of the p -values and the Storey's q -values were calculated using the q-value function in the q-value package (Storey and Tibshirani, 2003) from the p -values.

2.6.6 pH assay

Medium alkalization in *At* cell culture upon PAMP treatment was performed as described previously (Gust et al., 2007). The changes in pH were monitored and recorded by the Observer II program (Brainchild Electronics Co., Ltd, Taipei, Taiwan).

2.7 Microscopy and Histochemistry

2.7.1 Confocal microscopy

The visualization of fluorescence in samples was done using confocal laser scanning microscopy (TCS SP2, Leica). The images were taken using the 63x/1,2 PlanApo H₂O objective. The Software LCS Lite Version 2.61 was used for the processing of the images. As membrane-selective dye, 2 nM FM4-64 (diluted in ddH₂O, Invitrogen), was infiltrated into the leaves shortly before the microscopical analysis. Concave plasmolysis was induced by infiltrating the leaves with 850 mM NaCl, 0.01 % (v/v) Silwet L-77 prior microscopy.

2.7.2 Aniline blue stain

The induction of callose deposits upon PAMP treatment was analyzed by aniline blue (water blue) staining (Gómez-Gómez et al., 1999). Leaves were infiltrated with the different PAMPs and incubated for 24 hours and subsequently incubated with a fixing solution (1% (v/v) glutaraldehyde; 5mM citric acid; 90mM Na₂HPO₄; pH7.4) again for 24 hours at RT. After fixation the leaf tissue was bleached with 100% (v/v) EtOH for 1-2 days. The leaves were then transferred to 50% (v/v) EtOH and afterwards equilibrated in 67 mM K₂HPO₄ (pH 12.0) and finally stained for 1 h at RT in 0.1% (w/v) aniline blue dissolved in 67 mM K₂HPO₄ (pH 12.0). The stained leaves were transferred to a microscopic slide in 70% (v/v) glycerol and 30% (v/v) staining solution and examined under UV epifluorescence.

2.7.3 Trypan blue stain

The trypan blue stain was used to visualize dead cells and fungal structures after infections with necrotrophic fungi. Infected leaves were treated with for 1 minute with trypan blue stain (10 ml lactic acid, 10 ml 100% glycerol, 10ml Aqua-Phenol, 10 ml ddH₂O, 80 ml EtOH and 300 mg Trypan blue) and afterwards bleached with a 1mg/ml chloral hydrate solution.

2.7.4 GUS stain

The transgenic plants bear a cassette containing the uidA (gusA) gene under the control of a promoter of interest (Jefferson et al., 1987). For the histochemical detection of the enzymatic activity of the reporter gene β -glucuronidase (GUS) leaves were vacuuminfiltrated with a staining solution containing 50mM sodium phosphate buffer pH7.0, 0.021% (w/v) $K_4Fe(CN)_6$, 0.016% (w/v) $K_3Fe(CN)_6$, 1mM EDTA pH8.0, 0.5% Triton X-100 (v/v) and 0.05% (w/v) 5-bromo-4-chloro-3-indolyl β -D-glucuronide (X-Gluc). The leaves were incubated overnight at 37°C and subsequently chlorophyll was removed by shaking in 100% EtOH. The stain was examined under the microscope.

2.8 Statistical analysis

Statistical analysis was performed using Microsoft Office Excel. The data represent the average of replicates with standard deviation (SD) or standard error (SE). The significance for the differences of a data pair was calculated using the t-test.

3 Results

The aim of this work was to gain more insights into the perception system of the bacterial PAMP peptidoglycan in the model plant *Arabidopsis thaliana*. In vertebrates and mammals the action of PGN as PAMP and the corresponding perception systems have been extensively analysed (Dziarski and Gupta, 2005a; Dziarski and Gupta, 2006; Girardin and Philpott, 2004; Royet and Dziarski, 2007), whereas *in planta* peptidoglycan was only lately described as a novel elicitor of the innate immunity (Erbs et al., 2008; Gust et al., 2007).

3.1 Isolation and analysis of PGN from *P.syringae* and other bacteria

In previous studies peptidoglycan from the Gram-positive bacteria *Staphylococcus aureus*, as well as the Gram-negative bacteria *Escherichia coli* were shown to induce typical plant defense reactions, such as induction of defense-related gene expression, medium alkalization and accumulation of phytoalexins (Gust et al., 2007). Gram-positive bacteria are underrepresented among the plant-pathogenic bacteria, however it has been reported that *Streptomyces* spp. and also *S.aureus* are able to infect plants, including *Arabidopsis thaliana* (Joshi et al., 2007; Prithiviraj et al., 2005). The Gram-negative bacteria attacking plants include *Xanthomonas* spp., *Ralstonia solanacearum*, *Erwinia* spp. and the model plant pathogenic bacterium *Pseudomonas syringae* pv. *tomato* DC3000 (*Pto* DC3000) (Boch and Bonas, 2001). Since *Pto* DC3000 is routinely used in bacterial infection assays for monitoring effects of *Arabidopsis* mutants lines in bacterial resistance, it was logical to analyse the properties of its peptidoglycan as elicitor of the plant innate immunity. Therefore, a protocol for the isolation of highly purified PGN from Gram-negative bacteria was established and preparations of *Pseudomonas syringae* PGN (*Pto* PGN) along with other PGNs were tested in different bioassays. First, the purity of *Staphylococcus aureus* PGN (*Sa* PGN), *Pto* PGN, *Bacillus subtilis* PGN (*Bs* PGN), *Xanthomonas campestris* pv. *campestris* PGN (*Xcc* PGN) and muropeptides derived of *Xcc* PGN (Erbs et al., 2008) was analysed for protein contaminations using the sensitive silver staining method (Figure 3-1A). In all preparations no high molecular weight impurities could be observed. To monitor the immunogenic properties of the different PGNs in *Arabidopsis* plants, Col-0 seedlings were treated with 100 µg/ml PGN and the transcript accumulation of the immune marker gene *Flagellin-induced receptor kinase 1* (*FRK1*) was measured 6 hours post elicitation using quantitative RT-PCR (RT-qPCR, Figure 3-1B). *FRK1* is transcriptionally up-regulated relatively early upon treatment with several MAMPs, such as flg22, HrpZ (Harpin) and NPP1 (necrosis-inducing

Phytophthora protein 1) (Boudsocq et al., 2010; He et al., 2006). Treatment of seedlings with the tested peptidoglycans led to a four to 10-fold higher *FRK1* gene expression in comparison to water treatment. In addition to *FRK1* expression, the expression of the defense-related gene *pathogenesis related 1 (PR1)* was also analysed in adult leaves upon PGN treatment using a transgenic *pPR1::GUS* reporter line (Shapiro and Zhang, 2001). All tested PGNs and also the *Xcc* muropeptide induced the *PR1* promoter (Figure 3-1C). Water and flg22 treatments were used as negative and positive control, respectively. *Pto* PGN also triggers other early plant immune responses, as was observed in the medium alkalization assay with plant cell cultures (Figure 3-1D). In comparison to the rapid and transient flg22-induced pH shift, the PGN reaction is slower but still clearly measurable, as reported earlier (Gust et al., 2007). The deposition of the polysaccharide callose (β -1,3-glucan) between the plasma membrane and the plant cell wall as a rather late cellular response is triggered upon different abiotic or biotic stresses, such as wounding and microbial attack (Stone and Clarke, 1992), but also upon treatment with PAMPs (Gómez-Gómez et al., 1999). Upon infiltration of adult leaves with *Pto* PGN, *Xcc* PGN and *Xcc* muropeptides a weak but visible callose accumulation was observed (Figure 3-1E). As expected, the positive control flg22 induced a strong deposition of callose, whereas water treatment led to no callose accumulation.

The immunogenic properties of all tested Lys- and Dap-type peptidoglycans were generic suggesting that either there are several PGN recognition machineries present in *Arabidopsis* or that there is no discrimination between the different peptidoglycan types. The modification of the peptidoglycan either within the sugar backbone (acetylation) or peptide moiety (amino acid change) can change the immunogenic properties as reported by Erbs et al. (2008), but this did not seem to be the case for the examined PGNs. All in all, the PGN-mediated immune responses showed weaker levels when compared to the peptide PAMP flagellin, what might result from the polymeric structure of peptidoglycan and hence poor or delayed accessibility to the plant receptors at the plasma membrane.

Efforts of isolating peptidoglycan from the model phytopathogen *Pseudomonas syringae* pv. *tomato* DC3000 were profitable. The purified Dap-type *Pto* PGN was able to trigger both early and late defense responses (Figure 3-1). In addition, the usage of the highly pure *Pto* PGN in elicitation assays contributed to the identification of AtLYM3, a membrane-tethered LysM protein, as a putative PGN receptor protein (Willmann, 2011). Thus, the collection of plant immunity stimulating peptidoglycans is increased by the Dap-type PGN from *P. syringae*.

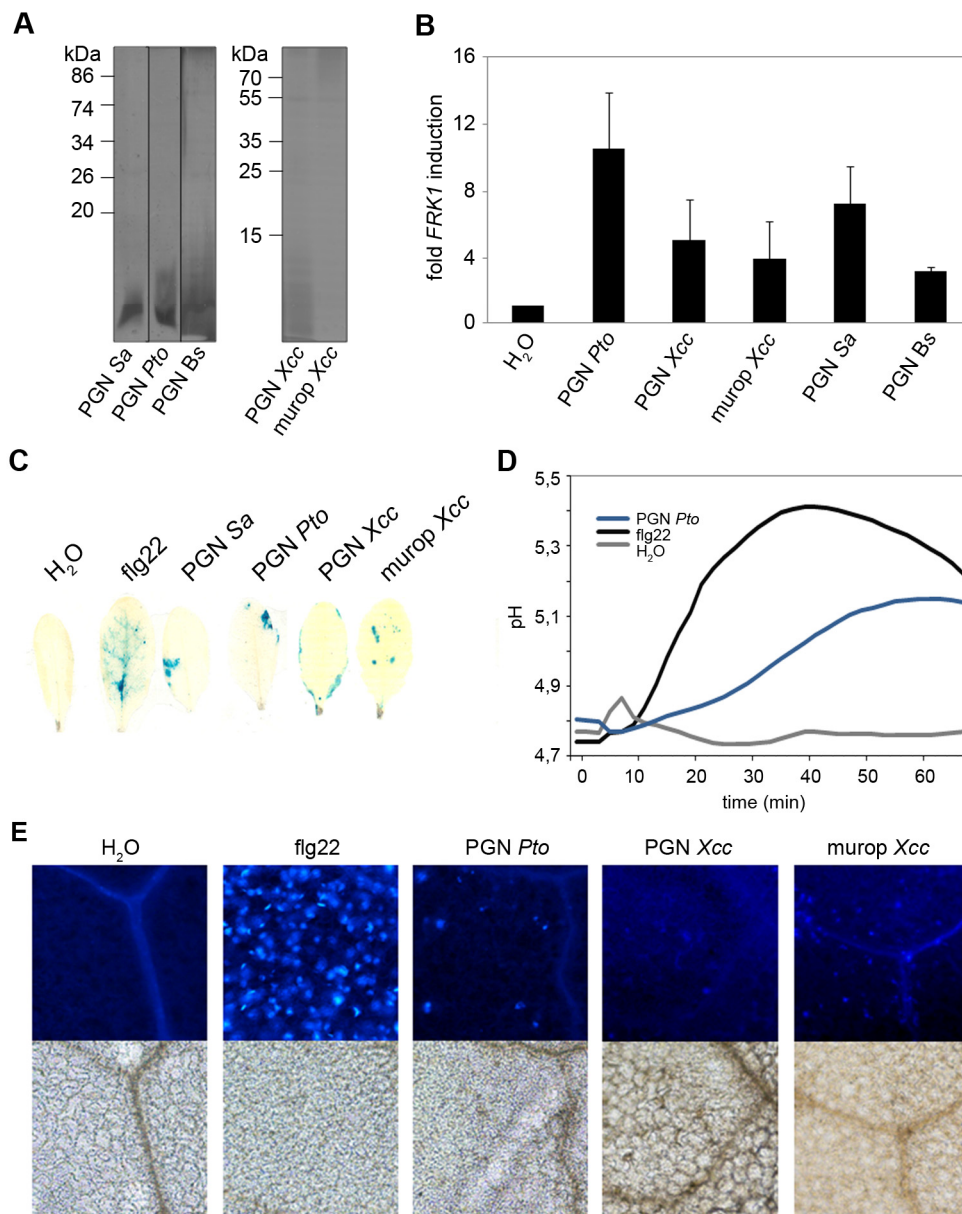


Figure 3-1: Peptidoglycan induces defense responses in *Arabidopsis thaliana*

(A) The purity of peptidoglycan and muropptides was analysed by silver staining. 100 μ g of different PGNs or muropptides (*Staphylococcus aureus*, Sa; *Pseudomonas syringae* pv. *tomato* DC3000, Pto; *Bacillus subtilis*, Bs; *Xanthomonas campestris* pv. *campestris*, Xcc; muropptides from *Xanthomonas campestris* pv. *campestris* PGN, murop Xcc;) were separated by SDS-PAGE and the proteinous contaminations in the samples monitored by silver staining. (B) PGN-induced *FRK1* gene expression in Col-0. Seedlings were treated with water or 100 μ g/ml PGN and subjected to RT-qPCR 6 hours post treatment. *EF1 α* transcripts served for normalization, corresponding water controls were set to 1. Data represent means \pm SD of three independent experiments with 4-6 seedlings/sample. (C) Induction of the reporter gene *PR1* upon PGN treatment. Adult leaves of transgenic *pPR1::GUS* plants were infiltrated with water, 100 μ g/ml PGN or 1 μ M flg22. Leaves were harvested 24 hours post treatment and stained for GUS activity. (D) Medium alkalinisation in Col-0 cell culture upon treatment with water, 100 μ g/ml PGN Pto or 1 μ M flg22. (E) Accumulation of callose deposition upon PGN treatment. Adult Col-0 leaves were infiltrated with water, 100 μ g/ml PGN or 1 μ M flg22 and stained with aniline blue 24 hours post treatment. Under UV light the callose deposits appear as light blue dots (upper panel). Lower panels show a light image of the leaf tissue.

3.2 Identification of putative PGN receptor(s) among the LysM-RLKs

Specific LysM domain proteins have been characterised in the binding and recognition of carbohydrate molecules structurally similar to peptidoglycan. In rice and *Arabidopsis*, the fungal carbohydrate elicitor molecule chitin is perceived by the receptor proteins OsCEBiP, OsCERK1 and AtCERK1, respectively (Kaku et al., 2006; Miya et al., 2007; Wan et al., 2008). Furthermore, LysM receptor proteins in the legumes *Medicago truncatula* and *Lotus japonicus* recognize bacterial lipochitooligosaccharides thereby establishing plant root symbioses with soil-borne rhizobacteria (Limpens et al., 2003; Radutoiu et al., 2003). In *Arabidopsis thaliana*, there are five genes encoding LysM receptor-like kinases (LYKs, Figure 3-2A). Due to the similarity between the LysM receptor proteins in the different plant species and the structural similarity between peptidoglycan, chitin and lipochitooligosaccharide, a targeted reverse-genetics approach was chosen to analyse the members of the *Arabidopsis* LysM receptor kinase family more in detail regarding peptidoglycan recognition and bacterial resistance. The predicted protein domain structures of the five LYKs harbour a signal peptide for secretion (SP), a transmembrane domain (TM), a serine/threonine protein kinase domain (PK) and one or several lysin motifs, with the exception of LYK2 (Figure 3-2B). The analysis of the absolute expression of the *LYK2* gene in Col-0 leaf tissue revealed extremely low values in comparison to the other members of the *LYK* family (data not shown, ATGenExpress Initiative). *LYK2* displayed relatively high expression levels in the 1st node and the pedicel of the flower, whereas *CERK1* (*LYK1*), *LYK3*, *LYK4* and *LYK5* were strongly expressed in leaves, suggesting that the four other *LYK* members possibly play a more important role within innate immunity to leaf pathogens such as *Pto*. Changes in the expression profiles of single genes upon different stimuli can give indications for an involvement of the gene products in corresponding signaling pathways or cellular mechanisms. Therefore, the ATGenExpress microarray data for *CERK1*, *LYK3*, *LYK4* and *LYK5* was analysed upon infection with different strains of *Pseudomonas syringae* (Figure 3-2C). *CERK1* expression was first slightly induced upon infection with the virulent *Pto* DC3000 (2h sample) but was already suppressed after 6 hours likely through effector-triggered suppression. After 24 hours *CERK1* expression showed control levels again. Infection with the type III secretion system-deficient strain *Pto* DC3000 hrcC⁻ or the non-host *Pseudomonas syringae* pv. *phaseolicola* (*Pph*) led to enhanced *CERK1* transcript levels at all investigated data points. In contrast, *LYK3* transcript levels were strongly suppressed upon infection with the three tested *Pseudomonas* strains and at all data points. The expression profile of *LYK4* resembled the one of *LYK3* upon infection with *Pto* DC3000 and *Pph*, and the one of *CERK1* upon *Pto* DC3000 hrcC⁻ infiltration. The expression of the *LYK5* gene showed a similar pattern than *CERK1* gene upon treatment with the three tested bacteria, however with a lower overall induction.

Alterations in the gene expression upon infection with bacterial pathogens suggest a role for the *Arabidopsis* LysM receptor kinases in the plant innate immunity. Hence, selected LYK family members were in the following characterised more in detail.

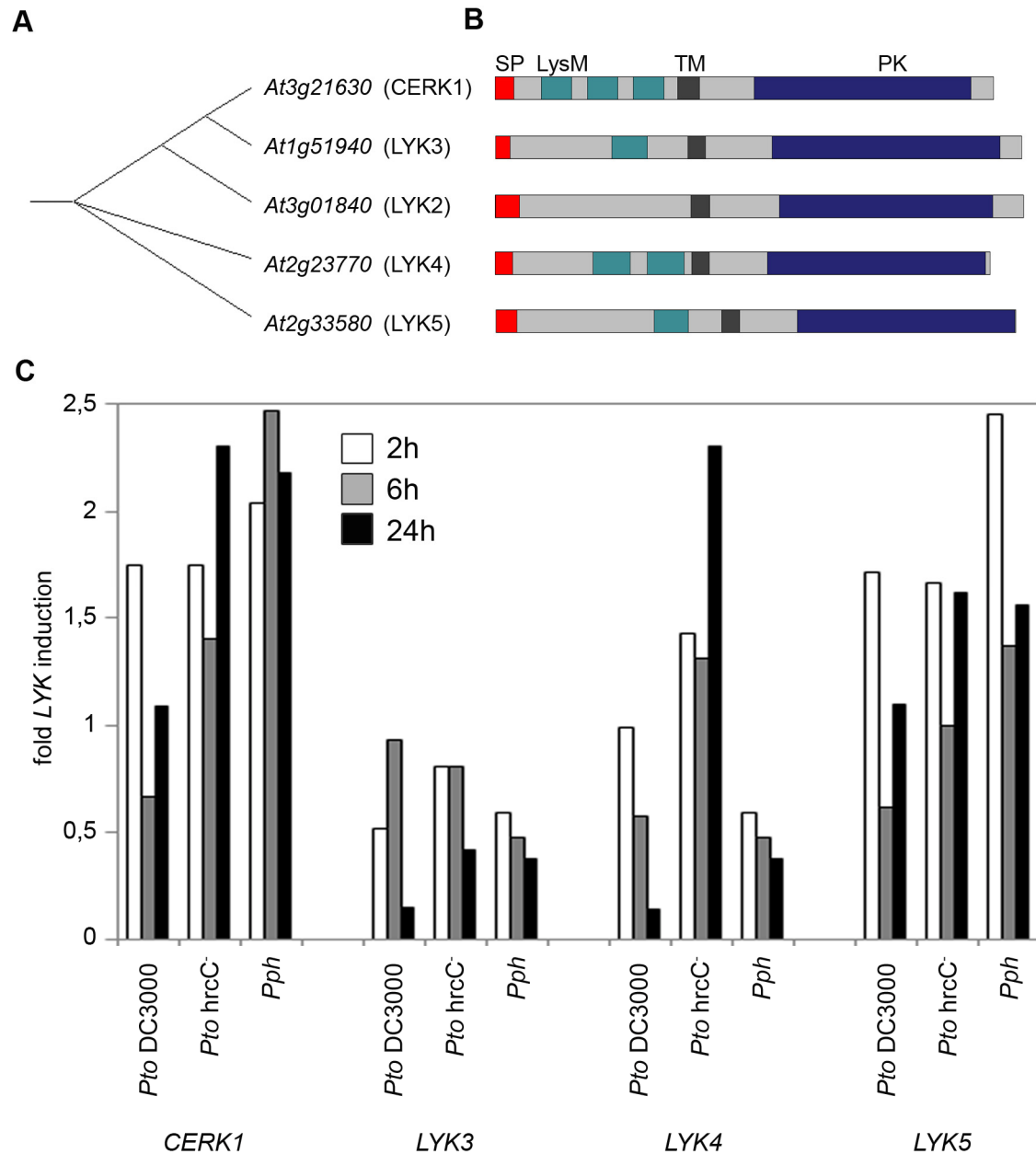


Figure 3-2: Arabidopsis LysM receptor-like kinase family

(A) A multiple sequence alignment of the full-length protein sequences of the five LysM-RLK (LYK) members using the ClustalW2 algorithm. **(B)** The predicted domain structures of the LYK proteins as annotated in the databases PFAM and SMART. Signal peptide, SP; LysM, Lysin motif; Transmembrane domain, TM; Protein kinase domain, PK. **(C)** Leaves of adult *Arabidopsis* Col-0 plants were infiltrated with the virulent *Pto* DC3000, the T3SS-deficient *Pto* DC3000 hrcC⁻ or the avirulent *Pseudomonas syringae* pv. *phaseolicola* (*Pph*) strain (10^8 cfu/ml) or 10 mM MgCl₂ as control. Leaves were harvested at indicated time points and total leaf RNA was used for microarray analysis. Data for *CERK1* (*At3g21630*), *LYK3* (*At1g51940*), *LYK4* (*At2g23770*) and *LYK5* (*At2g33580*) result from experiments performed within the ATGenExpress initiative (<http://www.arabidopsis.org/info/expression/ATGenExpress.jsp>). The gene transcription in the control treatment was set to 1.

3.2.1 Analysis of the *LYK* T-DNA insertion lines

For the functional analysis of the *LYKs* T-DNA insertion lines were obtained from Volker Lipka (Göttingen) and NASC (Nottingham Arabidopsis Seed Collection, UK). In the beginning of this work only one of the *LYK* members, *CERK1*, was characterised having a biological role as a chitin elicitor receptor kinase. The knock-out line for *CERK1*, *cerk1-2* was published by Miya et al. (2007). The exon-intron structure of the *CERK1* gene and the position of the T-DNA insertion in the 11th intron are depicted in Figure 3-3A. The homozygous genotype of the *cerk1-2* line and the absence of full-length *CERK1* transcript was confirmed by genotyping PCR and semi-quantitative RT-PCR, respectively (Figure 3-3A). Moreover, protein expression was absent in *cerk1-2* (Gimenez-Ibanez et al., 2009). For both *LYK3* and *LYK5* two independent T-DNA lines and double mutants (*lyk3-1 lyk5-1*; *lyk5-1 lyk3-1*) were available (Volker Lipka). The gene models and the T-DNA insertions for *LYK3* and *LYK5* are illustrated in Figure 3-3B and C. As for *CERK1*, also *LYK3* and *LYK5* T-DNA insertion lines were homozygous and showed no residual transcript as controlled by genotyping and transcript analysis (Figure 3-3B, C).

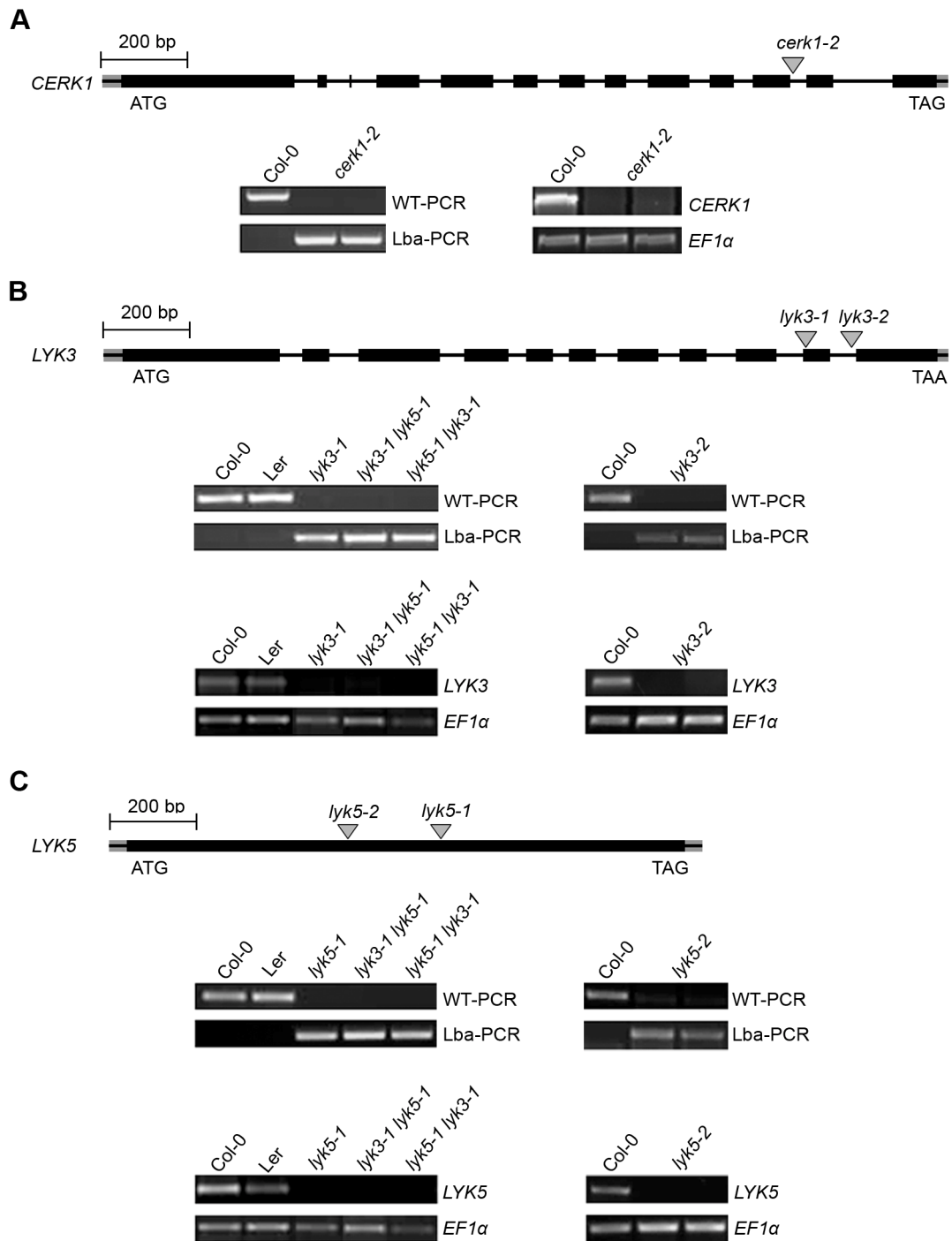


Figure 3-3: Characterisation of *CERK1*, *LYK3* and *LYK5* and their mutants

Gene models of *CERK1* (A), *LYK3* (B) and *LYK5* (C) including the positions of the T-DNA insertions. Exons and introns are indicated by black bars and black lines, respectively. 5'- and 3'-UTR regions are represented by grey bars and the T-DNA insertions by grey triangles. Leaf genomic DNA was isolated and genotyping PCRs were performed. Total RNA was isolated from leaves and transcribed into cDNA for transcript analysis using semi-quantitative RT-PCR. EF1a-s and EF1a-as primers were used to amplify the transcript of the house-keeping gene *EF1α*. (A) Genotyping of the *cerk1-2* mutant was done with the primers 580H03LP and 580H03RP (WT-PCR) and 580H03LP and Gabi-Kat-Lba (Lba-PCR). *CERK1* transcript was amplified with the primers 580H03LP and 580H03RP. (B) *Lyk3* mutants were genotyped with the primers 640374LP and 640374RP (WT-PCR) and 640374LP and SALK-Lba (Lba-PCR). *LYK3* transcript was amplified with primers 640374LP and 640374RP (*lyk3-1*) and N654015F2 and N660797R2 (*lyk3-2*). (C) *Lyk5* mutants were genotyped using the primers GT7089LP and GT7089RP2 (WT-PCR, *lyk5-1*), 631911LP and 631911RP (WT-PCR, *lyk5-2*), Ds3-1 + GT7089RP2 (Lba-PCR,

lyk5-1) and Salk-Lba and 631911RP (Lba-PCR, *lyk5-2*). *LYK5* transcript analysis was done with the primers GT7089LP and GT7089RP2.

T-DNA insertion lines for the *LYK2* and *LYK4* genes were also analysed with respect to homozygosity. The T-DNA insertion in the *lyk2-1* line is positioned in the first exon and the T-DNA insertion in the *lyk4-1* at position of 1615 bp (Figure 3-4). However, both lines turned out to be heterozygous as for some individual plants still WT-PCR product could be observed (Figure 3-4A, B). Candidate plants (*lyk2-1*, lane 3; *lyk4-1*, lanes 2 and 3) were chosen for production of seeds and the next generation has to be genotyped again to be subsequently used for further analyses.

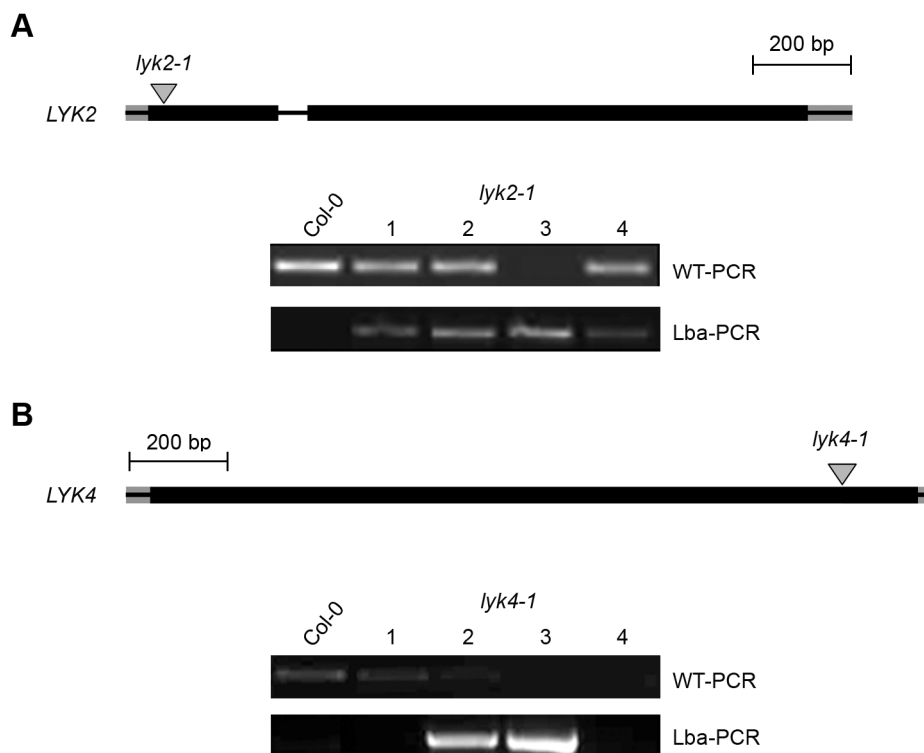


Figure 3-4: Characterisation of *LYK2* and *LYK4* and their mutants

Gene models of *LYK2* (A) and *LYK4* (B) including the positions of the T-DNA insertions. Exons and introns are indicated by black bars and black lines, respectively. 5'- and 3'-UTR regions are represented by grey bars and the T-DNA insertions by grey triangles. Genotyping analysis was performed as described in Figure 3-3. **(A)** Genotyping of the *lyk2-1* mutant was done with the primers 512441LP and 512441RP (WT-PCR) and Salk-Lba and 512441RP (Lba-PCR). **(B)** The *lyk4-1* mutant was genotyped with the primers 2g23770F2 and 2g23770R1 (WT-PCR) and 2g23770F2 and Gabi-Kat-Lba (Lba-PCR).

3.2.1.1 Phenotypic analysis of *lyk3* and *lyk5* single and double mutants

The T-DNA insertion mutant *cerk1-2* was published to have no visible phenotypic alteration from wild type (Col-0) plants (Gimenez-Ibanez et al., 2009). The phenotypes of the T-DNA insertion line *lyk5-1* and the double mutants *lyk3-1 lyk5-1* and *lyk5-1 lyk3-1*, however, differ from the phenotype of the corresponding ecotype. The *lyk5-1* (GT7089) mutant has the same

leaf morphology than the WT plant Ler, but shows an early flowering transition, whereas the *lyk3-1* (N654015) mutant resembles the Col-0 ecotype both in its morphology and flowering behavior (Figure 3-5B). Whether the observed developmental differences in the *lyk5* mutant line result from *LYK5* deletion or additional 2nd site insertions should be further investigated in future experiments. The double mutant lines *lyk3-1 lyk5-1* (LGK2-6-1-2, in Col-0) and *lyk5-1 lyk3-1* (LGK2-8-1-2, in Ler) display upward curled leaves, what might indicate defects in polarity and cell division (Liu et al., 2010). The production of seeds was unaltered in all T-DNA lines (data not shown). However, since changes in the reproduction process or leaf morphology should not negatively affect plant innate immunity, the lines were considered as suitable for further experiments. The *lyk2* and *lyk4* mutant lines were so far not included in the study.

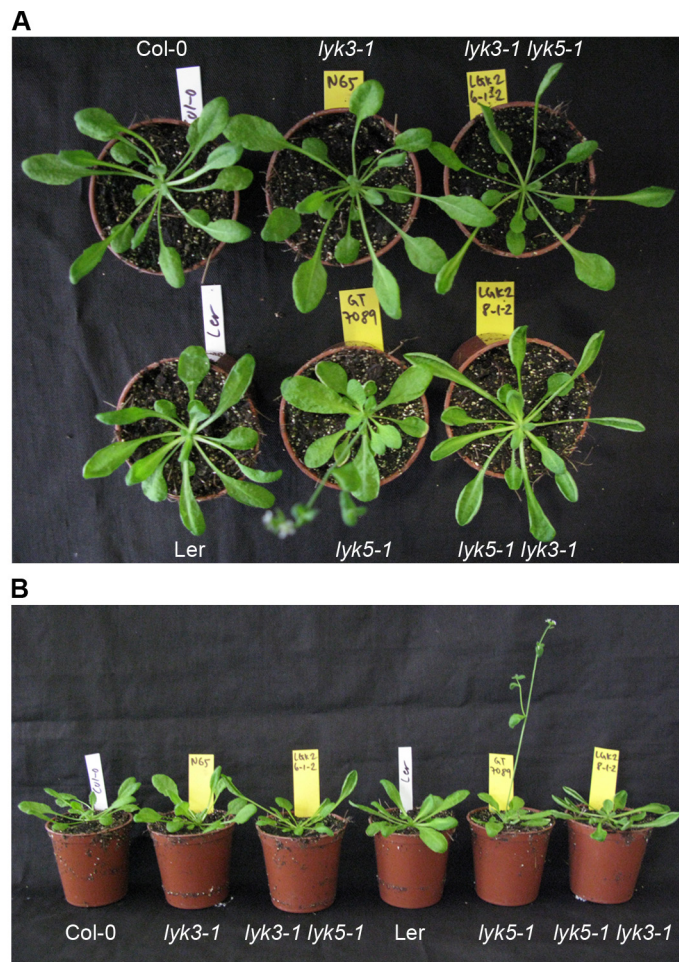


Figure 3-5: Phenotypes of *lyk3* and *lyk5* single and double mutants

Representative five week-old mutant plants of *lyk3-1* (N654015), *lyk5-1* (GT7089), *lyk3-1 lyk5-1* (LGK2-6-1-2, Col-0), *lyk5-1 lyk3-1* (LGK2-8-1-2, Ler) and the corresponding ecotypes (Col-0 and Ler) were photographed from the top (A) and the side (B) view.

3.2.2 Role of LYKs in fungal resistance

The importance of one of the LysM receptor-like kinases, CERK1, in the fungal resistance has been reported. Knock-out mutants displayed more fungal growth than WT plants upon infection with the biotrophic powdery mildew fungal pathogen *Erysiphe cichoracearum* (Wan et al., 2008) or larger lesions upon infection with the necrotrophic fungus *Alternaria brassicicola* (Miya et al., 2007). Microarray data upon infection with the necrotrophic fungal pathogen *Botrytis cinerea* (ATGenExpress initiative) suggest weak upregulation of the *CERK1* and *LYK5* gene expression, whereas the expression of *LYK3* is suppressed (Figure 3-6E). To gain additional information about the possible influence of the *CERK1*, *LYK3* and *LYK5* genes in resistance to fungal pathogens, the aggressive necrotrophic fungus, *Botrytis cinerea*, was employed.

Botrytis cinerea spore solution was droplet inoculated on the one half of the leaf and two leaves per plant were infected (2.6.3). The infection symptoms were monitored 2 and 3 days post infection. The infection site was already visible after two days showing necrotic tissue around the spore drop (data not shown) and after 3 days the necrotised leaf area was expanded (Figure 3-6A). All *lyk* mutant lines exhibited similar symptom development in comparison to WT plants. For disease analysis on a cellular level, dead plant cells and fungal hyphae were visualised using Trypan blue staining (2.7.3). Two days post infection all tested lines including Col-0 showed relatively loose fungal hyphae within the infection site, which was surrounded by an intensively stained ring, the cell death zone (Figure 3-6B). One day later (3 dpi) the cellular symptoms of the infection were more dramatic, i.e. the observed fungal hyphae were denser, however there were no differences between the lines (Figure 3-6C). Also the measurement of the lesion size three days post infection delivered no differential data, all tested *lyk* mutants behaved like the wild type (Figure 3-6D). Although the *cerk1-2* mutant showed a tendency of larger lesions and the *lyk3* and *lyk5* mutants of smaller lesions than the WT plants, these changes were not significant.

In summary, upon infection with *Botrytis cinerea* no significant mutant phenotype for the tested *LYK* genes was observed.

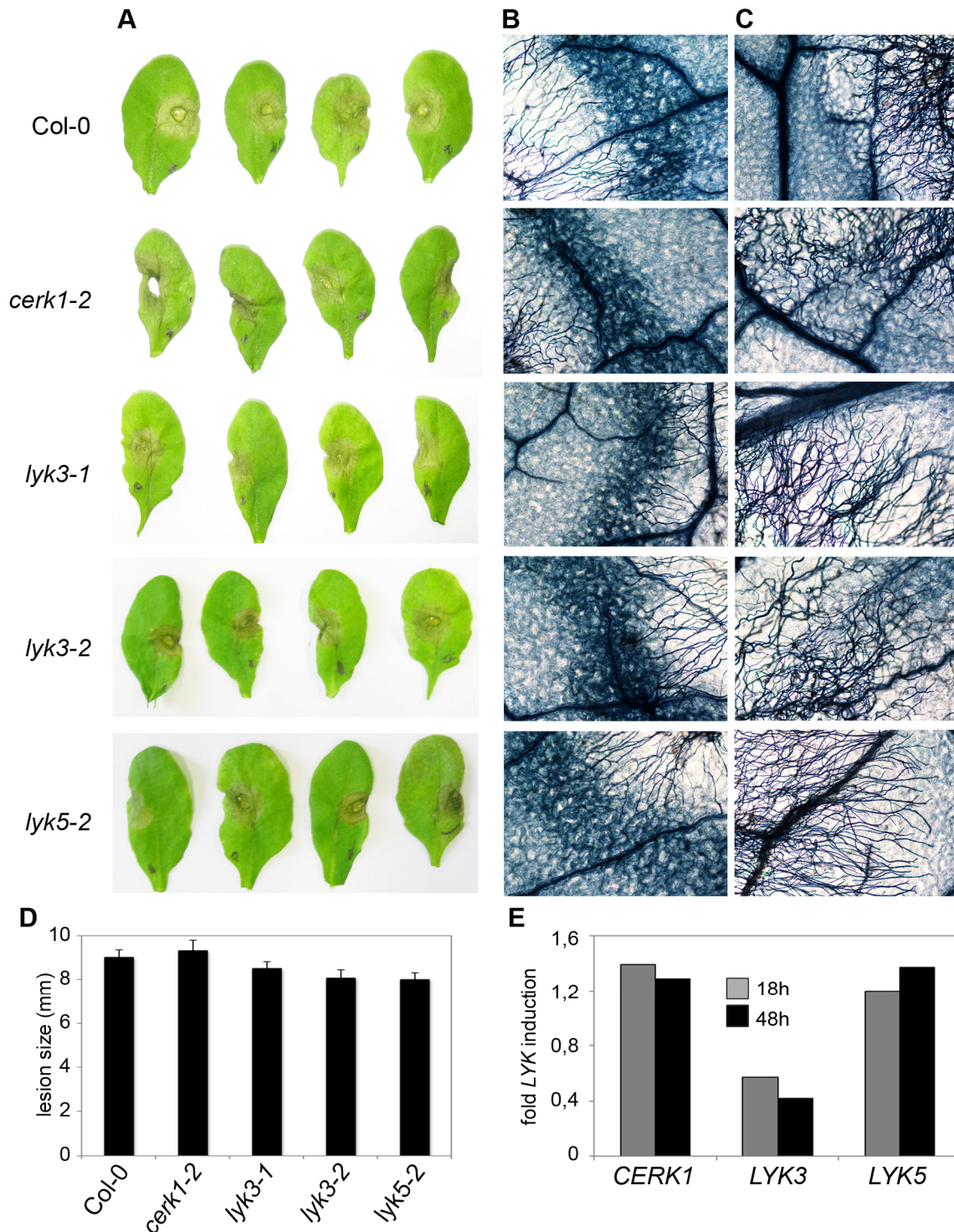


Figure 3-6: Infection of *lyk* mutants with *Botrytis cinerea*

Five week-old plants were infected with the necrotrophic fungus *Botrytis cinerea*. 5 μ l spore suspension of 5×10^5 spores/ml was drop-inoculated on the one half of the leaf, two leaves per plant were infected and analysed for symptom development after 2 or 3 days post infection. **(A)** Visible symptoms after 3 dpi. Microscopic analysis of the infection site and fungal hyphae visualised by Trypan blue stain 2 dpi **(B)** and 3 dpi **(C)**. **(D)** Measurement of the lesion size 3 days post infection. Shown are means and standard errors ($n=16$). **(E)** Leaves of adult *Arabidopsis* Col-0 plants were infected with *Botrytis cinerea* (10^5 spores/ml) or PDB medium as control. Leaves were harvested at indicated time points and total leaf RNA was used for microarray analysis. Data for *CERK1* (At3g21630), *LYK3* (At1g51940) and *LYK5* (At2g33580) genes result from experiments performed within the ATGenExpress initiative (<http://www.arabidopsis.org/info/expression/ATGenExpress.jsp>). The gene transcription in the control treatment was set to 1.

3.2.3 Influence of LYKs on bacterial resistance

Defects in the recognition process of pathogenic microbes can lead to enhanced virulence of the pathogens. For instance, *FLS2*-deficient plants, which no longer sense the bacterial PAMP flagellin, are more vulnerable to phytopathogenic bacteria (Zipfel et al., 2004). Also the deletion of the co-receptor of *FLS2*, *BAK1*, leads to enhanced disease symptoms upon bacterial infection in the mutant background (Kemmerling et al., 2007). In the following the homozygous T-DNA lines of the LYK family members were assayed for their bacterial resistance properties using different strains of the hemibiotrophic bacterium *Pseudomonas syringae*. Interestingly, a bacterial susceptibility phenotype of two independent *cerk1* mutant alleles reported recently implicated a role for *CERK1* in the perception of a bacteria-derived MAMP (Gimenez-Ibanez et al., 2009). Similar hypersusceptibility was observed for the tested *cerk1-2* mutant upon infection with the virulent *Pto* DC3000 4 days upon infiltration of the bacteria at a dose of 10^4 cfu/ml (Figure 3-7A, left diagram). Also the less-virulent mutant strain *Pto* DC000 Δ avrPto/PtoB and the type III secretion system (TTSS)-deficient mutant *Pto* DC3000 *hrcC*⁻ showed more growth in the mutant than in the WT plants as depicted in Figure 3-7A (middle and right diagram). Two independent *LYK3* knock-out mutants, *lyk3-1* and *lyk3-2*, were also subjected to infection assays with the same bacterial strains. Both mutant lines were more susceptible to *Pto* DC3000, whereas only *lyk3-1* allowed significantly more growth of the *Pto* DC3000 Δ avrPto/PtoB strain (Figure 3-7B, left and middle diagram). Despite of repetitive experiments, so far no significant differences in the growth of *Pto* DC3000 *hrcC*⁻ strain could be observed for the *lyk3* mutants in comparison to the WT (Figure 3-7B, right diagram). The two *lyk5* mutants, *lyk5-1* and *lyk5-2*, displayed no measurable changes to the corresponding WT upon infection with either *Pto* DC3000 or *Pto* DC3000 Δ avrPto/PtoB (Figure 3-7C). Infection with the *Pto* DC3000 *hrcC*⁻ strain was up to date only performed with the *lyk5-2* mutant, but it showed similar levels of bacterial growth than the WT as shown in Figure 3-7C (right diagram). Although single *lyk3-1* mutant did show a bacterial growth phenotype, the double mutants for the *LYK3* and *LYK5* genes behaved like WT plants upon infection with either virulent and or less-aggressive mutant strains (Figure 3-7D). However, crosses of two different ecotypes might be problematic and lead to such ambiguous results. Nevertheless, the bacterial infection experiments on the single mutants suggest that additionally to *CERK1* also *LYK3* as a member of the *LYK* family might have a role in resistance to bacterial pathogens.

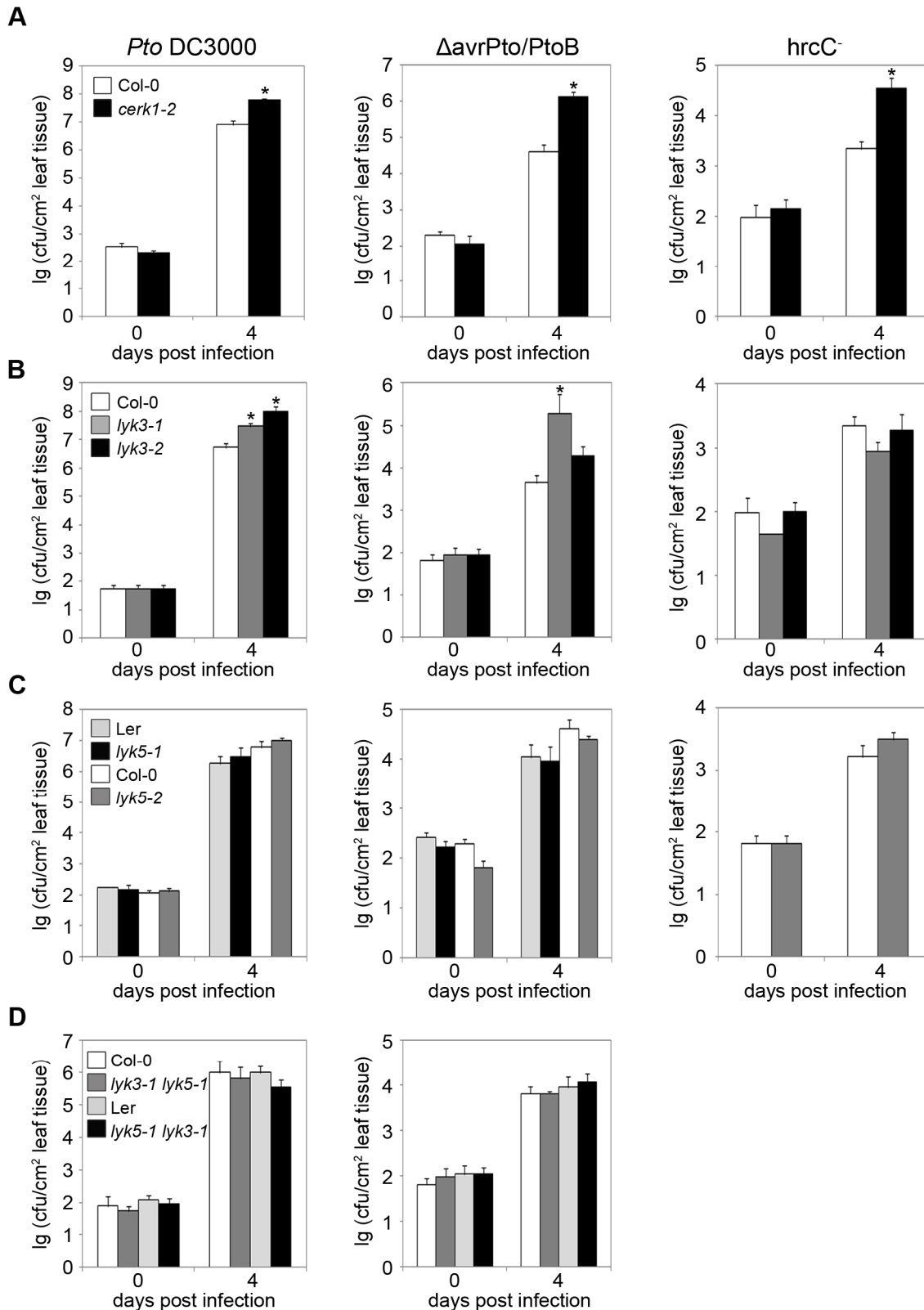


Figure 3-7: Infection of *lyk* mutants with *Pseudomonas syringae* strains

Bacterial infections of *Pto* DC3000 (left diagram), *Pto* DC3000 Δ avrPto/PtoB (middle diagram) and *Pto* DC3000 *hrcC*⁻ (right diagram) in the *cerk1-2* mutant (A), *lyk3* mutants (B), *lyk5* mutants (C) and *lyk3 lyk5* double mutants (D). Growth of bacteria was determined 4 days post infiltration with 10⁴ cfu/ml. Data represent means and standard errors (n=6/genotype/data point). Statistical significance compared to wild type ($p \leq 0.05$, Student's test) is indicated by asterisks. Shown are representative of at least 3 independent experiments.

3.2.4 Analysis of peptidoglycan responsiveness in *lyk* mutants

The structure of the PAMP chitin resembles the glycan backbone structure of peptidoglycan and CERK1 or the ectodomain of CERK1 containing all three LysM domains have been shown to bind to the ligand chitin *in vitro* (Iizasa et al., 2010; Petutschnig et al., 2010). In parallel, a LysM domain containing GPI-anchored protein, LYM3, was identified as a putative PGN-binding protein whereby the *lym3* mutant displays defects in PGN-triggered defense responses (Willmann, 2011). Since LYM3 lacks an intracellular signaling domain, a signaling partner might be found within the LYK family. The bacterial susceptibility phenotype observed for *cerk1* and *lyk3* mutants suggested that one or both of these receptor kinases might fulfill the missing part in the PGN recognition machinery. First, the responsiveness of the *cerk1-2* mutant to PGN was tested. Adult leaves were treated with 100 µg/ml *Xcc* PGN, 1 µM flg22 or 100 µg/ml chitin and subjected to RT-qPCR three hours post infiltration to monitor induction of the defense-related gene *FRK1* (Figure 3-8A). Similar transcript accumulation was observed upon flg22-treatment for Col-0, *cerk1-2* and the *lym3-1* mutant, which was included as a control. In PGN-treated leaves the transcript level of *FRK1* was reduced in the *lym3* and *cerk1* mutant backgrounds when compared to WT. As expected, the chitin-response was strongly reduced in the *cerk1-2* but not in the *lym3-1* mutant (Figure 3-8A). The PGN responsiveness of *cerk1-2* was also analysed in seedlings and here the *lyk3-1* mutant was also included into the assay. The *FRK1* transcript accumulation was monitored 6 hours post treatment with 100 µg/ml PGN *Pto* or chitin (Figure 3-8B). Whereas Col-0 and *lyk3-1* seedlings were sensitive towards PGN treatment, in *lym3-1* and *cerk1-2* mutant seedlings PGN failed to induce the expression of *FRK1*. The chitin-response was defective only in the *cerk1-2* mutant.

The elicitation experiments with peptidoglycan from two different Gram-negative bacteria indicate that of the so far tested *lyk* mutants only *cerk1-2* mutant is defective in the peptidoglycan-triggered defense response.

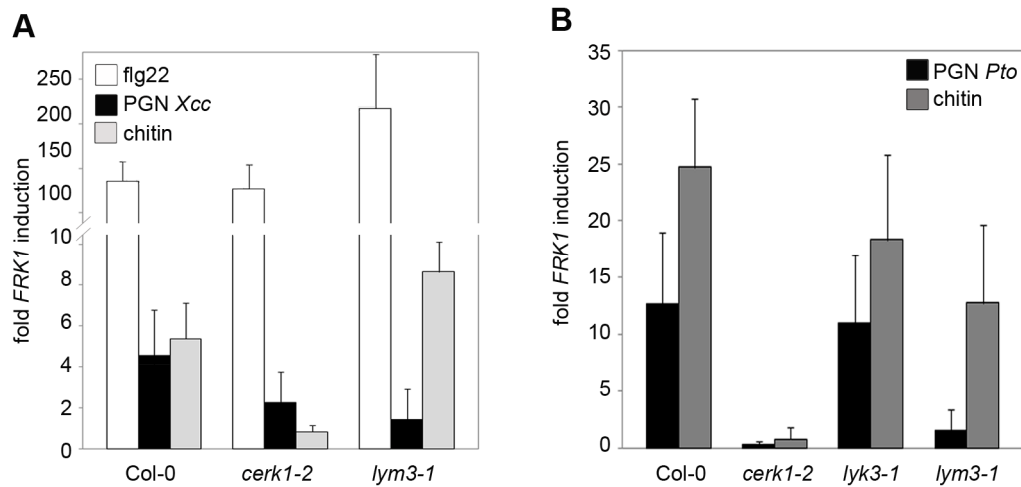


Figure 3-8: Analysis of PGN responsiveness in *lyk* mutants

Leaves of adult mutant plants and the corresponding wild type Col-0 were infiltrated with 100 $\mu\text{g/ml}$ PGN *Xcc*, 100 $\mu\text{g/ml}$ chitin, 1 μM flg22 or water as control, harvested three hours post treatment and analysed for *FRK1* transcript accumulation (A). RT-qPCR was performed as described in Figure 3-1B. Data represent means \pm SD of three independent samples each with two pooled leaves. Shown is representative of 3 independent experiments. (B) Seedlings were treated with 100 $\mu\text{g/ml}$ PGN *Pto*, 100 $\mu\text{g/ml}$ chitin or water and harvested 6 hours after treatment and monitored for *FRK1* gene expression as described in Figure 3-1B. Shown is the representative data of three independent experiments with means \pm SD from triplicate samples (4-6 seedlings per sample).

3.2.4.1 The LysM-receptor kinase CERK1 mediates sensitivity to PGN

Microarray analyses were performed using the *cerk1-2* mutant and the corresponding wild type to survey the effects of PGN elicitation on the global gene expression in *Arabidopsis thaliana* (in collaboration with Fumiaki Katagiri and Kenichi Tsuda, University of Minnesota). Leaves of five week-old plants were infiltrated with either water or 100 $\mu\text{g/ml}$ *Xcc* PGN and analysed 6 hours post treatment. In total 682 genes were either significantly induced or repressed by peptidoglycan in WT plants. Interestingly, the gene ontology (GO) analyses showed among the PGN-inducible genes an over-representation of those known to be induced upon stress (12 %) and biotic stimulus including bacterial infection (9.5 %) as depicted in Figure 3-9. The genes repressed by PGN-treatment showed a highly similar functional classification (data not shown). Among the affected genes were many genes implicated in plant defense including *FRK1*, *ADR1* (*Activated disease resistance 1*, NBS-LRR protein), *At1g51890* (LRR receptor-like kinase), *PAD3* (*Phytoalexin deficient 3*, phytoalexin biosynthesis), *NPR1* (*Nonexpresser of PR genes 1*, key regulator of SA-mediated SAR pathway), *MYB7* (*MYB domain protein 7*, transcription factor) and *MLO12* (*Mildew resistance locus 12*, disease resistance protein).

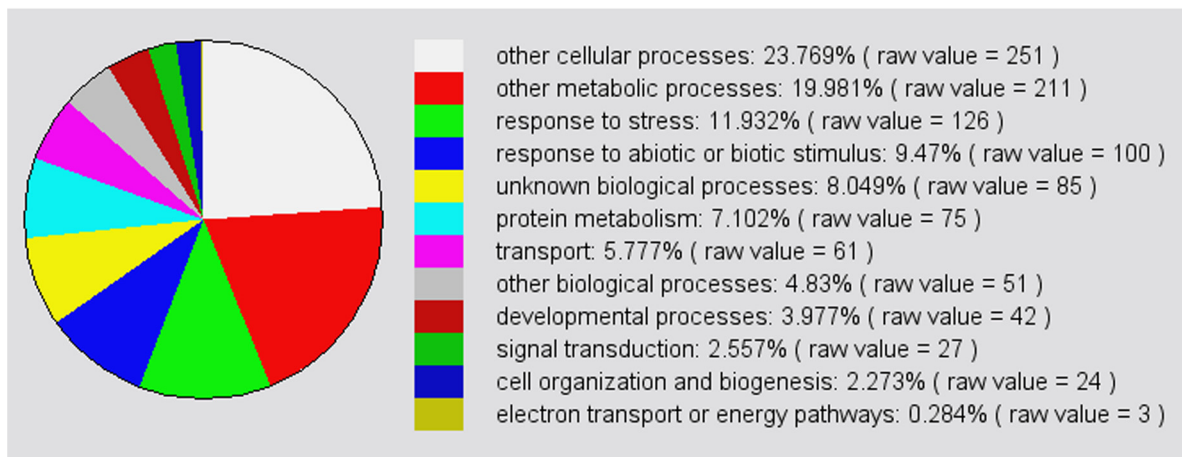


Figure 3-9: Functional characterisation of PGN-induced genes by GO analysis

The global PGN-inducible gene expression in wild type plants was analysed using microarray experiments. PGN treatment was performed as described in Figure 3-8A and harvested after 6 h and extracted RNA was used for microarray analyses. Significantly induced or repressed genes by either treatment were chosen (682 genes; Storey's q -value < 0.15) and functionally analysed using GO slim Classification for plants (GO Biological Process, TAIR). The genes were organized into sets according to broad GO ontology categories and percentage of the genes belonging to a specific biological process was calculated ($[\text{number of annotations to terms in this GOslim category} \times 100] / \text{number of total annotations in this ontology} = \%$).

A strong deregulation of both up- and down-regulated genes was revealed in the *cerk1-2* mutant when compared to Col-0 plants as visualised by a heat map in Figure 3-10A. The Michael-Eisen cluster analysis was facilitated for clustering of the affected genes. Similarly striking deregulation pattern of the gene expression in *cerk1-2* mutant is visible when the \log_2 ratios of the PGN-treated transcript levels are plotted against water samples (WT, Figure 3-10B upper diagram; *cerk1-2*, Figure 3-10B; lower diagram, red line indicates the regression line for WT). To verify the microarray data the expression levels of randomly selected genes (*At1g51890*, *MLO12* and *PAD3*) were monitored using quantitative RT-PCR (Figure 3-10C, performed by Roland Willmann). All three tested genes show a strong reduction in PGN-induced accumulation of their transcripts in the *cerk1-2* mutant in comparison to the WT. Additionally, to confirm that the PGN-insensitivity is not restricted to the one tested T-DNA insertion mutant, a second independent allele, *cerk1-3* (Gimenez-Ibanez et al., 2009), which is in Ws-4 background was also tested and found also to be insensitive towards peptidoglycan (data not shown).

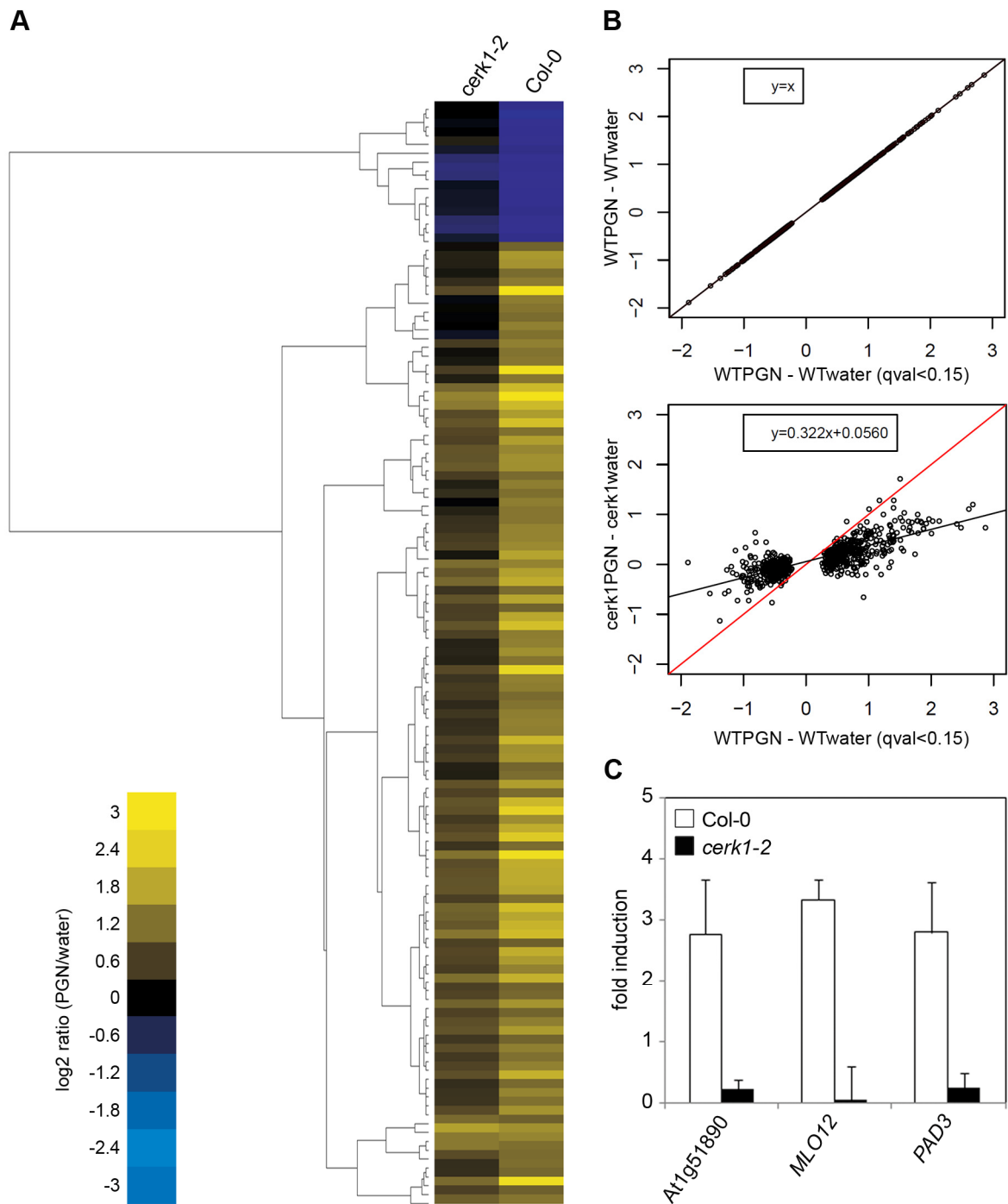


Figure 3-10: CERK1 mediates PGN sensitivity

Microarray analysis of global PGN-inducible gene expression in wild type and *cerk1-2* mutant plants. PGN treatment was performed as described in Figure 3-8A and harvested after 6 h and extracted RNA was used for microarray analyses. Significantly induced or repressed genes by either treatment were chosen (682 genes; Storey's q -value < 0.15). **(A)** Heat map comparing the changes in gene expression in the tested lines. Legend indicates values that correspond to the color scale; \log_2 ratio (PGN/water). The responsive genes were clustered using Michael-Eisen cluster (uncentered correlation) and visualized by tree view. **(B)** The \log_2 ratios of transcript levels observed PGN-treated Col-0 and *cerk1-2* plants were plotted vs. water controls. The linear regression line indicates gene expression levels in Col-0 (black line in the upper diagram, red in the lower diagram) or *cerk1-2* (black line in the lower diagram). **(C)** Transcript accumulation of *At1g51890*, *MLO12* and *PAD3* genes in PGN treated *cerk1-2* and Col-0 are shown relative to those detectable in water-treated plants. Seedlings were treated with 100 $\mu\text{g/ml}$ PGN *Xcc* and subjected to RT-qPCR as described in Figure 3-1B.

3.2.5 Analysis of potential redundancy among *LYK* genes

Gene families with several members are common in plants (Vandepoele and van de Peer, 2005). Individual genes may exhibit differential temporal expression patterns or they can be expressed in different tissues. However, these genes may also have redundant functions, with differences in dose requirements. Regarding the *LYK* gene family, the expression patterns indicate that *LYK2* might have a very tissue-specific task in *Arabidopsis*. The other *LYK* members are strongly expressed in the leaf, one of the main infection sites of the plant, suggesting potentially redundant roles or completely different functions. The generation of double, triple or quadruple *lyk* mutants could help elucidating the roles of the single genes. The data presented so far supported the importance of *CERK1* and possibly also *LYK3* in the bacterial resistance and in the first round of crossing the *cerk1-2* mutant was crossed with both the *lyk3-1* single mutant and also the *lyk3-1 lyk5-1* double mutant (both mutants in Col-0 background). An additional benefit from the crossing of the *cerk1-2* with the double mutant was to get an additional back-crossing in Col-0 background for minimising the Ler portion still left in the genotype of the double mutant. The crossing was successful for both combinations and the obtained offspring was monitored for heterozygous individuals by genotyping PCR analysis (data not shown). The F2 generation of the generated *lyk* triple mutant *cerk1-2 lyk3-1 lyk5-1* contained some candidate individuals showing amplification products only in the Lba-PCR reactions, indicating that these plants could be fully homozygous for all three T-DNA insertions within the *CERK1*, *LYK3* and *LYK5* genes in the following generation (Figure 3-11; lane 1-2, 4-6). The phenotype of this newly generated triple mutant can in future be analysed with respect to PGN sensitivity and bacterial resistance. WT plants and the mutant lines *cerk1-2*, *lyk3-1* and *lyk3-1 lyk5-1* were included as controls in the genotyping analysis (Figure 3-11). As soon as the *lyk4-1* mutant is homozygous it can also be used for a further crossing with the *cerk1-2 lyk3-1 lyk5-1* triple mutant to generate a quadruple *lyk* mutant.

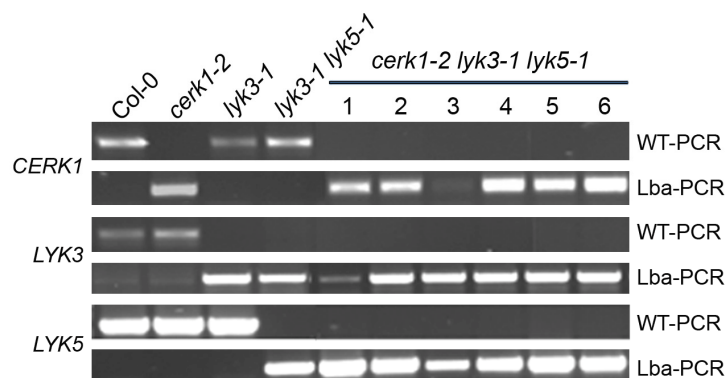


Figure 3-11: Generation of triple *lyk* knock-out mutants

Genotyping analysis of the triple mutant *cerk1-2 lyk3-1 lyk5-1* in Col-0 background. Genomic DNA was isolated from leaves and genotyping PCR reactions were performed with the primer combinations described in Figure 3-3A-C.

3.3 The role of PGN hydrolysis in the PGN sensing process

Peptidoglycan recognition proteins (PGRPs) mediate beside the LRR-receptor proteins TLR2 and NOD1/2 recognition of PGN, and are conserved between insects and higher animals, including humans (Bischoff et al., 2006; Cho et al., 2005; Dziarski and Gupta, 2010; Kurata, 2010). Among these PGRPs are both PRRs as perception and signaling molecules and proteins with PGN hydrolysing properties (Bischoff et al., 2006; Dziarski and Gupta, 2010; Gelius et al., 2003; Kurata, 2010; Wang et al., 2003). PGRPs act together with other innate immunity proteins to effectively combat pathogens. One example for such innate immunity protein is lysozyme, which is able to lyse bacteria by massive PGN hydrolysis and thus boosts the antibacterial defense (Callewaert and Michiels, 2010). It has been also shown to synergistically function together with the human PGLYRP1 and to contribute to the innate immunity by killing Gram-negative bacteria trapped by the neutrophils (Cho et al., 2005). Besides the direct bacteriolytic activity, it has been suggested that the PGN fragments released by the lytic activity of lysozyme have an impact on bacteria-host interactions by modulating the activation of the immune response and inflammation pathways (Chaput and Boneca, 2007). Such processing of polymeric carbohydrates derived of pathogenic cell walls and release of immunogenic fragments by host enzymes has also been reported in plants. In the legume plant soybean a β -glucan-binding protein (GBP) harbours two carbohydrate-active protein domains; on the one hand a binding site for a β -glucoside ligand derived from the cell wall of the oomycete *Phytophthora sojae* and on the other hand an endoglucanase activity (Fliegmann et al., 2004; Mithöfer et al., 2000). Hence, during contact with *Phytophthora* hyphae the intrinsic 1,3- β -glucanase activity of the GBP produces soluble oligoglucoside fragments enriched in motifs that are ligands for the high-affinity binding site present in the same protein (Fliegmann et al., 2004). However, GBP does not contain any signal transmitter domains leaving the question open how the defense mechanism triggered by β -glucan perception is transduced across the plasma membrane.

In order to find a connecting link between PGN processing and receptor-mediated PGN recognition *in planta* the general plant PGN hydrolase properties as well as the immunogenic nature of PGN fragments were examined. Previous studies demonstrated that soluble oligomeric PGN fragments derived from peptidoglycan of the Gram-negative phytopathogen *Xanthomonas campestris* pv. *campestris* (*Xcc* muropeptides) were able to induce defense reactions in *Arabidopsis thaliana* (Erbs et al., 2008). This muropeptide mixture was used to infiltrate adult leaves of the *cerk1-2* and *lym3-1* mutants and Col-0 plants. The following RT-qPCR analysis revealed that the muropeptide-induced expression of the immune marker genes *FRK1* and *MLO12* was clearly reduced in both mutant lines (Figure 3-12A, B). The

results indicate that soluble muropeptides derived from polymeric PGN are sensed in a receptor-mediated manner via LYM3 and CERK1.

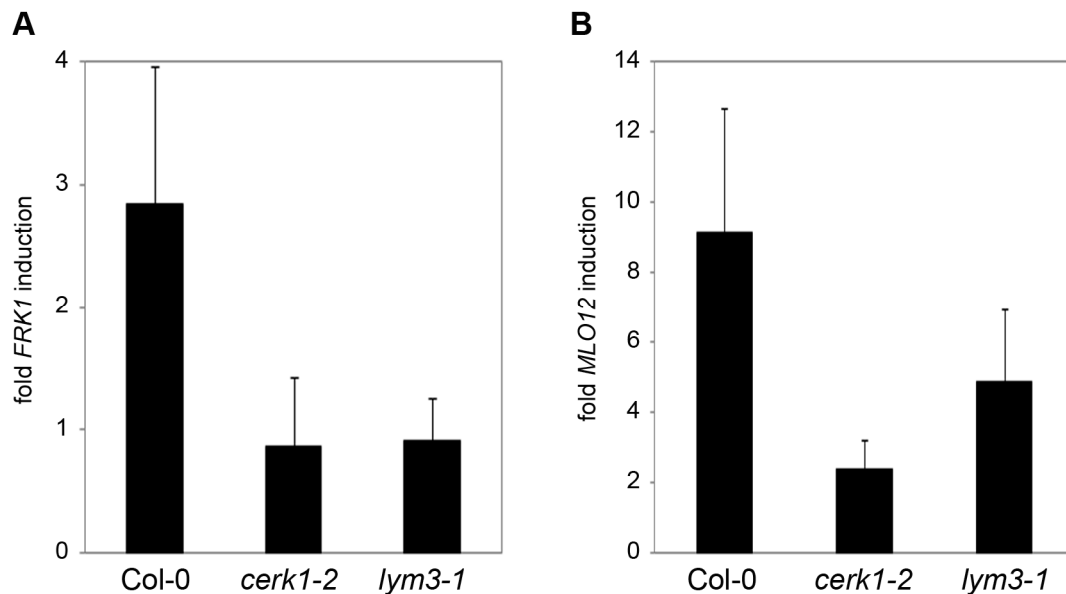


Figure 3-12: Muropeptide-induced gene expression requires LYM3 and CERK1

Leaves were infiltrated with 100 µg/ml muropeptides derived from PGN *Xcc* and analysed 3 hours post treatment for the transcript accumulation of the defense-related genes *FRK1* (**A**) and *MLO12* (**B**) using RT-qPCR as described in Figure 3-8A.

3.4 Identification of a putative PGN hydrolase in *Arabidopsis thaliana*

Lysozyme-encoding sequences are restricted to animal genomes. Nevertheless, a subset of plant enzymes (hevamine-like chitinases) have been reported to possess PGN hydrolase activity *in vitro* (Bokma et al., 1997; Park et al., 2002). Interestingly, also some lysozymes are able to hydrolyse N-acetyl glucosamine substrates and have thus chitinase activity (Miyachi et al., 2006; Nilsen et al., 1999; Xue et al., 2004). Based on these informations it was likely to find a putative PGN hydrolase among the *Arabidopsis* chitinases. In *Arabidopsis*, 24 chitinases are annotated and they are subdivided into 5 classes according to their sequence and structural features (Passarinho and De Vries, 2002). The arrangement of the chitinases into classes I to V is illustrated by the alignment of the full-length amino acid sequences using the ClustalW2 algorithm (Figure 3-13). The class III is represented by only one member, CHIA (*At5g24090*).

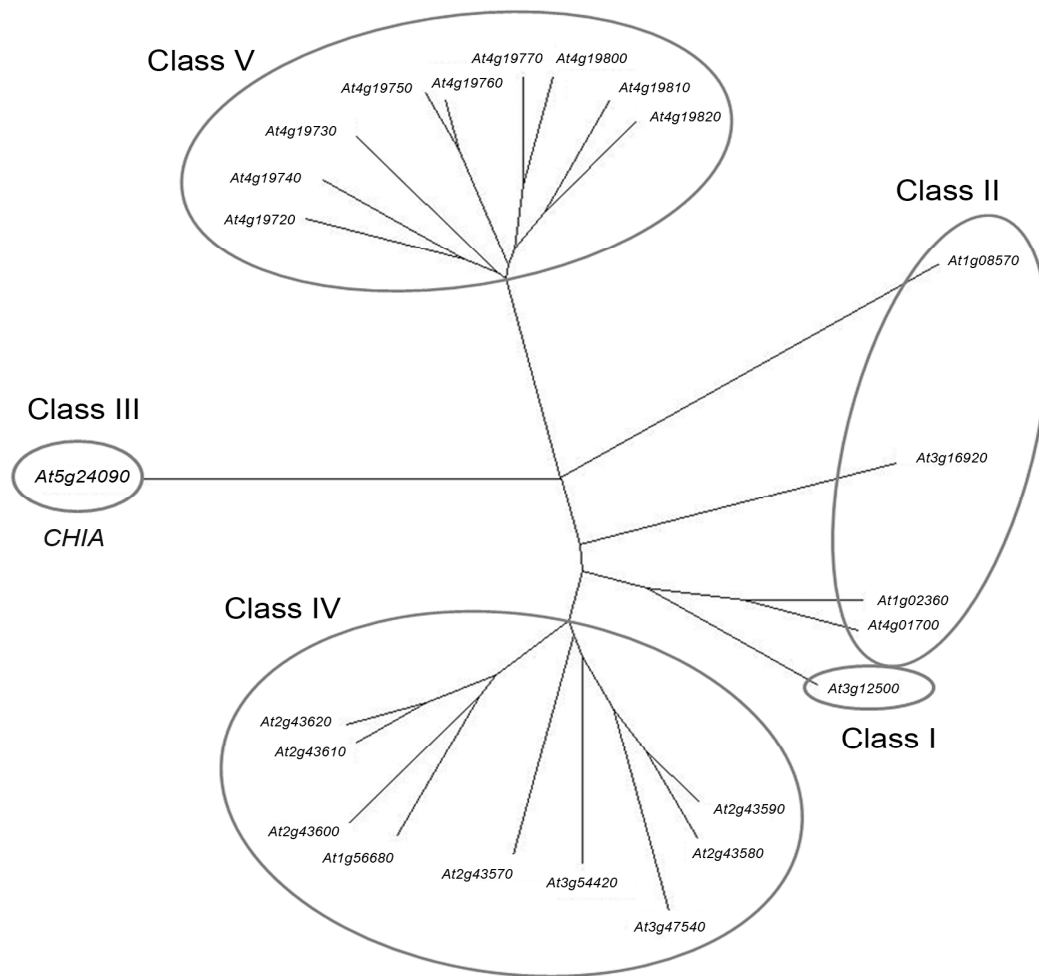


Figure 3-13: Sequence alignment of the *Arabidopsis* chitinases

A multiple sequence alignment of the 24 annotated members of the chitinase family in *Arabidopsis thaliana* using the ClustalW2 algorithm. Full-length amino acid sequences were aligned and subgroups (I-V) were classified according to Passarinho and De Vries (2002). *Arabidopsis* CHIA (At5g24090) represents the only member of class III.

3.4.1 Analysis of the class III chitinase CHIA

The rubber tree hevamine is a class III chitinase and has been reported to display additionally to chitinolytic activity also PGN hydrolysing properties (Bokma et al., 1997). A BLAST (Basic Local Alignment Search Tool) search using the protein sequence of *Hevea brasiliensis* hevamine revealed only one *Arabidopsis* chitinase, the putative acidic endochitinase CHIA, as homologous to the rubber tree enzyme. Alignment of these two protein sequences using the ClustalV algorithm resulted in approximately 70 % identity (see Figure 3-14A). The CHIA protein contains the conserved catalytic core with an glutamic acid residue (E-157; Figure 3-14A, blue box) and almost all residues essential for substrate-binding (Figure 3-14A, blue asterisks) as shown for the rubber tree hevamine (Terwisscha van Scheltinga et al., 1996). The protein sequence of CHIA was also analysed for the

presence of a signal peptide and subcellular protein localisation using the SignalP 3.0 program and Cell EFP Browser (BAR, The Bio-Array Resource for Plant Biology) and a high probability was calculated for a putative secretion signal (amino acids 2-22) targeting CHIA to the extracellular space (Figure 3-14A, B). The calculated isoelectric point of CHIA (pI 9.3) (The Arabidopsis Information Resource, TAIR) is similar to that of *Hevea brasiliensis* hevamine (Tata et al., 1983).

Due to the presence of all essential enzymatic residues known to date to be required for chitinase activity and the predicted secretion into the plant apoplast, the endochitinase CHIA makes a perfect candidate for a putative PGN hydrolase.

A

```

1 M THNMTLRKHVIYFLFFISCSLS KPSDASRGGIAIYWGQNGNEGNLSATCATGRYR at5g24090
1 M AK--- R QRA I L L L L L L A I S L I H S S H V D G G G I A I Y W G Q N G N E G L L Q T C S T R K Y S hevamineA
                                     *

56 Y V N V A F L V K F G N G Q T P E L N L A G H C N P A A N T C T H F G S Q V K D C Q S R G I K V M L S L G G G at5g24090
53 Y V N A F L M K F G N G Q T P Q I N L A G H C N P A A G G C T I V S N G I R S C Q I Q G I K V M L S L G G G hevamineA
                                     * * *

111 I G N Y S I G S R E D A K V I A D Y L W N N F L G G K S S S R P L G D A V L D G I D F N I E L G S P Q H W D D at5g24090
108 I G S Y F L A S O R D A K N V A D Y L W N N F L G G K S S S R P L G D A V L D G I D F D I E H G S F L Y W D D hevamineA
* * * * *

166 L A R T L S K F S H R G R K I Y L T G A P Q C P F P D R L M G S A L N T K R F D Y V W I Q F Y N N P P C S Y S at5g24090
163 L A R M L S R Y S K G G K K V Y L T N A P Q C P F P D R V L G T A L N T G L F D Y V W V Q F Y N N P P C O Y S hevamineA
                                     * * * * *

221 S G N T Q N L F D S W N K W T T S I A A Q K F F L G L P A A P E A A G S G Y I P P D V L T S Q I L P T L K K S at5g24090
218 S G N I N N I I N S W N R W T T S I N A G K I F L G L P A A P E A A G S G Y V P P D V L I S R I L P E I K K S hevamineA

276 R K Y G G V M L W S K F W D D K N G Y S S S I L A S V at5g24090
273 P K Y G G V M L W S K F V D D K N G Y S S S I L D S V L F L H S E E C M T V L hevamineA
                                     *

```

B

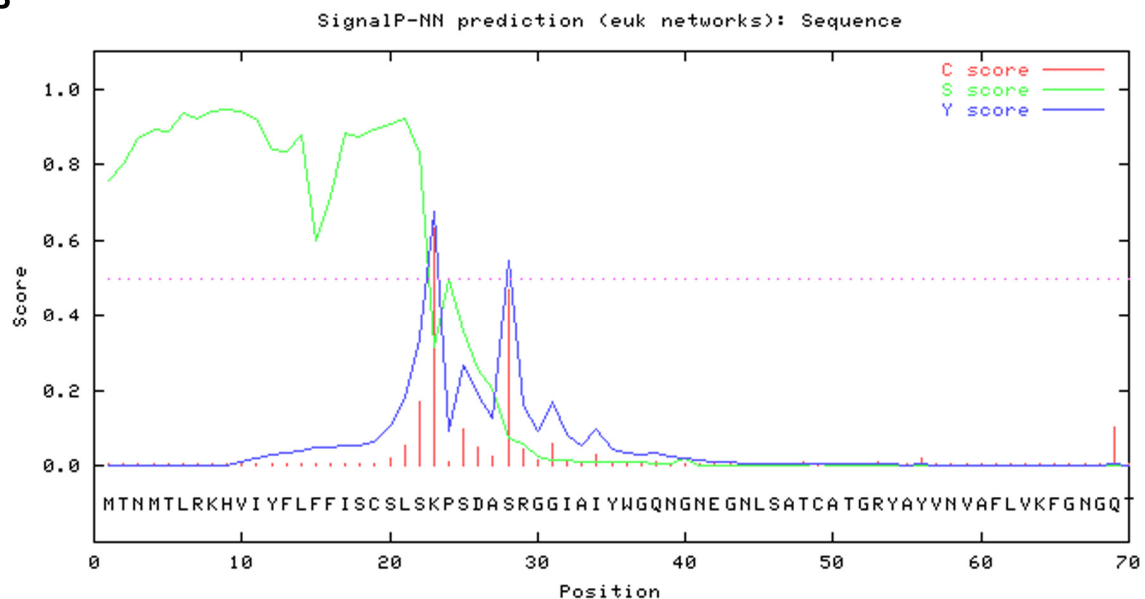


Figure 3-14: CHIA protein sequence and annotated features

(A) Alignment of the full-length amino acid sequences of the *Arabidopsis thaliana* CHIA (*At5g24090*) and its homolog *Hevea brasiliensis* HevamineA using the ClustalV algorithm. The sequences share 70 % identity, grey boxes underline differences and the red box depicts the predicted secretion signal. The amino acid sequence after the secretion signal is annotated as acidic endochitinase domain (glycoside hydrolase family 18, EC 3.2.1.14). The blue box indicates the conserved catalytic site with a glutamic acid residue and the blue asterisks the substrate-binding sites (Terwisscha van Scheltinga et al., 1996). (B) Secretion signal prediction for the CHIA protein sequence performed with the SignalP 3.0 program using neural networks (NN) and hidden Markov models (HMM) trained for eukaryotes. The most likely cleavage site is between aa pos. 22 and 23 (SLS-KP).

3.4.2 Expression pattern of the *CHIA* gene upon biotic stress

According to the publicly available microarray data from the ATGenExpress initiative the *CHIA* gene is expressed at relatively low levels in most plant tissues, including leaves of different stages (data not shown). In certain stages of the flower development the *CHIA* transcript is abundantly present in anthers. In addition, studies using promoter-GUS reporter lines showed that *CHIA* was also expressed in hydathodes and stomatal guard cells (Samac and Shah, 1991). Upon infection with the fungal pathogen *Rhizoctonia solani* the expression of *CHIA* was induced around the lesion sites (Samac and Shah, 1991). Furthermore, *CHIA* expression was inducible by different strains of the plant phytopathogenic bacterium *Pseudomonas syringae* (ATGenExpress, Figure 3-15A). Whereas the induction of *CHIA* expression was less than two-fold after 24 hours upon infection with the virulent *Pto* DC3000 strain in comparison to control treatment, infection with the non-virulent mutant strain *Pto* DC3000 hrc⁻ yielded nearly 2.5-fold induction (Figure 3-15A). The infection of *Arabidopsis* leaves with the non-host pathogen *Pph* resulted in a relatively fast and strong induction of *CHIA* transcription with already 2.2-fold induction after 6 hours and 2.4-fold induction upon 24 hours when compared to the mock treatment (Figure 3-15). The expression of *CHIA* was also induced 48 hours after inoculation with the necrotrophic fungi *Botrytis cinerea* as depicted in Figure 3-15B.

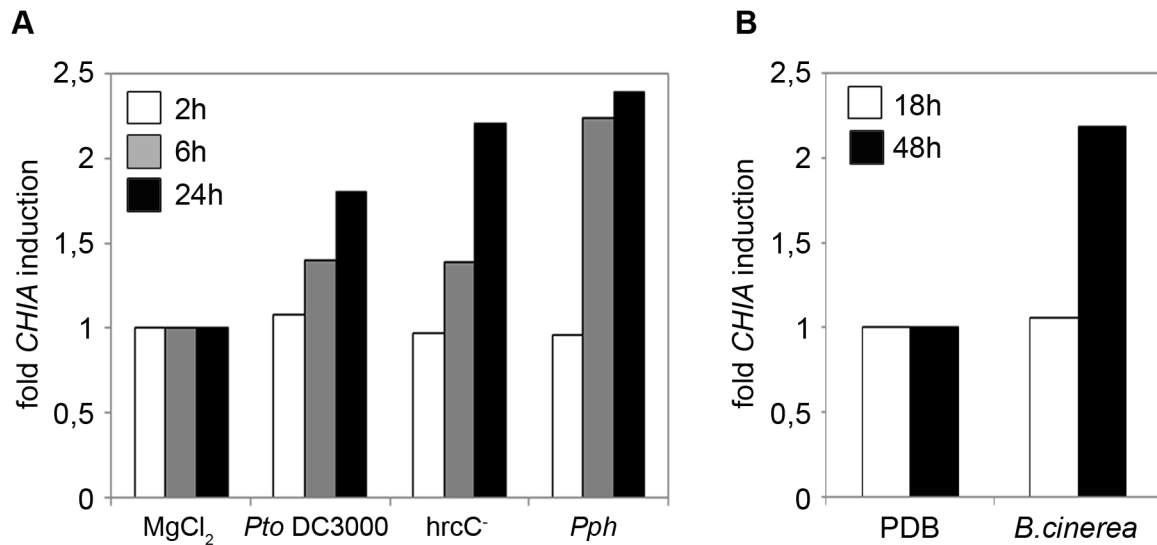


Figure 3-15: *CHIA* expression profile upon biotic stress

Microarray analyses were performed within the ATGenExpress initiative using Col-0 plants infected with different *Pseudomonas syringae* strains (**A**) and *Botrytis cinerea* (**B**) as described in detail in Figure 3-2C (*P.syringae* infection) and Figure 3-6E (*B.cinerea* infection).

To analyse the mode of *CHIA* expression in more detail transgenic promoter-GUS reporter lines were generated containing the β -glucuronidase (*GUS*) reporter gene under the control of a 2 kb long fragment of the *CHIA* promoter (see 2.4.15). One half of the leaves of homozygous plants was infiltrated with either water or 100 μ g/ml PGN *Bs*, chitin or 1 μ M flg22 and stained for GUS activity 24 hours post treatment (Figure 3-16A). Transgenic *pPR1::GUS* reporter plants served as control (Shapiro and Zhang, 2001). No GUS staining was observed in the water-treated leaves of both reporter lines. Also peptidoglycan from *Bacillus subtilis* failed to induce the *CHIA* promoter and the treatment with chitin resulted in very weak activation of the promoter (Figure 3-16A, second and third upper panel from left). However, elicitation with the proteinaceous bacterial PAMP flg22 led to a visible GUS staining indicating activation of the *CHIA* promoter (Figure 3-16A, upper right panel). The *pPR1::GUS* line showed similar GUS staining pattern as the *pCHIA::GUS* line but the *PR1* promoter was slightly more sensitive showing visible activation also upon PGN and chitin treatments (Figure 3-16A, second and third lower panel from left). The flg22-treatment induced a strong GUS staining of infiltrated half of the leaf (Figure 3-16A, lower right panel). The PAMP treatment led in general to a local induction of the promoters, thus GUS staining was only detected within the infiltrated leaf tissue (Figure 3-16A). The ability of the necrotrophic fungi *Alternaria brassicicola* and *Botrytis cinerea* to induce the *CHIA* promoter was also explored. 48 hours after infection of *pCHIA::GUS* leaves with *Alternaria* weak GUS stain at the site of the drop-inoculation was observed (Figure 3-16B, second upper panel from right). Similar

activation of the *CHIA* promoter was visible upon *Botrytis* infection, but also the PDB medium used as control induced the promoter in a weak manner (Figure 3-16B, third and fourth upper panel from left). The *PR1* promoter showed stronger activation upon *Alternaria* and *Botrytis* infections than the *CHIA* promoter and especially the infection with *Botrytis* resulted in GUS activity beyond the inoculation site (Figure 3-16B, lower panel). Finally, the promoter GUS reporter plants were also infected with *Pseudomonas syringae* strains to monitor effects of bacterial phytopathogens on the activity of the *CHIA* promoter. Here, infection with the virulent *Pto* DC3000 showed no induction of the *CHIA* promoter, when leaves were observed 24 hours post infection (Figure 3-16C, second upper panel from left). *Pto* DC3000 *hrcC*⁻ and *Pph* strains both activated the *CHIA* promoter, however the GUS stain upon *Pph*-infection was clearly stronger than upon infection with *Pto* DC3000 *hrcC*⁻ (Figure 3-16C, third and fourth upper panel from left). The *pPR1::GUS* line responded to all three *Pseudomonas* strains (Figure 3-16C, lower panel). Also, the bacterial infections resulted similar to the PAMP treatments only in a local promoter activation.

The expression of the *CHIA* gene is differentially regulated upon infection with fungal or bacterial pathogens. Whereas virulent *Pseudomonas* strains seem to suppress the *CHIA* expression, non-host bacterial pathogens like *Pph* and and also the bacterial PAMP flg22 induce it, thus indicating a possible relevance for *CHIA* within plant defense against biotic stress.

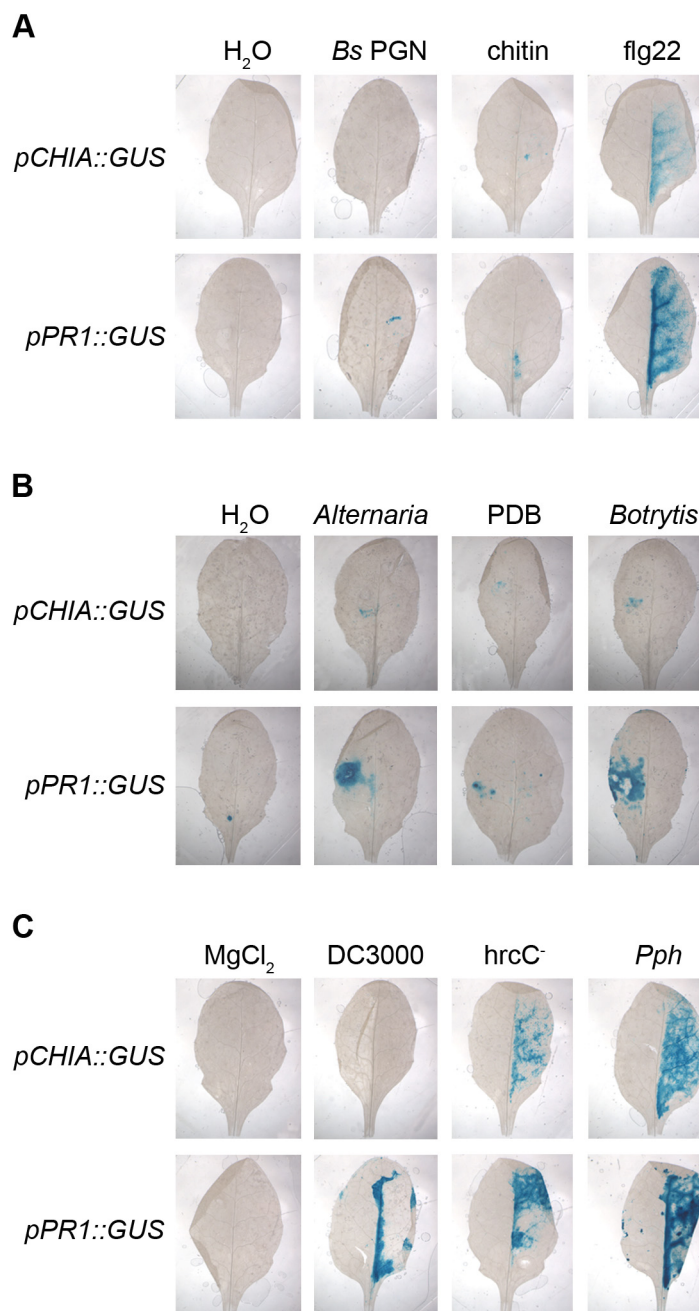


Figure 3-16: *CHIA* expression analysis using a *pCHIA::GUS* reporter line

The expression of *CHIA* in transgenic *pCHIA::GUS* reporter plants was monitored 24 hours post treatment with indicated PAMPs (**A**), 48 hours upon infection with the necrotrophic fungi *Alternaria brassicicola* or *Botrytis cinerea* (**B**) and 24 hours post infection with different *Pseudomonas syringae* strains (**C**). The treatment of the leaves and used concentrations were described in Figure 3-1D (PAMP infiltration), Figure 3-2C (infection with *Pseudomonas*) and Figure 3-6E (Infection with *Botrytis*). The leaves were harvested after indicated time points and stained for GUS activity. The *pPR1::GUS* line containing the promoter of the defense-inducible gene *PR1* (Shapiro and Zhang, 2001) was used as control.

3.4.3 Analysis of the transgenic *CHIA* lines

Three independent T-DNA insertion lines for the *CHIA* gene were obtained from NASC and CSHL (Cold Spring Harbor Laboratory, NY, USA) for the characterisation of the importance of *CHIA* in resistance to bacteria and PGN perception. The *chia-1* mutant line (WiscDsLox387C11) contains a T-DNA insertion ~500 bp upstream of the start codon in the promoter region, the T-DNA insertion in the *chia-2* mutant (SALK_095362) is in the end of the third exon and the third mutant line, *chia-3* (CSHL_ET14179), carries an Enhancer Trap (ET) transposon insertion within the first intron. The gene structure of *CHIA* and the positions of the insertions are depicted in Figure 3-17A. The genotyping analysis using gene- and insertion-specific primers could verify that all three *chia* mutant lines were homozygous for the corresponding insertions (Figure 3-17B). However, the subsequent transcript analysis using semi-quantitative RT-PCR revealed that these mutant lines still had *CHIA* transcript even to similar extent than the corresponding wild types (Figure 3-17C). Thus, *chia-1*, *chia-2* and *chia-3* were not suitable for analysis of the *CHIA* mutant phenotype.

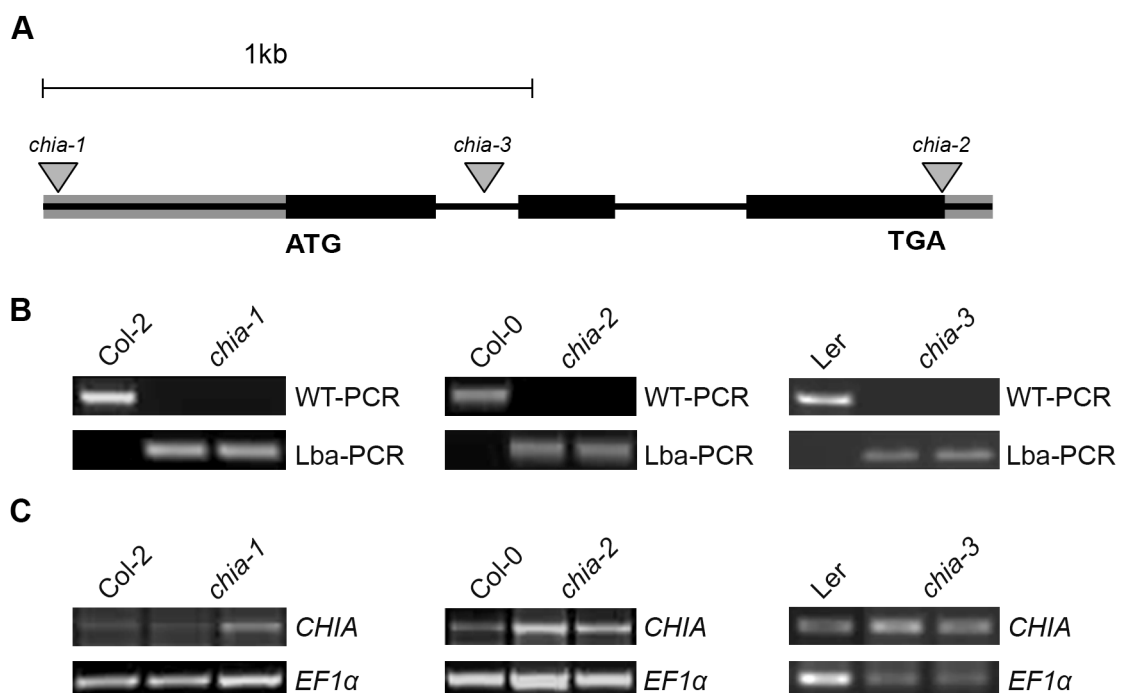


Figure 3-17: Characterisation of *CHIA* T-DNA insertion lines

(A) Gene model of *CHIA* with the T-DNA insertions indicated by grey triangles. The exons, introns and the untranslated regions (3'-UTR, 5'-UTR) are depicted as described in Figure 3-3. **(B)** The T-DNA insertion lines and the corresponding ecotypes were genotyped using following primer combinations: LP_853931 and RP_853931 (WT-PCR, *chia-1*), Wisc-Lba and RP_853931 (Lba-PCR, *chia-1*), LP_N595362 and RP_N595362 (WT-PCR, *chia-2*), Salk-Lba and RP_N595362 (Lba-PCR, *chia-2*), At5g24090F1 and At5g24090R1 (WT-PCR, *chia-3*) and Ds5-1 and At5g24090R1 (Lba-PCR, *chia-3*). **(C)** The *CHIA* transcript analysis was done using following primer combinations: At5g24090F and At5g24090R (*chia-1* and *chia-2*) and At5g24090F and At5g24090RP2 (*chia-3*).

In a parallel approach, transgenic *CHIA* knock-down (*chia-kd*) lines were generated using the artificial microRNA technology (2.4.13), which can be used to effectively silence specific genes in plants (Ossowski et al., 2008). The sequence region used for the generation of the *CHIA*-specific amiRNA is indicated by a grey triangle in Figure 3-18A. Also *CHIA* overexpression (*CHIA-oe*) lines carrying a *p35S::CHIA-GFP* cassette were created in Col-0 background as described in chapter 2.4.14. Two independent lines of both *CHIA* knock-down and overexpression plants were further analysed. The genotyping PCRs showed that both *CHIA-oe* lines contained additionally to the genomic *CHIA* fragment (gDNA) also the introduced cDNA using primers that amplify the whole gene, and also the 35S promoter was detectable (Figure 3-18B, WT- and 35S-PCR). AmiRNA-specific primers were used to detect the amiRNA-cassette in the *chia-kd-1* and *chia-kd-2* mutant lines, which was absent in Col-0 plants (Figure 3-18B, amiRNA-PCR). Since the effects of the amiRNA-mediated gene silencing act at a posttranscriptional level, the full-length genomic *CHIA* gene product can be amplified also in the knock-down lines (Figure 3-18B, WT-PCR). The *CHIA* transcript levels were monitored via RT-qPCR. Whereas *CHIA* overexpression lines displayed massively elevated transcription of *CHIA* (250 to 400-fold transcript levels in comparison to WT; Figure 3-18C, left diagram), the *CHIA* knock-down lines contained only approximately 5 - 10 % of the WT *CHIA* transcript amounts (Figure 3-18C, right diagram). Hence, the *CHIA* amiRNA and overexpression lines displayed the expected genetic properties and could be used for further experiments.

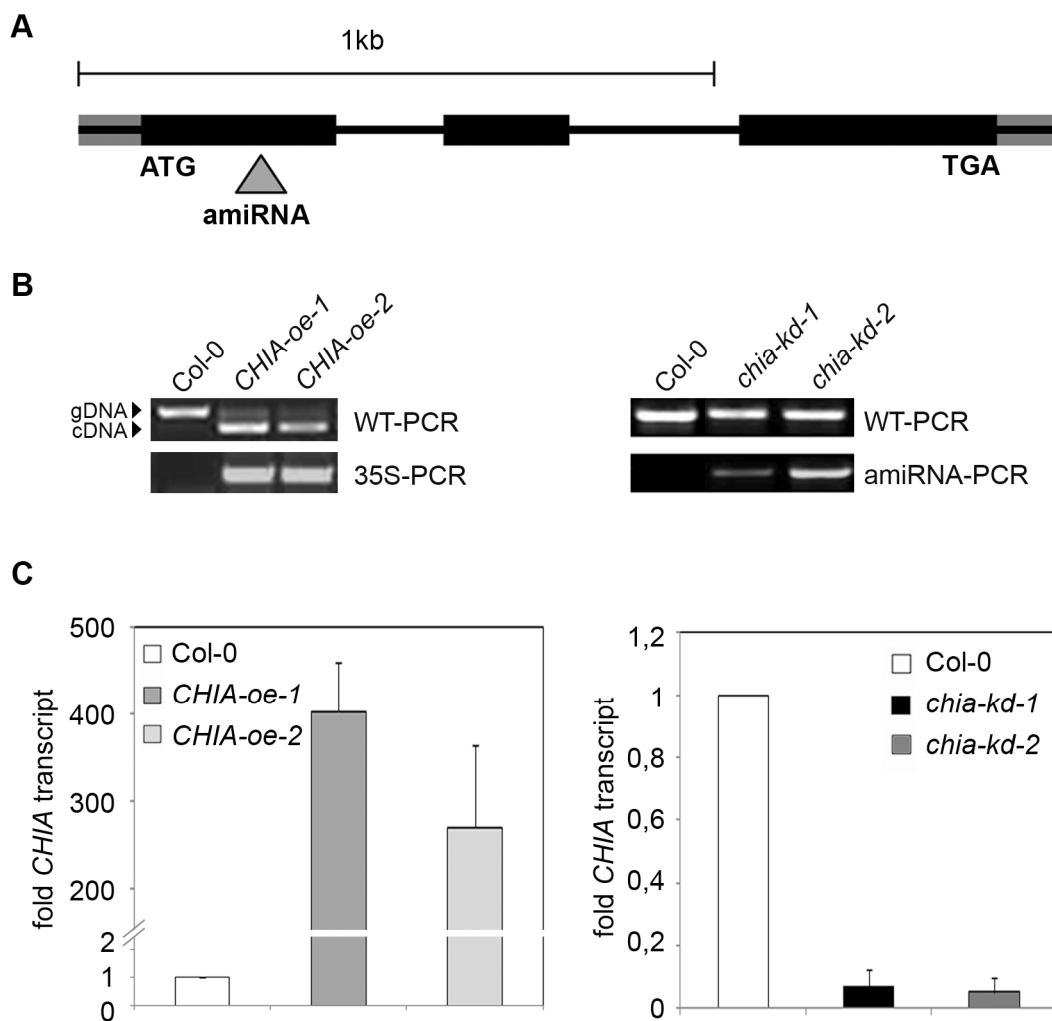


Figure 3-18: Characterisation of *CHIA* knock-down and overexpression lines

(A) Gene model of *CHIA* with the 20 bp region targeted for artificial microRNA-mediated gene silencing (grey triangle). Exons and introns are indicated by black boxes and black lines, respectively. The 3'- and 5'-UTR regions are shown as grey boxes. (B) Leaves of two independent plants of the *CHIA* overexpression lines (*CHIA-oe*) and *chia* knock-down lines (*chia-kd*) were genotyped using two sets of PCR reactions with the primer combinations: At5g24090F and At5g24090R (WT-PCR, *CHIA-oe* and *chia-kd*), GC248 and At5g24090R (35S-PCR, *CHIA-oe*), A-PRS300 and B-PRS300 (amiRNA-PCR, *chia-kd*). (C) *CHIA* transcript accumulation was monitored using RT-qPCR and the primers At5h24090Fq and At5g24090Rq in the *CHIA-oe* lines (left diagram) and the *chia-kd* lines (right diagram).

3.4.3.1 Phenotypic analysis of the *CHIA* overexpression and knock-down lines

Under control cultivation conditions in short day both the *CHIA* knock-down and overexpression plants exhibited normal phenotypes comparable to Col-0 (Figure 3-19A, upper row from left: Col-0, *CHIA-oe-1*, *CHIA-oe-2*, lower row from left: Col-0, *chia-kd-1*, *chia-kd-2*). Under low light intensity the leaves of the *CHIA* overexpression lines were somewhat stunted in comparison to WT leaves (Figure 3-19B, upper row from left: Col-0, *CHIA-oe-1*, *CHIA-oe-2*, lower row from left: Col-0, *chia-kd-1*, *chia-kd-2*). But as all the bio assays were

always performed in short day and under controlled cultivation conditions the “low-light” aberrance of the *CHIA-oe* lines was of no consequence.

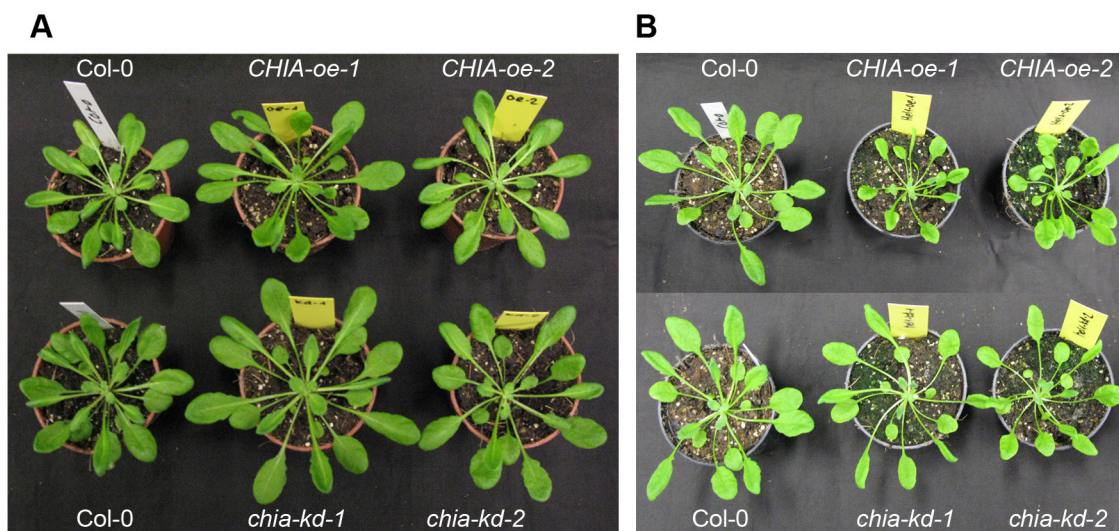


Figure 3-19: Phenotypes of CHIA overexpression and knock-down lines

CHIA-oe-1, *CHIA-oe-2*, *chia-kd-1*, *chia-kd-2* and the corresponding ecotype were cultivated in the short day either under normal conditions (**A**) or under low light intensity (**B**) and photographed in the age of 5 weeks from the top view.

3.4.4 Subcellular localisation of CHIA

According to the Bio-Array resource analysis tool (BAR) the CHIA protein is localised outside the plasma membrane in the apoplastic space. To visualise the localisation of the GFP-tagged CHIA protein leaves of two transgenic *Arabidopsis* CHIA overexpression lines were investigated using the confocal laser-scanning microscope. The GFP fluorescence was localised in both *CHIA-oe* lines in the cell periphery showing a slightly patchy and irregular pattern (Figure 3-20). As negative control leaves of Col-0 plants were monitored using the same excitation setup and laser intensity.

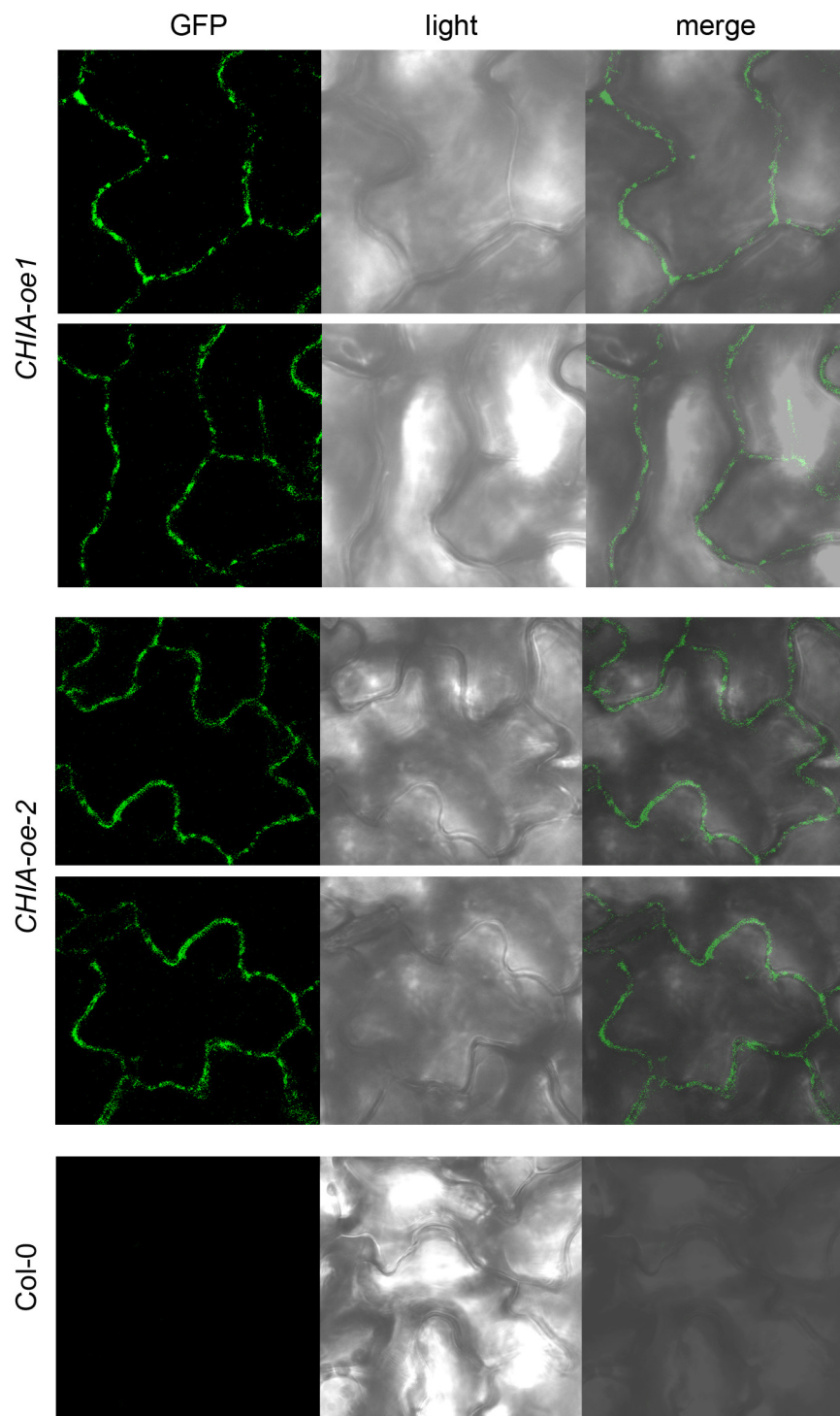


Figure 3-20: Localisation of CHIA-GFP in *Arabidopsis*

GFP fluorescence in the leaf epidermal cells of the two independent transgenic lines stably expressing a *35S::CHIA-GFP* construct (*CHIA-oe-1*, *CHIA-oe-2*) was analysed using confocal laser-scanning microscopy. Col-0 leaves served as control. Argon/Krypton laser was used to excite the fluorescence at 488 nm, the light emission was monitored between 500 and 600 nm. Left panel (GFP channel), middle panel (light) and right panel (merge of GFP and light).

To gain more insights into the subcellular localisation of CHIA the transient expression system in *Nicotiana benthamiana* was used (see chapter 2.4.11). It allowed, beside the expression of a WT CHIA-GFP construct, also the expression and rapid analysis of a mutated version of CHIA lacking the putative secretion signal peptide (CHIA Δ SP-GFP). The WT CHIA-GFP displayed a similar patchy localisation pattern in tobacco as in *Arabidopsis* (compare Figure 3-20 and Figure 3-21, CHIA-GFP). The plasma membranes of two adjacent plant cells appeared as one thick layer as stained by FM4-64 and the GFP fluorescence was detected in distinct areas around this layer as shown in the close-up picture (Figure 3-21, CHIA-GFP, lower panel). The deletion of the signal peptide led to a dramatic change in the localisation of the fluorescence signal. In leaves expressing CHIA Δ SP-GFP the GFP fluorescence was present in the cytosol, showing an evenly spread signal completely different to the patchy localisation pattern of the WT CHIA (Figure 3-21, compare close-ups for CHIA-GFP and CHIA Δ SP-GFP). Unfortunately, the membrane stain FM4-64 was no longer detectable at the plasma membrane but was weakly visible in distinct cytosolic structures. FM4-64 is rapidly taken up by endocytosis into the cytoplasm and thus does not stably stain the plasma membrane (Bolte et al., 2004; Ueda et al., 2001). GFP alone was expressed as a positive control for cytoplasmic localisation and mock-infected tobacco leaves served as negative control (Figure 3-21, GFP and negative control). Approaches to induce plasmolysis in leaf epidermal cells and to observe whether fluorescence signal is truly between the cells turned out to be technically challenging. The plasmolysis did not take place evenly in many surrounding cells, so that the possible fluorescence signal outside of an affected cell could not be distinguished from the normal signal of a neighboring unaffected cell (data not shown). The direct microscopical evidence for apoplastic localisation of CHIA is not trivial, also because the low apoplastic pH additionally quenches the fluorescence signal (Scott et al., 1999). Nonetheless, the microscopical localisation studies suggest that the CHIA protein is indeed secreted into the plant apoplast and that the signal peptide is essential for this targeted localisation. Moreover, this prediction is supported by a proteomic approach using *Arabidopsis thaliana* cell cultures that revealed the CHIA chitinase among the secreted, apoplastic proteins (Kwon et al., 2005).

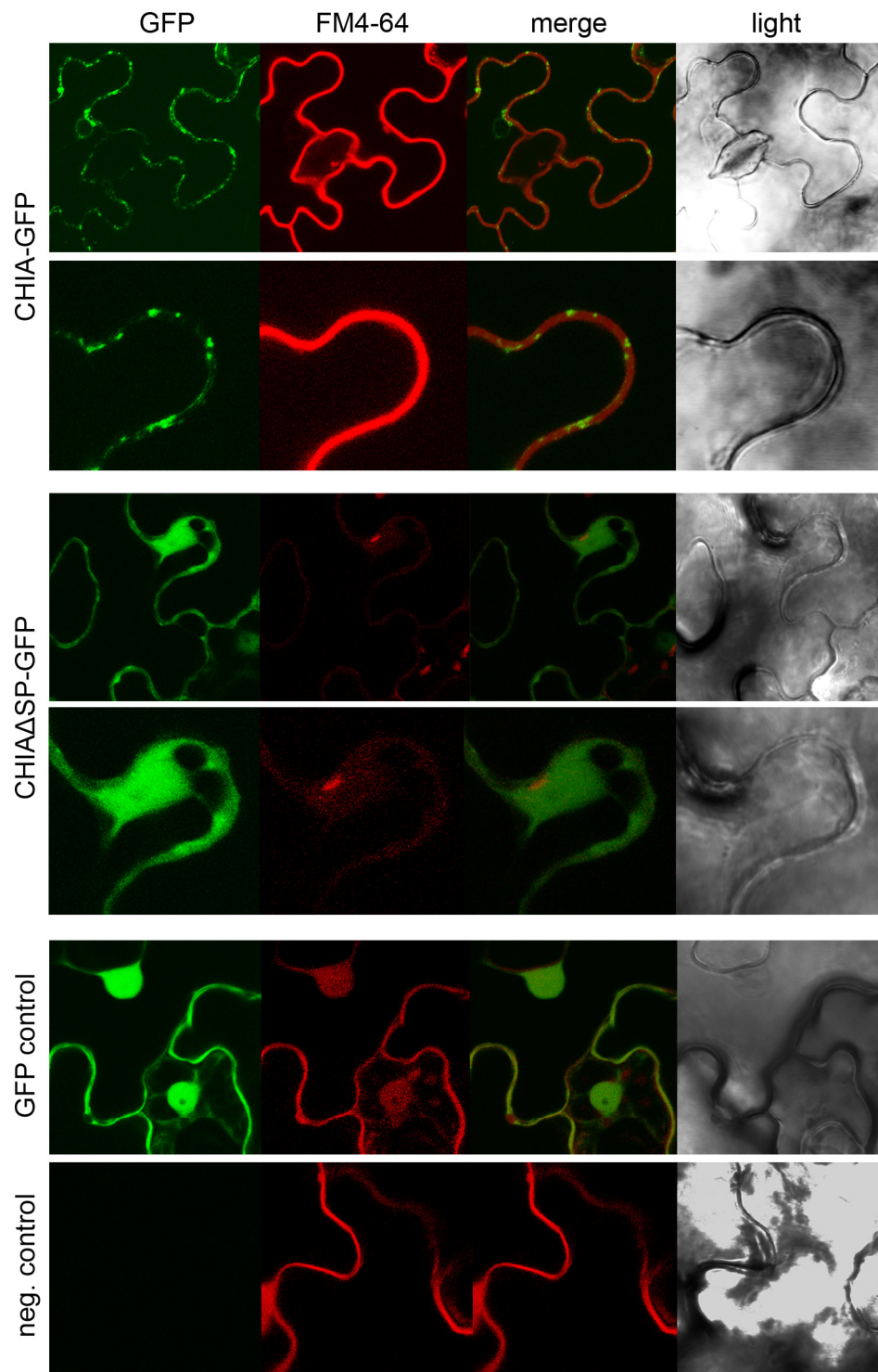


Figure 3-21: Localisation of CHIA-GFP and CHIA Δ SP-GFP in tobacco

The *35S::CHIA-GFP* and *35S::CHIA Δ SP-GFP* constructs were transiently expressed in *Nicotiana benthamiana* leaves using *Agrobacterium tumefaciens*-mediated transformation. GFP fluorescence in the leaf epidermal cells was analysed 3 days post infection. As positive GFP control leaves were transfected with the pK7WGF2.0 vector. As negative control uninfected leaves were used. FM4-64 was used to stain the plasma membrane. Argon/krypton laser was used for excitation of GFP at 488 nm and the 543 nm line of helium/neon laser for the excitation of FM4-64. Detection wavelengths of emitted light were 500 nm to 600 nm (GFP) and 560 nm to 615 nm (FM4-64). Panels from left: GFP, FM4-64, merge of GFP and FM4-64 and light.

3.4.5 Detection of CHIA protein in the transgenic *CHIA* lines

To monitor the CHIA protein levels in the generated transgenic *CHIA* lines two antibodies were available. First, antibodies raised against GFP could be used to detect the GFP-tagged CHIA in the *CHIA-oe* plants. Second, an antibody raised against the tobacco class III chitinases (α -class III chitinase antibody from rabbit, provided by Frédéric Brunner) could be tested for recognition of the *Arabidopsis* class III chitinase homolog CHIA. The α -GFP antibody detected specific bands in leaf extracts of *CHIA-oe* lines in the sizes of approximately 60 kDa and 30 kDa, which correlated with the expected sizes of CHIA-GFP (60.1 kDa) and GFP alone (27 kDa) (Figure 3-22A). The detection of CHIA using the α -class III chitinase revealed a more complex pattern of protein bands. In the *CHIA* overexpression plant extracts a clear band was visible below the 35 kDa marker. This protein band possibly represents the CHIA protein, which has the calculated size of 33.1 kDa, without the GFP tag (Figure 3-22B). In the WT lane no protein band was visible between 25 and 35 kDa (Figure 3-22B). Weak bands in the size of the CHIA-GFP fusion protein were also present in the overexpressor extracts (Figure 3-22B). It is possible that the large GFP tag is disturbing the recognition of the CHIA protein by the α -class III chitinase antibody leading to weaker detection of the tagged protein or indeed most of the protein is cleaved. The additional bands visible on the immunoblot might present cross-reacting bands. The presence of the secreted form of GFP protein in the transgenic *p35S::secGFP* line was also confirmed by immunoblot analysis (Teh and Moore, 2007). SecGFP could be detected using α -GFP antibody in the expected size of approximately 30 kDa (Figure 3-22C). The exact size of secGFP is due to an additional c-myc tag 31 kDa (Teh and Moore, 2007). In the same immunoblot analysis also the absence of CHIA-GFP in the *chia-kd* line was investigated (Figure 3-22C).

In order to purify and enrich the CHIA-GFP fusion protein from the *CHIA-oe* total leaf extracts an immunoprecipitation approach was exploited. The purified CHIA-GFP sample could then be used for further experiments, such as activity assays. Agarose A beads coupled with the antibody against GFP were used to pull down the GFP-tagged CHIA protein. The immunoprecipitation functioned well and CHIA-GFP could be detected at the expected size of approximately 60 kDa as shown in Figure 3-22D. Interestingly, upon immunoprecipitation specific high-molecular weight bands appeared in both *CHIA-oe* samples, but were not present in present in WT samples possibly representing CHIA-GFP multimers (Figure 3-22D, asterisk). Also here degradation of CHIA-GFP was observed since GFP was visible as a separate band at about 30 kDa.

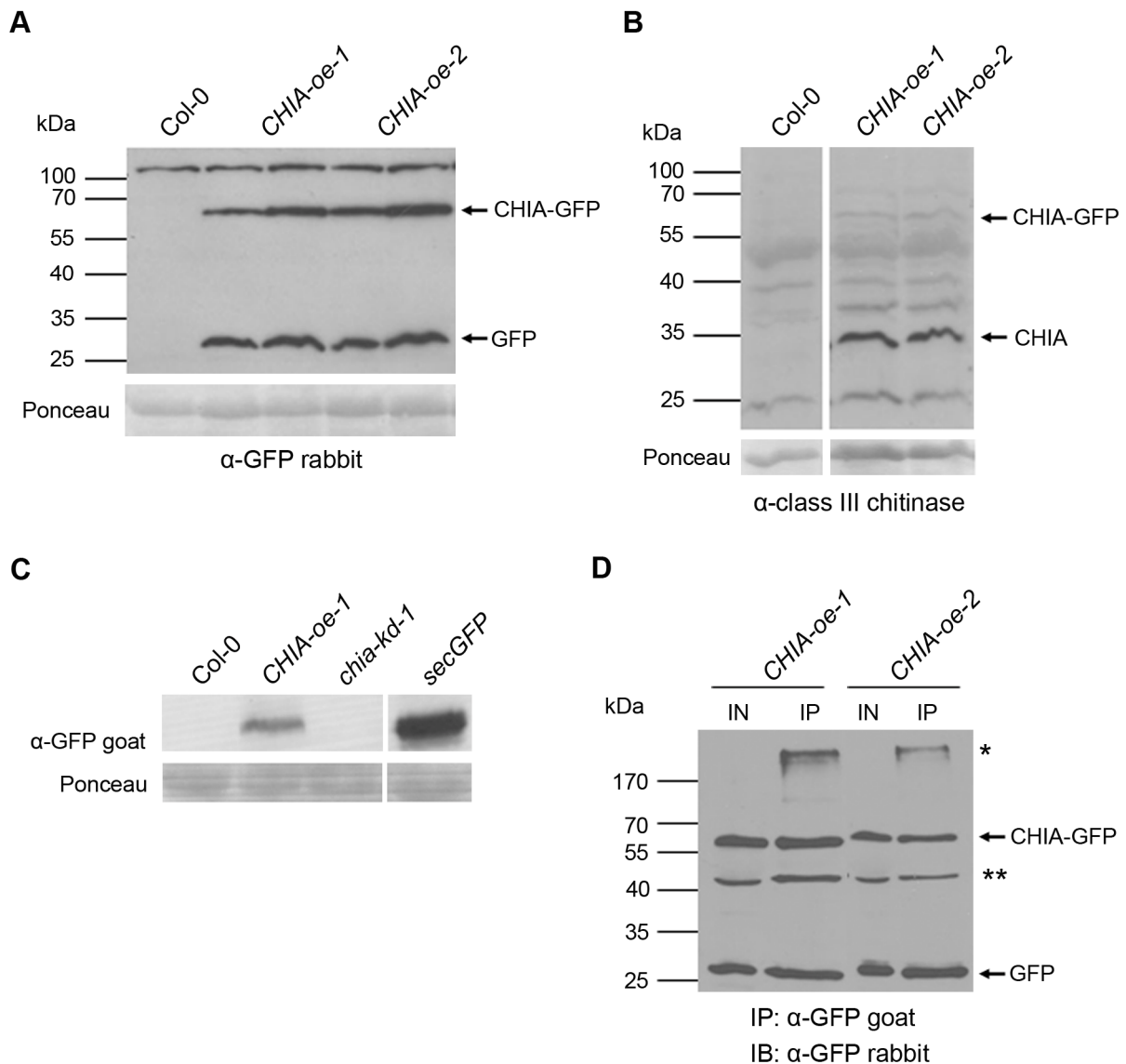


Figure 3-22: Detection of CHIA protein in *Arabidopsis*

Immunoblot analysis of protein extracts from leaves of transgenic *CHIA* lines and Col-0 plants. Total leaf protein was separated by SDS-PAGE and blotted onto a nitrocellulose membrane. The immunodetection was carried out using α -GFP rabbit (**A**), α -class III chitinase rabbit (**B**) or α -GFP goat antibody (**C**). The α -mouse-HRP and α -goat-HRP were used as secondary antibodies and the protein bands were visualized by chemiluminescence. Ponceau staining of the large subunit of RuBisCO served as loading control. Transgenic plants expressing a *p35S::secGFP* construct was used as control for GFP. (**D**) Total leaf protein of *CHIA* overexpression lines was subjected to immunoprecipitation using α -GFP goat antibody and agarose A beads. The immunodetection was performed with rabbit α -GFP and α -rabbit-HRP antibodies. IN, protein input; IP immunoprecipitated sample; * indicates a specific high-molecular weight band present in IP samples; ** indicates the band of the heavy chain of the α -GFP goat antibody.

3.4.6 Posttranslational modification of the CHIA protein

Posttranslational modifications of plant proteins include glycosylation (Tekoah, 2004). As in mammals both N- and O- linked glycosylation takes place in plants, although the mechanisms vary. The attachment of N-linked glycans to proteins begins in eukaryotes in the

endoplasmic reticulum (ER), where glycosylation sites, tripeptides N-X-S/T (X can be any amino acid except proline and aspartic acid) are recognised (Lerouge et al., 1998). The CHIA protein sequence contains two putative N-glycosylation sites (N44 and N113). As many secretory proteins undergo this type of posttranslational modification, it is possible that also the CHIA chitinase is chemically altered in this way. Depending on the amount and size of attached N-glycans the modification leads to an increased size of the glycosylated protein. This glycosylation-dependent size shift can be exploited in the analysis of posttranslational modification. Thus, total leaf protein extracts of either *Arabidopsis CHIA-oe* plants or tobacco transiently expressing *p35S::CHIA-GFP* or *p35S::CHIA Δ SP-GFP*, were subjected to deglycosylation and afterwards the possible reduction in the size of the CHIA-GFP fusion protein due to the action of the glucosidases was detected by immunoblot analysis (Figure 3-23). For both *Arabidopsis* CHIA-GFP and in *Nicotiana* expressed CHIA-GFP a small size shift was observable in the deglycosylated sample in comparison to the untreated protein sample. In contrast, the CHIA Δ SP-GFP fusion protein lacking the secretion signal displayed no reduction in the protein size after deglycosylation treatment (Figure 3-23), probably because of missing glycosylation due to misregulated targeting.

The deglycosylation experiments revealed that the CHIA-GFP fusion protein was glycosylated both in *Arabidopsis thaliana* and *Nicotiana benthamiana* and that this modification was dependent on the presence of the secretion signal.

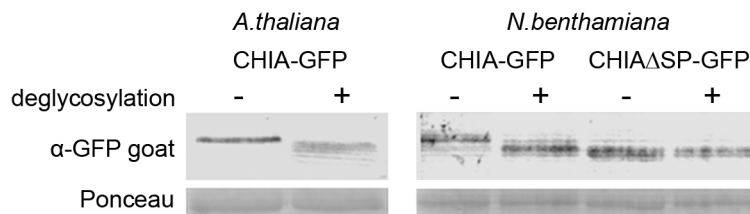


Figure 3-23: Deglycosylation of CHIA-GFP and CHIA Δ SP-GFP

Protein extracts from leaves of transgenic *Arabidopsis CHIA-oe-1* plants (A) and *Nicotiana* expressing either *p35S::CHIA-GFP* or *p35S::CHIA Δ SP-GFP* were subjected to deglycosylation with a mixture of deglycosylases. The negative control (-) was treated as the deglycosylation sample (+) but without addition of the deglycosylation enzyme mix. The immunoblot analysis was carried out as described in Figure 3-22.

3.4.7 Expression of CHIA protein using heterologous expression systems

To analyse the enzymatic properties of the CHIA chitinase *in vitro* it was expressed heterologously in *E.coli*. The expression of the His₆-CHIA fusion protein in BL21AI cells was induced by L-arabinose for 3 hours at 18 °C and after lysis of the cells the soluble protein fraction was subjected to affinity-purification using a Ni²⁺-NTA column. The His₆-CHIA could be purified to high extent and most protein was eluted from the column in the first two elution

steps as visualised by Coomassie stain and immunoblot analysis (Figure 3-24A, B; lanes 3 and 4). The majority of the protein was visible at the expected size of approximately 35 kDa, but also an additional double band was running at the size of about 65 kDa (Figure 3-24B). Afterwards, the PGN-hydrolytic activity of the fusion protein was assessed in a turbidity assay using *Micrococcus luteus* cells as substrate. The cell walls of the Gram-positive bacteria *Micrococcus luteus* are widely used as crude peptidoglycan substrate for enzymatic assays (Biswas et al., 2006; Brunner et al., 1998; de Azambuja et al., 1991; Park et al., 2002). The reduction in the turbidity of the suspension due to PGN-hydrolysis is thereby monitored and the absolute reduction of the OD or the relative activity (comparison to control PGN-hydrolysing enzymes like lysozyme) can be measured. The purified His₆-CHIA protein or the corresponding uninduced sample (negative control) were incubated together with the *M.luteus* substrate and the hydrolytic activity was monitored after 2 and 20 hours (Figure 3-24C). After 2 hours of incubation the relative activity of the His₆-CHIA protein was approximately 10 % of the lysozyme activity and 20 hours after incubation a relative activity of 40 % was measured. Unluckily, the negative control showed similar activities than the His₆-CHIA sample, indicating that the background activity resulting from bacterial enzymes was very high. It is also possible that traces of lysozyme, used for the lysis of the BL21AI cells, were present in the samples despite the affinity purification. All in all, the measured enzyme activity after 2 hours of incubation was very weak implicating that the prokaryotic *E.coli* system might be suboptimal for the expression of CHIA, which seems to be posttranslationally modified (Figure 3-23).

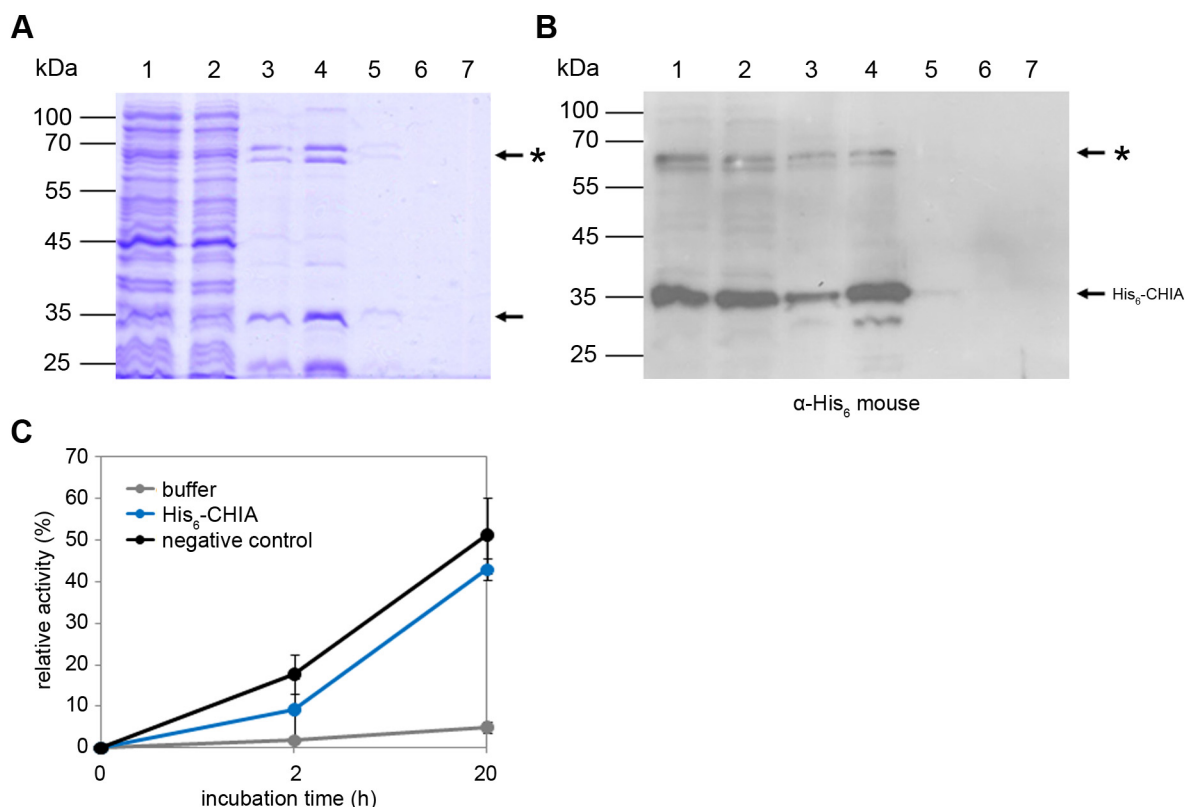


Figure 3-24: Expression of His₆-CHIA in *Escherichia coli*

His₆-tagged CHIA expression in the *E.coli* strain BL21AI was induced by L-arabinose and the bacteria were harvested after incubation for 3 hours at 18 °C. The soluble His₆-CHIA protein was purified using Ni²⁺-NTA affinity column. The protein amounts in the input (lane 1), flow-through fraction (lane 2) and 5 elution fractions (lanes 3-7) were analysed by Coomassie blue stain (**A**) or immunoblot using the α-His₆ mouse and α-mouse-HRP antibodies (**B**). Arrows indicate purified proteins and the asterisk putative CHIA oligomers. (**C**) The PGN-hydrolysis activity of the His₆-CHIA protein was monitored in a turbidity assay. 20 µg of the purified His₆-CHIA protein was incubated with *Micrococcus luteus* cells and the reduction in turbidity (OD_{570nm}) was monitored over time. The relative activity was calculated using the hen egg-white lysozyme as standard (lysozyme activity was set as 100 %). As negative control the bacterial protein extract of the uninduced sample and elution buffer were used.

Fungal expression systems can be used for expressing active plant enzymes (Park et al., 2002; Petersen et al., 2009). Therefore, for the second approach of expressing active CHIA protein the methylotrophic yeast *Pichia pastoris* was chosen. Two different vectors enabling secretion of the expressed protein in the culture medium were used (pPICZαC and pPIC9K, Invitrogen). The protein expression was induced by methanol and monitored after 1 to 4 days of cultivation of the yeast cells at 30 °C (Figure 3-25A, B). However, the expression of the CHIA protein was not induced in any of the tested clones. The protein patterns in the cells transformed with the CHIA constructs resembled the patterns in the empty vector (ev) controls.

The approaches to heterologously express an active CHIA chitinase failed so far. Nonetheless, especially the eukaryotic *Pichia* system has still potential and new expression constructs and the usage of other tags could solve the induction problems.

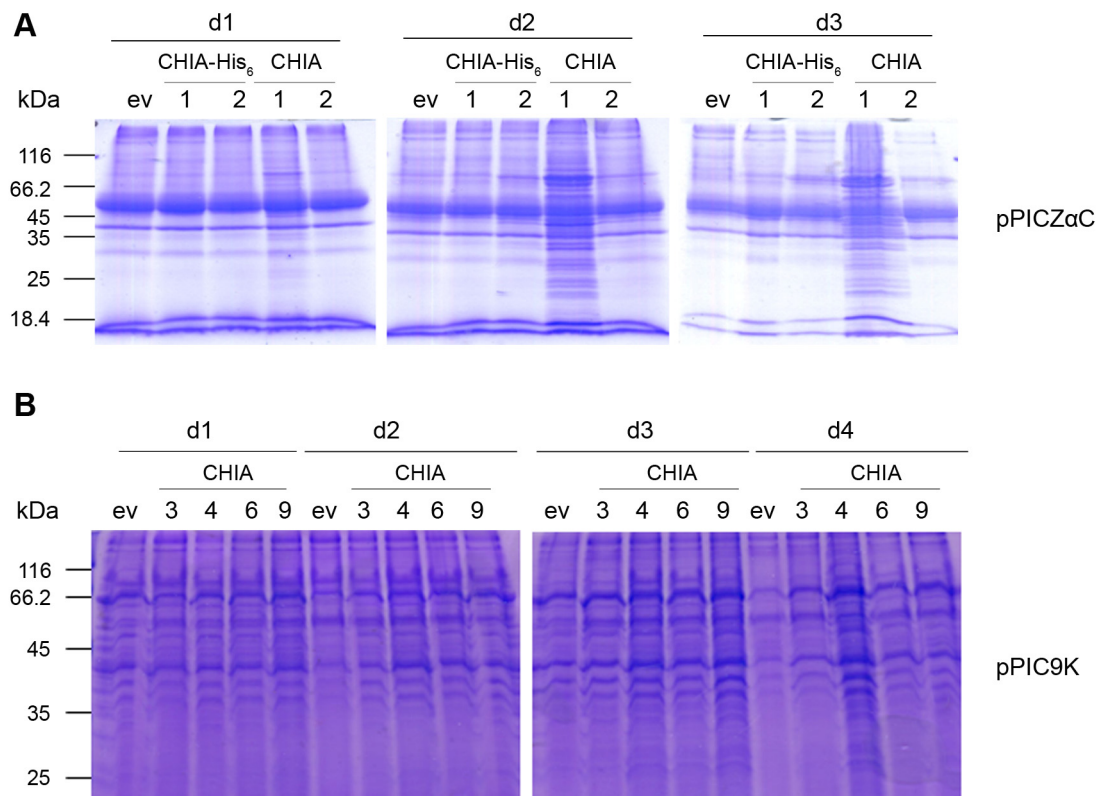


Figure 3-25: Expression of CHIA in *Pichia pastoris*

Expression of His₆-tagged or untagged CHIA in the yeast *Pichia pastoris* was induced by methanol. The cells were harvested after 1 to 4 days incubation at 30 °C. The secreted protein in the medium was precipitated by TCA and analysed by Coomassie blue stain. **(A)** Expression of CHIA-His₆ and untagged CHIA using the pPICZαC expression vector. **(B)** Expression of untagged CHIA using the pPIC9K vector. The empty vector sample is indicated by ev.

3.4.8 Analysis of homo-oligomerisation properties of CHIA

Since some CHIA-specific high-molecular weight protein bands were detected both in *Arabidopsis* (Figure 3-22D) and *E.coli* (Figure 3-24A, B) protein extracts, the homo-oligomerisation properties of CHIA were analysed more in detail in a yeast two-hybrid (Y2H) assay (Figure 3-26). The Y2H system is based on the ability of two hybrid proteins to interact with each other inducing thereby the induction of GAL4-regulated transcription of reporter genes. One of the hybrid proteins contains the DNA binding domain (DB) of the GAL4 transcription factor and the other the GAL4 activation domain (AD). The two constructs are combined with different selection markers (BD: tryptophan, W; AD: leucine, L). An interaction between the CHIA-BD and CHIA-AD due to homo-oligomer formation would then lead to the

reconstitution of the GAL4 transcription factor and induction of the transcription of reporter genes. The gene product of the reporter gene *Ade2* encodes an enzyme enabling the biosynthesis of adenine and the usage of specific media lacking adenine can be used to assay the interaction of the constructs. First, the transformation of the yeast cells was monitored using a drop test and medium lacking the amino acids tryptophan and leucine (Figure 3-26, -LT). Here all the tested combinations showed growth. The interaction medium contained no tryptophan, leucine and adenine (Figure 3-26, -LTA) and allowed growth of yeast cells only in the positive control. The positive control was the interaction between the SV40 large T-antigen and the murine p53 (pGAD-T + PGBK-53). The protein expression in the different combinations was verified using immunoblot analysis (data not shown). Thus, an ability of CHIA to form homo-oligomers was not detectable in the yeast two-hybrid assay. However, since Y2H assay is an artificial system further studies *in planta* are necessary.

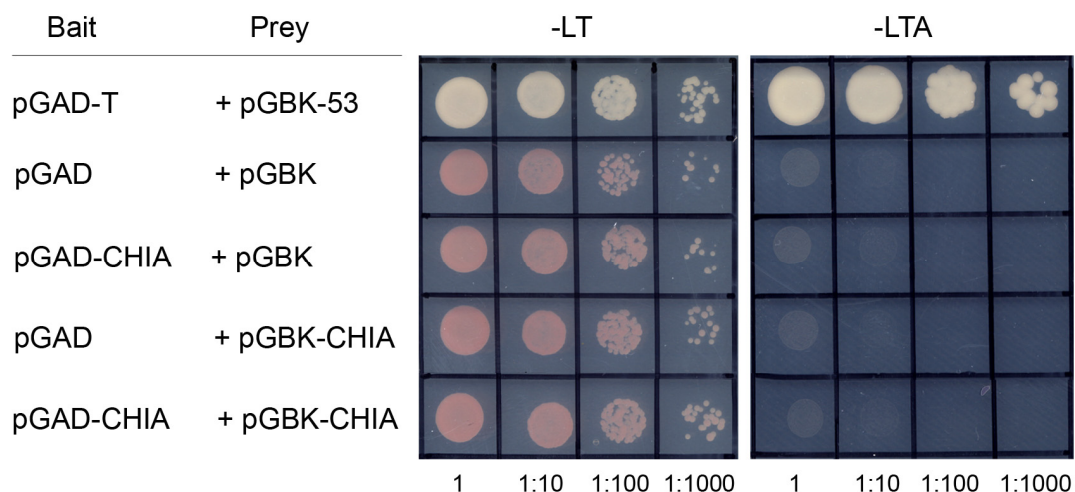


Figure 3-26: Yeast two-hybrid analysis

The homo-oligomerization property of CHIA was tested in an Y2H analysis. *CHIA* was cloned into the vectors pGADT7 and pGBKT7 and used against each other. Interaction was tested using synthetic dropout medium not containing leucine, tryptophan and adenine (-LTA). Shown are serial dilutions (1, 1:10, 1:100, and 1:1,000) of the corresponding yeast culture. The positive control was the interaction between the SV40 large T-antigen and murine p53 (pGAD-T and pGBK-53). The combinations pGAD + pGBK (empty vector), pGAD-CHIA + pGBK (auto-activation) and pGAD + pGBK-CHIA (auto-activation) served as negative controls.

3.4.9 Assessment of the chitin- and PGN-hydrolase activity of CHIA

To learn more about the function of the *Arabidopsis* CHIA chitinase its enzymatic properties in hydrolysis of chitin and peptidoglycan were assessed (chapters 2.5.11, 2.5.12 and 2.5.13). First, the chitinolytic activity of leaf extracts from transgenic *CHIA* lines and Col-0 plants towards the chitin derivate 4-methylumbelliferyl- β -D-N, N', N'' triacetylchitotriose (4-MUCT)

was measured after 4 hours of incubation (Figure 3-27A). The relative enzymatic activity was calculated using the activity of *Streptomyces griseus* chitinase as standard (*S.griseus* activity was set as 100 %). The transgenic *secGFP* line expressing secreted GFP was used as a control for external GFP. The background activity observed in the buffer control was approximately 5 % and the relative activities measured in the WT, *chia-kd* and *secGFP* samples were roughly 10 % of the *S. griseus* chitinase activity. The most active sample hydrolysing 4-MUCT was the *CHIA-oe* leaf protein extract, which showed a relative activity of almost 250 %. The strong activity of the *CHIA-oe* sample was already visible after 2 hours (data not shown). As another chitin substrate, colloidal chitin was used in a hydrolysis assay. In this assay the Col-0 leaf protein sample displayed approximately 27 % relative activity, whereas the two tested *CHIA-oe* samples showed a relative activity between 38 - 40 % (Figure 3-27B). However, these increased relative activities in the *CHIA-oe* samples were not significantly different from the Col-0 sample. Possibly the general chitinolytic activity against colloidal chitin resulting from other *Arabidopsis* chitinases present in the crude leaf extract add up to the resulting enzymatic activity. In contrast, 4-MUCT, might represent a specific substrate for class III chitinases. To explore the peptidoglycan hydrolysis capacity of the transgenic *CHIA* lines complex Lys-type peptidoglycan from intact Gram-positive *M.luteus* cells were used as substrate in a turbidity assay (Figure 3-27C). Here, similar activity patterns were observed as for the 4-MUCT substrate; Col-0, *chia-kd* and *secGFP* leaf samples showed similar activity levels (around 20 % of lysozyme activity which was set to 100%), whereas the *CHIA-oe* sample displayed the clearly strongest hydrolytic activity (120 %). In parallel, also the immunoprecipitated CHIA-GFP samples (see chapter 3.4.5 for details) were subjected to turbidity assay with *M.luteus* cells as substrate, but no activity was measured (data not shown). The lack of enzymatic activity in the IP samples might be due to sterical hindrance by the beads or the absence of essential co-factors, which were not immunoprecipitated. Ultimately, also purified insoluble Dap-type PGN from *Bacillus subtilis* was subjected to hydrolysis by the total leaf protein samples (Figure 3-27). Once again the leaf sample of the transgenic line overexpressing *CHIA* was most active (40 %) and the other tested leaf samples showed slightly higher activity than the buffer control (buffer: 3 %; Col-0, *chia-kd* and *secGFP*: 8 %).

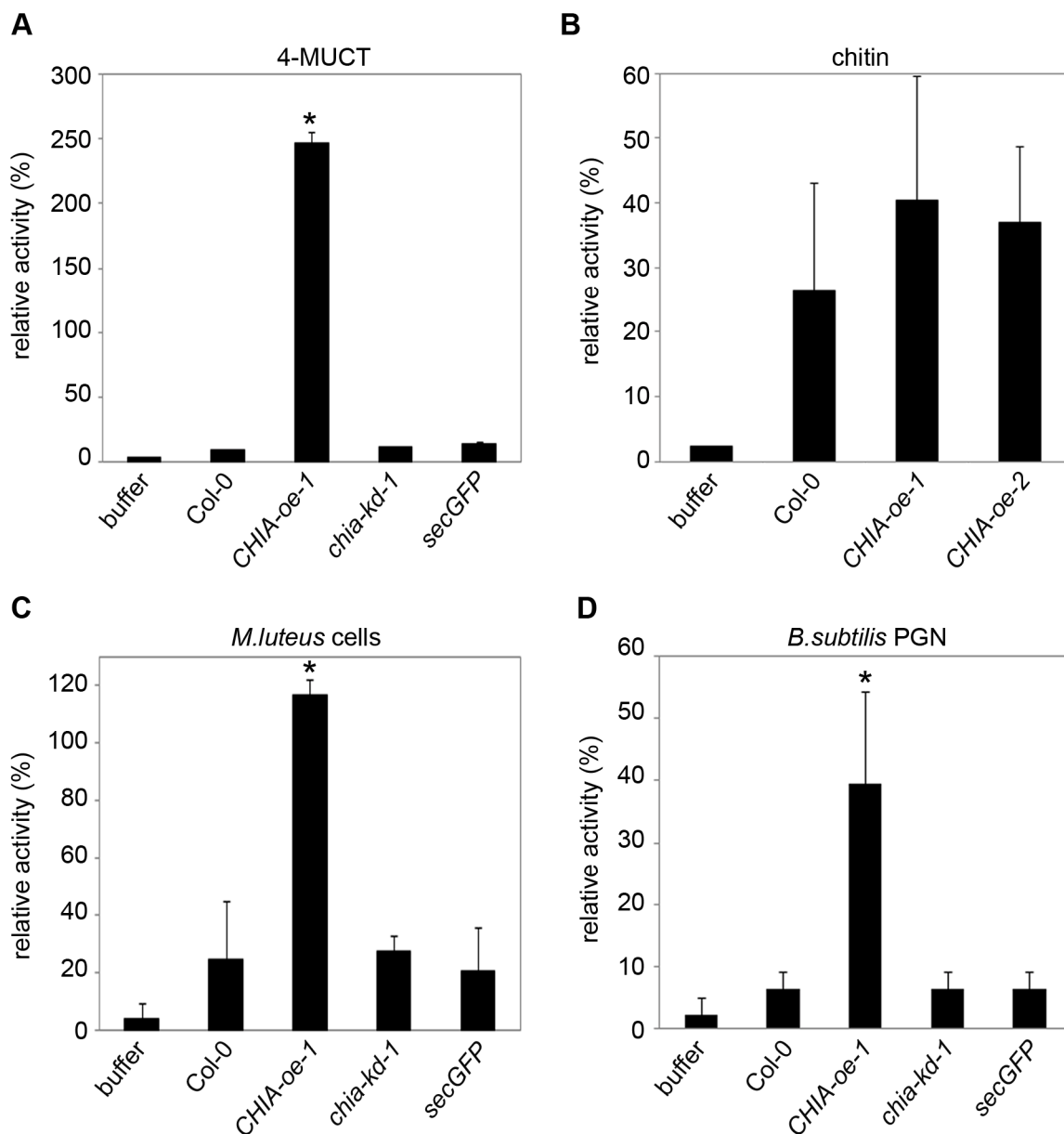


Figure 3-27: Chitin- and PGN-hydrolysis activity of CHIA leaf protein

Protein extracts from leaves of adult homozygous lines (*CHIA-oe*, *chia-kd*) were assayed for chitinolytic activity with 4-MUCT substrate (**A**) and colloidal chitin (**B**) or for PGN-hydrolytic activity against *M. luteus* cells in a turbidity assay (**C**). Relative activities (4 hrs post treatment) were calculated using *Streptomyces griseus* chitinase (A, B) or hen egg-white lysozyme (C) as standards. Plants expressing secreted GFP (secGFP) served to control the effect of external GFP. (**D**) *Bs* PGN was subjected to hydrolysis by leaf extracts for 2 hours, and PGN solubilization was calculated as in (C). 60 μ g total leaf protein was used per sample. Means and standard errors of two replicates per sample are given. Significant differences in enzyme activities relative to those in Col-0 are indicated (asterisks, $p \leq 0.05$ for A and C and $p \leq 0.09$ for D; Student's t-test).

The activity assays performed with the crude leaf protein extracts give no additional information about the localisation of the enzyme activity. To address the question, whether CHIA is really secreted and acts as an enzyme in the apoplast an approach using protoplasts was exploited. Protoplasts were isolated from WT and transgenic plants and incubated

overnight in the dark. The protoplasts were then gently separated from the medium and the secreted proteins in the medium were concentrated before usage in hydrolytic activity assays. In the 4-MUCT assay the majority of the chitinolytic activity was present in the secreted (supernatant) fraction of the *CHIA-oe* protoplast sample (Figure 3-28, 70 %) but a lot of activity was also present in the *CHIA-oe* protoplast pellet (40 %) indicating possible overexpression-related artefacts. The relative activity measured in the other samples was either very low (*chia-kd* and *secGFP* samples, 5%) or not detected at all (control samples and Col-0 samples). The PGN hydrolysis assay using *M. luteus* cells as substrate revealed that the secreted protein present in the *CHIA-oe* protoplast sample had the strongest PGN-hydrolysing properties (*CHIA-oe-S*, 50 %) compared to lysozyme activity. The *CHIA-oe* protoplast pellet displayed together with the Col-0 and *secGFP* samples relative activity levels between 10 - 15 %. Notably, the secreted protein fraction of the *chia-kd* protoplast sample was significantly less active than the corresponding WT sample. The presence of CHIA protein in the protoplast samples was confirmed by immunoblot analysis (Figure 3-28C). CHIA protein was detectable both in the *CHIA-oe* supernatant and protoplast sample. Interesting was the finding, that whereas in the pellet sample only CHIA-GFP could be visualised using the α -GFP antibody, in the supernatant sample exclusively processed CHIA protein lacking the GFP tag was detected with the α -class III chitinase antibody. A possible explanation for the differences in the protein pattern in the supernatant and pellet samples could be of biological but also technical nature. It is conceivable that the recombinant CHIA-GFP is proteolytically processed during the secretion pathway or that the additional enrichment step of the secreted protein samples led to enhanced protein degradation (2.5.4).

In conclusion, *CHIA* overexpression plants can hydrolyse both peptidoglycan and substrates derived from chitin indicating that the *Arabidopsis* CHIA protein represents an enzyme harboring both chitinolytic and PGN-hydrolysis activity. Furthermore, CHIA was able to degrade both Lys-type and Dap-type peptidoglycan substrates, presented by *M.luteus* and *B.subtilis* respectively, suggesting similarly broad PGN-specificity than the mammalian peptidoglycanolytic PGLYRP2 (Gelius et al., 2003). Detailed analysis using protoplasts showed also that the majority of the CHIA activity was indeed present in the secreted protein fraction of *CHIA-oe* protoplasts. The CHIA protein levels in uninduced wild type leaves are probably too low to be able to result in differences between WT and *chia-kd* protein extracts. Removal of the plant cell wall during protoplast preparation might lead to stress-induced induction of CHIA in the WT but not *chia-kd* sample. Hence, differences were visible only using protoplast samples (Figure 3-27), but not with leaf extracts (Figure 3-28). The inducibility of CHIA-derived activity in wild type plants and also the possibility of using

immunoprecipitated CHIA-GFP samples for the activity assays have to be further investigated.

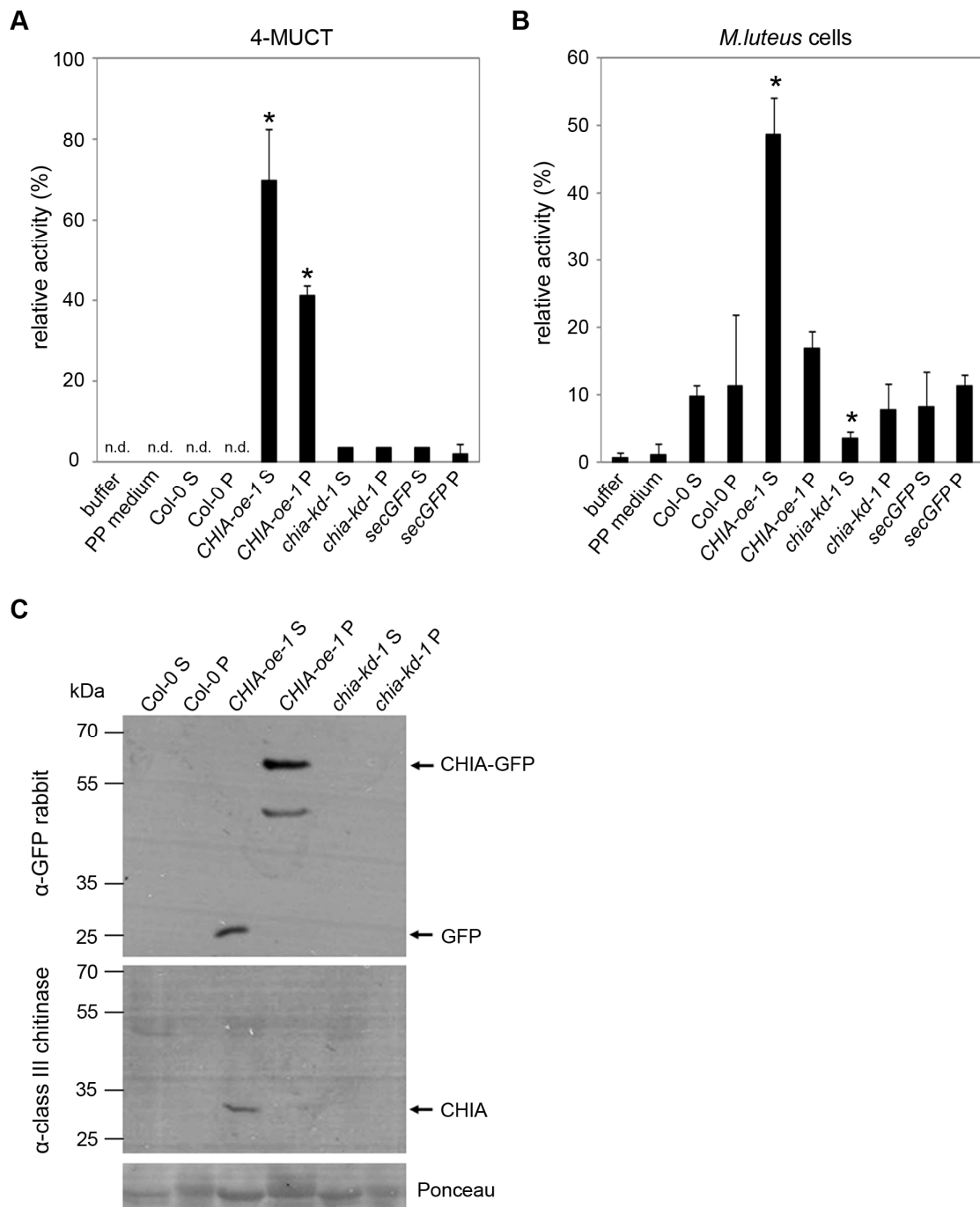


Figure 3-28: Chitin- and PGN-hydrolysis activity of CHIA protoplast samples

Protoplasts of transgenic lines were pelleted, and protein extracts of the pellet (P) or supernatant (S) was subjected to either hydrolysis of 4-MUCT (**A**) or *M.luteus* cells (**B**). The relative activities were calculated 3 hours post treatment as described in Figure 3-27. 15 μ g of total protein was used per sample. Means and standard errors of two replicates per sample are given. Significant differences in enzyme activities relative to those in Col-0 are indicated (asterisks, $p \leq 0.05$; Student's t-test). Samples with no measurable activity are indicated accordingly (not detected, n.d.). (**C**) CHIA protein levels in the supernatant and pellet samples were analysed by immunoblotting. The immunoblot analysis using α -GFP rabbit, α -class III chitinase rabbit and α -rabbit-HRP antibodies was carried out as described in Figure 3-22.

3.4.10 Role of *CHIA* in fungal resistance

The CHIA protein belongs to the family of chitinases, which are generally considered as pathogenesis-related (PR) proteins. Members of this family have been shown to degrade fungal cell walls and inhibit fungal growth *in vitro* (Arlorio et al., 1992; Mauch et al., 1988; Schlumbaum et al., 1986). Since CHIA also exhibited chitinolytic activity its influence in defending the plant from fungal infections was analysed.

3.4.10.1 Infection of the transgenic *CHIA* lines with *Botrytis cinerea*

Leaves of transgenic *CHIA* lines and WT plants were infected by drop-inoculation with the necrotrophic fungus *Botrytis cinerea* and kept under high humidity to provide optimal infection conditions for the pathogen. The disease symptoms were monitored two and three days post infection. A Trypan blue stain was used to visualise both fungal hyphae and dead plant cells (Figure 3-29A, B). The infection site after 2 days post infection appeared similar in all tested lines as shown in Figure 3-29A. Also the analysis of disease symptoms at a cellular level revealed no differences between the analysed lines (Figure 3-29B). The hyphal outgrowth and the cell death zones observed in the transgenic lines resembled the ones in WT plants. In addition to the infection symptoms also the size of the lesions was measured three days post infection (see Figure 3-29C). However, no significant differences were seen in the lesion sizes between transgenic *CHIA* lines and Col-0 plants. In total, the infection of the aggressive fungus *B.cinerea* proceeded in the *CHIA* overexpression and knock-down lines similarly as in the WT plants.

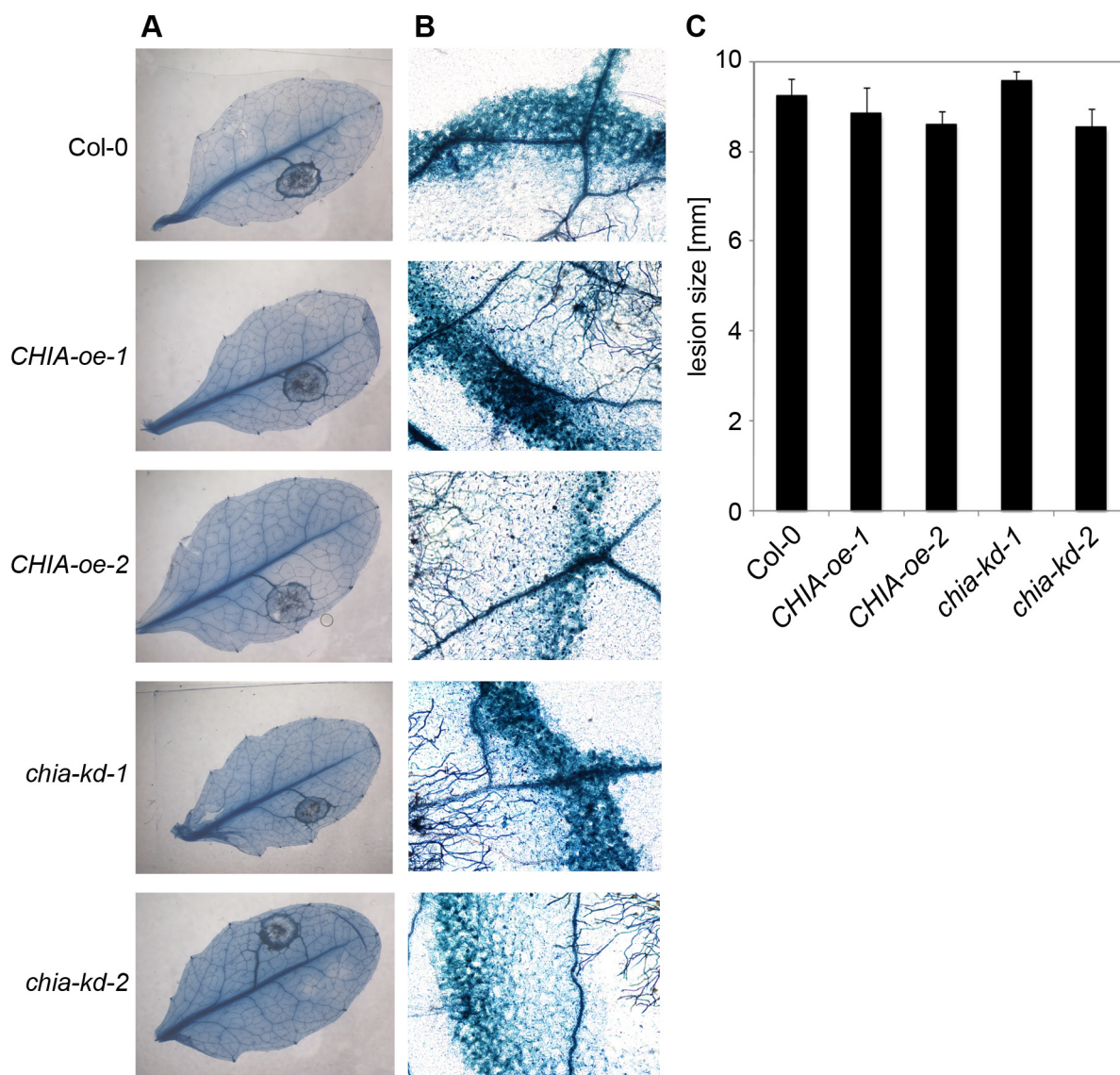


Figure 3-29: Infection of the transgenic *CHIA* lines with *Botrytis cinerea*

Five week-old plants were infected with the necrotrophic fungus *Botrytis cinerea*. 5 μ l spore suspension of 5×10^5 spores/ml was drop-inoculated on the one half of the leaf, two leaves per plant were infected. The plants were analysed for symptom development after 2 and 3 days post infection. **(A)** Trypan blue stain showing visible symptoms after 2 dpi. **(B)** Microscopic analysis of the infection site and fungal hyphae 2 dpi visualised by Trypan blue stain. **(C)** Measurement of the lesion size 3 days post infection. Shown are means and standard errors (n=16).

3.4.10.2 Infection of the transgenic *CHIA* lines with *Alternaria brassicicola*

Botrytis cinerea is an aggressive pathogen leading to massive maceration and cell death in the host tissue already at very early stages in the infection (Glazebrook, 2005). Thus, a weaker fungal pathogen causing disease symptoms after a longer time period might evoke differences in the progression of infection in the *CHIA-oe* or *chia-kd* lines when compared to WT plants. Therefore, fungal infection assays with the weaker necrotroph, *Alternaria*

brassicicola, were performed. Like *Botrytis*, *Alternaria* spores were also drop-inoculated on the leaf surface of the different lines and the infected plants were cultivated under high humidity. After 14 days post infection the leaves showed chlorosis and also necrosis spreading from the inoculation sites (Figure 3-30A, B). All the tested lines showed these disease symptoms, although the necrotic lesions displayed by the two *CHIA* overexpression lines appeared smaller and the lesions in the knock-down lines more drastic than in the WT plants. The microscopical analysis of the infection sites could not reveal major differences in the fungal hyphal growth in the tested lines as visualised by Trypan blue stain (Figure 3-30C). Additionally, also the course of the infection was monitored over a 14-day period and the degree of symptoms was determined as described in 2.6.2 (Figure 3-30D). After 7 days of infection the disease index was roughly 200 for all included lines. After 11 and 14 days the infection was more advanced and a slight tendency was visible; the *CHIA-oe* lines showed less and the *chia-kd* lines slightly more symptoms than the corresponding WT plants. However, these subtle differences could not be verified as being significant.

The results of the fungal infections cannot completely rule out the possibility that the *CHIA* chitinase is involved in fungal resistance. It is possible that it has a supportive role acting together with other chitinases or defense-related enzymes, like β -1,3-glucanases. In that case the generation of multiple KO mutants is most likely necessary to be able to get clear phenotypes in fungal defense.

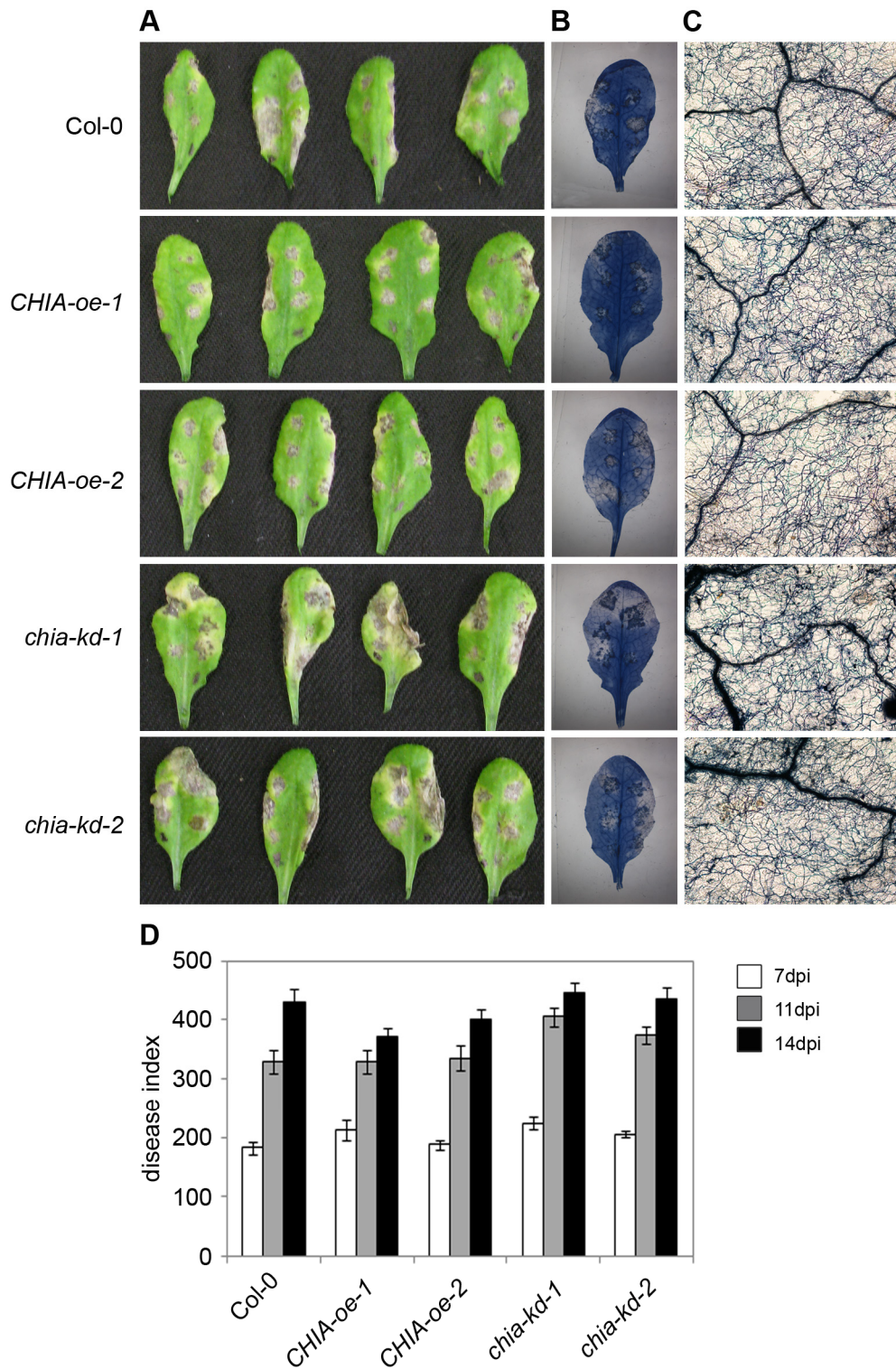


Figure 3-30: Infection of the transgenic CHIA lines with *Alternaria brassicicola*

Five week-old plants were infected with the necrotrophic fungus *Alternaria brassicicola*. Six 5 μ l droplets of spore suspension of 5×10^5 spores/ml were inoculated on the leaf, two leaves per plant were infected. The plants were analysed for symptom development after 7, 11 and 14 days post infection. **(A)** Visible symptoms of four independent leaves after 14 dpi. **(B)** Disease symptoms after 14 dpi visualised by Trypan blue stain. **(C)** Microscopic analysis of the infection site and fungal hyphae 14 dpi visualised by Trypan blue stain. **(D)** Calculation of the disease index 7, 11 and 14 days post infection. Shown are means and standard errors ($n=16$).

3.4.11 Impact of CHIA on bacterial resistance

As CHIA also had PGN-lytic activity, its importance in defending the plant against bacterial pathogens was assessed in bacterial infection assays (2.6.1). *Pseudomonas syringae* strains with different virulence properties were tested. First, leaves of transgenic *CHIA* lines and Col-0 plants were infiltrated with virulent *Pto* DC3000 bacteria and the growth of the bacteria was measured 4 days post infection (Figure 3-31A). Importantly, directly after the infiltration similar amounts of bacteria were counted in the leaves of the different lines enabling the comparison between the lines at later time points (0 days post infection). During the 4 days of infection the bacterial cells had propagated strongly, in the wild type leaves 10^7 colony forming units per cm^2 leaf tissue were measured (Figure 3-31A, Col-0). The two independent *CHIA* knock-down lines were significantly more susceptible to the virulent *Pseudomonas* strain than Col-0 (Figure 3-31A, *chia-kd-1* and *chia-kd-2*) indicating that CHIA is essential for the bacterial resistance. Unexpectedly, also the *CHIA-oe* plants allowed *Pto* DC3000 to grow better (nearly 10^9 cfu/ cm^2 leaf tissue) than WT plants. The susceptibility phenotype of the *CHIA-oe* lines was already visible 2 days post infection (data not shown). Next, the hypovirulent *Pto* DC3000 strain lacking *avrPto* and *PtoB* ($\Delta\text{avrPto/PtoB}$) was tested. The growth of *Pto* DC3000 $\Delta\text{avrPto/PtoB}$ was monitored 2 days after infiltration; both the two *chia-kd* lines and the two *CHIA-oe* lines showed significantly enhanced bacterial growth rates compared to WT plants (Figure 3-31B). 4 days post infection the susceptibility phenotype of the transgenic *CHIA* lines was no longer detectable (data not shown). The infection assays with the type III secretion system-deficient strain *Pto* DC3000 *hrcC*⁻ could so far deliver no significant differences between the transgenic *CHIA* lines and wild type plants (data not shown). Additionally, also the infection of the *CHIA* lines with the non-host strain *Pseudomonas syringae* pv. *phaseolicola* should be investigated.

The absence of *CHIA* led to a susceptibility phenotype upon infection with both the hypervirulent phytopathogenic bacteria *Pto* DC3000 and the less virulent mutant strain *Pto* DC3000 $\Delta\text{avrPto/PtoB}$. These data suggest that lack of PGN-degrading activity dampens plant immunity. The results showing more bacterial growth also in the *CHIA* overexpressing plants was unexpected. It seems that changes in the PGN-lytic activity provided by CHIA no matter in what direction lead to distorted bacterial resistance behavior. Follow-up experiments are needed to clarify the role of CHIA and its PGN-hydrolase activity in the protection against bacterial attack.

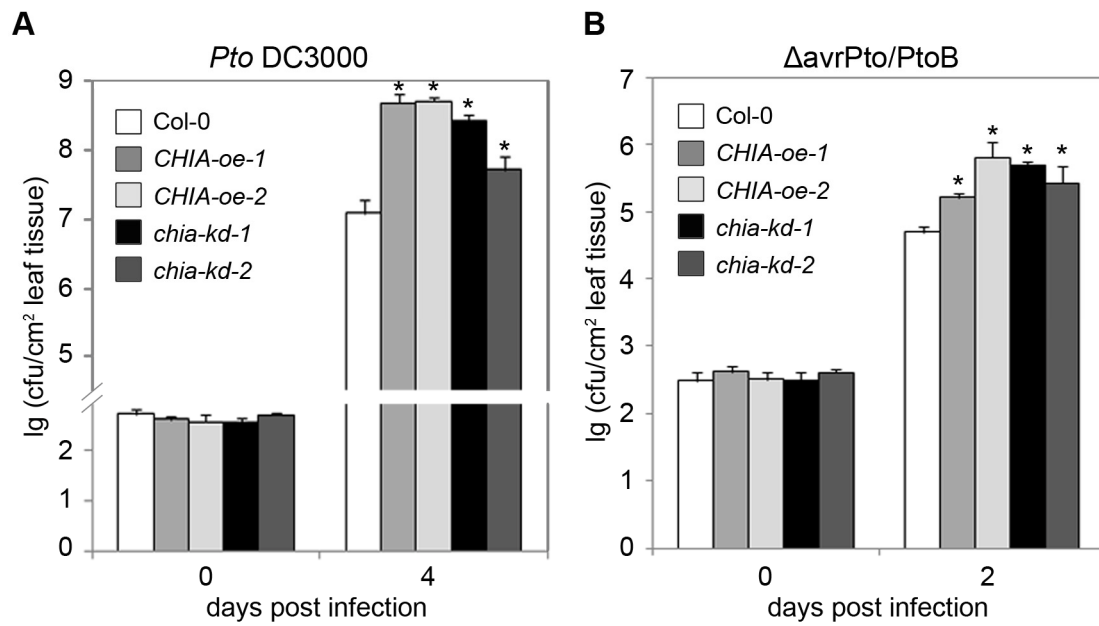


Figure 3-31: Infection of the transgenic *CHIA* lines with *Pseudomonas syringae*

Transgenic *CHIA* plants are hypersusceptible to bacterial infection. Growth of *Pto* DC3000 (**A**) and *Pto* DC3000 Δ avrPto/PtoB (**B**) was determined 2 or 4 days post infiltration of 10^4 colony forming units ml^{-1} (cfu/ml). Data represent means \pm SD of six replicate measurements/genotype/data point. Statistical significance compared to wild-type ($p \leq 0.05$, Student's t-test) is indicated by asterisks. Representative data of at least four independent experiments are shown.

4 Discussion

Although preliminary knowledge has been gathered in the past few years regarding bacterial peptidoglycans as bioactive stimuli of the plant immune response (Erbs et al., 2008; Gust et al., 2007), the molecular details of the perception mechanisms were still unresolved. In animals, the PGN sensing machinery is widely understood and distinct pathways encompassing a large variety of membrane-tethered and cytosolic receptors, PGN recognition proteins and PGN hydrolytic enzymes have been unraveled in the past decades (Royet and Dziarski, 2007). Several plant LysM-domain containing receptor-like kinases (LysM-RLKs or LYKs) are implicated in the recognition of glycan moieties, either during pathogenic host-fungi or symbiotic host-rhizobacteria interactions (Limpens et al., 2003; Miya et al., 2007; Radutoiu et al., 2003). Hence, a targeted reverse genetics approach was undertaken to search for peptidoglycan receptor(s) among the *Arabidopsis* family of LysM-RLKs.

Complex polymeric carbohydrates derived from pathogenic cell walls, such as fungal chitin and oomycete β -glucan, are preferably bound by corresponding plant high-affinity binding proteins in specific oligomeric fragment lengths (Fliegmann et al., 2004; Ito et al., 1997). Also polymeric peptidoglycan is processed by metazoan enzymes into smaller, yet still immunostimulatory fragments, which can then activate the corresponding signaling pathways (Chaput and Boneca, 2007; Wang et al., 2006; Zaidman-Rémy et al., 2006). As it could be shown that *Arabidopsis* is able to perceive not only complex but also fragmented peptidoglycan (Figure 3-12), it was also assayed whether PGN processing enzymes, which show similar activity than the animal PGN hydrolases, are present in *Arabidopsis thaliana* and contribute to bacterial immunity.

4.1 LYKs contribute to plant innate immunity

4.1.1 Effects of LYK gene deletions in plant fungal and bacterial resistance

Many proteins are controlled already at the level of gene transcription allowing stimulus-dependent increase or reduction of the gene products (Singh, 1998). Hence, changes in the gene expression pattern upon different developmental or environmental cues can give indications for possible protein functions. Interestingly, the expression of all investigated *LYK* genes showed a clear suppression either 6 or 24 hours after infection with the virulent *Pseudomonas syringae* pv. *tomato* DC3000 (Figure 3-2). Among the genes encoding *Arabidopsis* LysM proteins, also *LYM3* was similarly suppressed upon *Pto* DC3000 treatment (Willmann, 2011). Such infection-mediated transcriptional reduction has been shown to result

from the effector activity of plant pathogens (He et al., 2006). In contrast, the application of hypovirulent (*Pto hrcC*⁻) or non-host (*Pph*) strains led to an upregulation of the expression of *CERK1*, *LYK4* and *LYK5* genes (Figure 3-2). The expression profile of the *LYK3* gene differed most from the other *LYKs* upon bacterial infection displaying mainly different degrees of repression (Figure 3-2), however whether this *P.syringae*-dependent repression of *LYK3* also has a biological role remains to be clarified.

LYK2 gene was omitted from the analysis since the extremely low expression levels in leaf tissue make it the poorest receptor candidate during pathogen attack. In addition, the prediction of protein domains for *LYK2* gave no clear results regarding a LysM domain, however this might be due to some sequence variability within the lysin motif (Figure 3-2).

The expression profile analysis of the *LYK* gene family members is suggestive of a possible participation of *CERK1*, *LYK3*, *LYK4* and/or *LYK5* in bacterial resistance. *CERK1* was the first *Arabidopsis* *LYK* to be ascribed in pathogen resistance. Transgenic plants containing T-DNA insertions within the *CERK1* gene displayed severe reduced chitin-mediated defense responses and resulted in enhanced susceptibility against *Alternaria brassicicola* and *Erysiphe cichoracearum* (Miya et al., 2007; Wan et al., 2008). However, neither the tested *cerk1-2* mutant nor two other *lyk* mutants, *lyk3* and *lyk5*, showed more disease symptoms against the necrotrophic fungus *Botrytis cinerea* than wild type plants (Figure 3-6). This result suggests that either the loss of plant resistance to fungal pathogens is species-specific or that the degree of susceptibility is mild, hence the determination of disease symptoms requires more sophisticated detection methods. For instance, the amount of fungal growth in the infected leaves could be measured using quantitative RT-PCR to be able to discriminate between subtle differences in the WT and mutant plants (Gachon and Saindrenan, 2004). Additionally, the deletion of several *LYK* genes might result in a stronger fungal phenotype than observed for the single *cerk1* mutant (Miya et al., 2007; Wan et al., 2008). Therefore, it would be intriguing to analyse the generated triple mutant *cerk1 lyk3 lyk5* (Figure 3-11).

The impact of *LYK* mutations in the resistance against phytopathogenic bacteria was assessed using the Gram-negative hemibiotroph *Pseudomonas syringae*. Besides the hypervirulent WT strain *Pto* DC3000, also strains with diminished virulence due to deletion of certain effectors or the essential type III secretion system (no secretion of effectors at all) can be used to monitor the importance of host genes within bacterial immunity. Gimenez-Ibanez et al. (2009) reported that *CERK1* is additionally to its role in chitin perception a determinant of bacterial resistance. The *CERK1* gene depletion led to loss of bacterial growth restriction, thus allowing the TTSS-mutant strain *Pto hrcC*⁻ but also the virulent *Pto* DC3000 to propagate in an enhanced manner in the two independent mutant alleles in comparison to

WT plants. This susceptibility phenotype for *CERK1* depletion could also be observed in the infection assays performed in the frame of this work. Increased bacterial propagation was visible in the *cerk1-2* mutant post infection with *Pto* DC3000, *Pto* Δ avrPto/PtoB and *Pto* *hrcC*⁻ (Figure 3-7). Interesting was the result that also *lyk3* mutants displayed a susceptibility phenotype towards the virulent *Pseudomonas syringae* strain, *Pto* DC3000, indicating that LYK3 might, together with CERK1, contribute to plant immunity. The *lyk5* single mutants, but surprisingly also the *lyk3 lyk5* double mutants behaved similarly to wild type plants in bacterial infection assays (Figure 3-7). Possibly, the *lyk3* susceptibility phenotype is masked by the Landsberg erecta ecotype portion present in the double mutants. The bacterial susceptibility phenotype mediated by the *cerk1* and *lyk3* gene depletions and the repression of *CERK1* and *LYK3* expression upon the hypervirulent *Pto* DC3000 treatment together with the finding that the *Pseudomonas* effector protein AvrPtoB specifically targets CERK1 for degradation to promote bacterial virulence (Gimenez-Ibanez et al., 2009) deliver strong evidence for essential participation of CERK1, but maybe also of LYK3, in the formation and maintenance of bacterial immunity.

4.1.2 CERK1 serves together with LYM3 peptidoglycan recognition

Bacteria harbor a whole battery of known but also so far uncharacterised PAMPs (Nürnberg et al., 2004; Zipfel, 2009). To find out whether the recognition of the cell wall-derived PAMP peptidoglycan is connected to the discovered *cerk1*- or *lyk3*-dependent limitation of bacterial resistance, PGN-induced expression of defense-related genes was analysed in the *cerk1* and *lyk3* mutants. Interestingly, the depletion of the *CERK1* gene resulted in a similarly diminished response upon treatment of leaves or seedlings with Gram-negative PGN as seen for the *lym3* mutant (Figure 3-8 and Willmann (2011)). LYM3 was shown to bind both Gram-negative and Gram-positive peptidoglycan in a reversible and ligand-specific manner and transgenic *Arabidopsis* plants lacking the functional *LYM3* gene were not only PGN-insensitive but allowed also more growth of *Pseudomonas syringae* (Willmann, 2011). The assessment of the effects of PGN treatment on the global gene expression revealed a dramatic PGN-insensitivity in the *cerk1* mutant when compared to WT plants (Figure 3-10). Also mutants lacking LYM3 were not responsive to PGN treatment and showed a massive deregulation of the global gene expression (Willmann, 2011). The reduction of PGN-mediated defense gene expression both in the *cerk1* and *lym3* mutants was not only measured for Dap-type but also for Lys-type PGN derived from *Staphylococcus aureus* (Willmann, 2011), suggesting that the identified LysM receptor proteins are part of a peptidoglycan sensing system, which is responsible for the perception of different peptidoglycan subtypes. In addition, also soluble PGN structures activated the defense gene

expression in a LYM3/CERK1-dependent manner (Figure 3-12 and Willmann (2011)). The obvious lack of discrimination between differences in complexity and peptide bond of peptidoglycan resembles the broad ligand specificity of the mammalian PGN receptor Nod2 (Girardin et al., 2003b; Inohara et al., 2003), however the minimal PGN motif recognised by Nod2, the muramyl dipeptide (MDP), is not able to activate the plant immune response (Gust et al., 2007). Instead, the results obtained so far substantiate the significance of the glycan moiety for the *Arabidopsis* perception system. Mutanolysin-mediated complete digestion of the glycosyl bonds of peptidoglycan but not the cleavage of glycyglycine bonds within the peptide moiety by lysostaphin abolished the immunogenic properties of *Sa* PGN (Gust et al., 2007). Thus, it is likely that the chain length and possibly also the spatial structure of peptidoglycan are crucial parameters for the recognition. For instance, the *Drosophila* PGRP-LC cannot sense PGN monomers or dimers, indicating similar recognition preferences for longer glycan chains than the *Arabidopsis* PGN complex (Leulier et al., 2003). Moreover, the *Drosophila* PGRP-SA apparently perceives only PGN, which was preprocessed by the glucanase activity of GGBP1 (Filipe et al., 2005; Wang et al., 2006). Also plant LysM proteins seem to prefer carbohydrate ligands of specific chain length, because the rice LysM-domain receptor protein CEBiP was shown to require for binding chitin oligomers a degree of polymerisation (DP) > 6 (Ito et al., 1997; Okada et al., 2002).

Interestingly, the plant LysM proteins mediate via recognition of oligosaccharide structures as different processes as defense activation and symbiotic interactions. The lipochito-oligosaccharide-induced nodulation processes in leguminous plants require LysM-containing receptor kinases. For instance, the receptor pairs of NFR1/NFR5 (Figure 4-1) and LYK3/LYK4 are essential for the establishment of symbiosis with rhizobacteria in *Lotus japonicus* and *Medicago truncatula* respectively (Limpens et al., 2003; Radutoiu et al., 2003). Unfortunately, the formation of hetero-oligomeric complexes or direct binding to Nod factors has not been shown for neither in *Lotus* nor *Medicago* systems. The perception of chitin in rice is coordinated by the two receptor proteins CEBiP and OsCERK1 (Kaku et al., 2006; Miya et al., 2007; Wan et al., 2008) (Figure 4-1). In the presence of chitin oligosaccharides a portion of these proteins form a heteromeric complex in rice cells, however only CEBiP has been shown to bind to chitin (Kaku et al., 2006; Shimizu et al., 2010). In *Arabidopsis*, CERK1 is the only so far characterised LysM receptor protein essential for chitin-triggered activation defense responses and it also binds directly chitin *in vitro* (Iizasa et al., 2010; Miya et al., 2007) (Figure 4-1). The *Arabidopsis* PGN perception system mediated by CERK1 and LYM3 adds up to the versatility of LysM-protein functions in plants (Figure 4-1). As CERK1 displays no or only very weak PGN binding (Willmann, 2011), it seems to function exclusively as signal transducer upon PGN recognition by LYM3. There are *in vitro* indications for the

formation of an CERK1/LYM3 complex, as interaction was observed both in yeast two hybrid-assay and far western analysis (Willmann, 2011). Whether the functional PGN receptor consisting of CERK1 and LYM3 requires physical interaction between these two proteins *in planta*, remains to be elucidated. Similarly, the possible participation of additional LysM proteins, like LYK3, within the recognition process is still unclear. Although all these plant carbohydrate ligand receptors share many structural characteristics with each other, there are yet differences in their binding and signaling properties rendering the needed specificity (Nakagawa et al., 2010; Wan et al., 2008). Intriguingly, the discovery of the *Arabidopsis* CERK1/LYM3-based PGN perception system, that is analogous to the rice OsCERK1/CEBiP complex detecting chitin, indicates that plants employ two types of PRRs for the recognition of distinct types of PAMPs. The LRR-receptor kinases preferentially detect proteinous microbial signatures, whereas the LysM-domain containing receptor proteins contribute to plant innate immunity by perceiving carbohydrate-derived PAMPs.

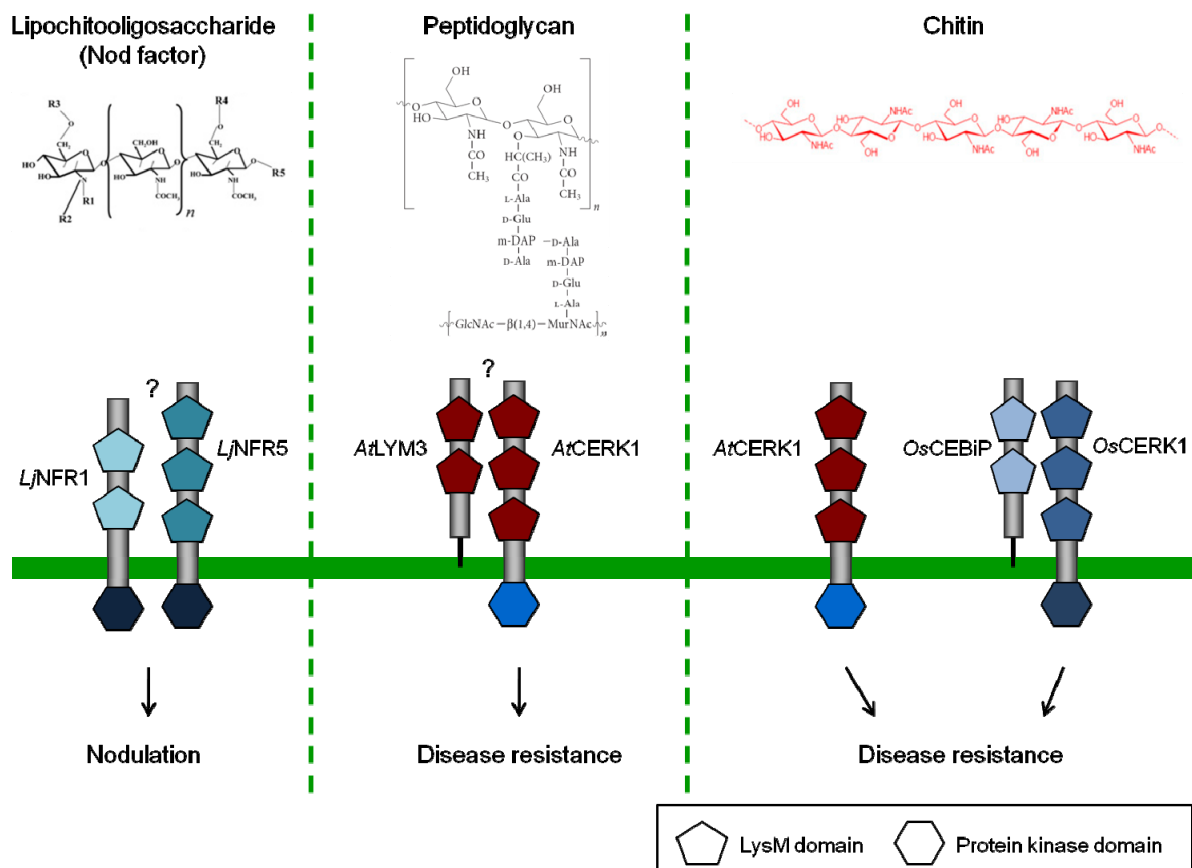


Figure 4-1: Plant perception and signaling of carbohydrate PAMPs/MAMPs

Bacterial peptidoglycan is structurally similar to fungal chitin and rhizobacteria-derived lipochitooligosaccharides (Nod factors). The corresponding LysM receptor kinases or proteins from *Arabidopsis thaliana* (*At*), *Oryza sativa* (*Os*) and *Lotus japonicus* (*Lj*) also share sequence similarities. OsCEBiP and OsCERK1 interact with each other *in planta* (Shimizu et al., 2010). Based on Eckardt (2008).

4.2 CHIA chitinase is involved in plant innate immunity

PGRPs and lysozymes carry out various tasks in metazoan innate immunity. The enzymatically active PGRPs and lysozymes can act directly bactericidal but also modulate the defense responses by PGN hydrolysis (Callewaert and Michiels, 2010; Dziarski and Gupta, 2010; Royet and Dziarski, 2007). Plants possess neither lysozyme nor PGRP encoding genes. However, among plant chitinases are members, which harbor lysozyme-like peptidoglycan hydrolysis activity (Heitz et al., 1994; Majeau et al., 1990; Park et al., 2002). One such well-characterised enzyme is the class III chitinase hevamine from *Hevea brasiliensis* (Bokma et al., 1997). Lysozyme and hevamine both hydrolyse $\beta(1\rightarrow4)$ glycosidic bonds in the glycan backbone, however they differ in the cleavage sites. Lysozyme cleaves between MurNAc and GlcNAc (muramidase activity) and hevamine between GlcNAc and MurNAc (glucosaminidase activity) (Bokma et al., 1997; Tipper et al., 1964). Only one *Arabidopsis* chitinase could be identified sharing high sequence homology to the rubber tree hevamine, and this acidic endochitinase (CHIA) is additionally the only member of the class III chitinases (Figure 3-13 and Figure 3-14).

Chitinases similar to other plant PR proteins are characterised by the inducibility of their expression upon pathogen infection (Kasprzewska, 2003). The analysis of the expression profile of *CHIA* revealed that its transcription in leaves was induced not only upon fungal infection but additionally also upon infection with phytopathogenic *Pseudomonas syringae* (Figure 3-15). The verification of the microarray data was achieved using transgenic *CHIA* promoter-GUS reporter plants. As GUS activity can be irreversibly stained in the analysed leaf tissue even weak activation of the promoter can be visualised. The fungal infections with *Alternaria brassicicola* and *Botrytis cinerea* resulted in relatively low but visible activation of the *CHIA* promoter (Figure 3-16B). Earlier data showed similar *CHIA* promoter activation upon treatment with *Rhizoctonia solani* (Samac and Shah, 1991). Bacterial infection turned on the *CHIA* promoter in a strong manner, however only using the less-virulent *Pto* hrcC⁻ and the non-compatible *Pph* strains (Figure 3-16C). The *CHIA* promoter was not activated upon treatment with the virulent *Pto* DC3000 strain. These results point to effector-mediated suppression indicating that *CHIA* might be essential combating bacterial pathogens. The activation of the *CHIA* promoter took exclusively place within the infected tissue region in the leaf, suggesting a local host response only. The slight discrepancy between the results with *Pto* DC3000 infection in the microarray and in the promoter-GUS analysis might result from differences in the condition of the used strains (Figure 3-15 and Figure 3-16). Depending on the age of the plated culture, the bacteria can display differences in their virulence. It is possible that the strain used for the microarray was less aggressive still allowing some stimulation of the *CHIA* promoter, whereas the strain used for the infection of *pCHIA::GUS*

plants was highly virulent suppressing the promoter completely. Interesting was also the observation that peptidoglycan and chitin treatment led either to no or only to moderate activation of the *CHIA* promoter, but the strong PAMP flagellin induced the promoter almost as good as *Pto hrcC* (Figure 3-16A and C). Obviously not only pathogenic fungi and bacteria but also conserved and highly immunogenic bacterial signatures are sufficient to trigger the expression of the *CHIA* gene.

CHIA is expressed constitutively at low levels in natural openings like hydathodes and stomatal guard cells (Samac and Shah, 1991). Although the accumulation of CHIA protein in the apoplastic space connected to these specific leaf regions has not been shown yet, it suggests that CHIA is indeed a part of the secreted defense armory of the plant. Possibly, some CHIA protein is always present but that a pathogenic attack leads to its enhanced production and accumulation in the apoplast. This postulation is supported by the finding that CHIA was among the secreted cell wall proteins in non-stressed cultured *Arabidopsis* cells (Kwon et al., 2005).

4.2.1 Chitinolytic activity of CHIA and its impact on fungal immunity

Many plant chitinases have been characterised regarding their ability to hydrolyse fungal cell walls and to contribute to innate immunity (Arlorio et al., 1992; Boller et al., 1983; Mauch et al., 1988; Onaga and Taira, 2008). However, so far only few *Arabidopsis* chitinases have been functionally analysed (Passarinho and De Vries, 2002). The enzymatic properties of the *Arabidopsis* class III chitinase, CHIA, were assayed using protein extracts from transgenic *CHIA* overexpression and knock-down lines. CHIA protein was detectable in the overexpression plants via the GFP-tag but also using an antibody against tobacco class III chitinases (Figure 3-22A-C). The class III chitinase antibody seemed also to recognise the *Arabidopsis* class III chitinase present in high amounts in the *CHIA-oe* leaves (Figure 3-22B). However, in the WT leaves the CHIA amounts were probably too low for detection.

The *CHIA-oe* leaf extracts displayed a very strong hydrolytic activity towards a chitin-derivate, 4-MUCT, in comparison to the WT extract, which only showed basal activity (Figure 3-27A). Colloidal chitin was more or less equally hydrolysed by the *CHIA-oe* and WT extracts (Figure 3-27B). The obtained experimental data strongly implicates that CHIA is a functional enzyme possessing chitinolytic activity. The results further suggest, that 4-MUCT could be a chitin substrate, which is preferentially cleaved by the class III chitinase, whereas colloidal chitin might be rather favoured by the other *Arabidopsis* chitinases, present in both *CHIA-oe* and WT leaf extracts. In fact, similar strong activity towards 4-MUCT was also obtained for tobacco class III chitinases, whereas chitinases of the classes I, II, IV and V showed only

little or no enzymatic activity (Brunner et al., 1998). The analysis of the protoplast samples showed that the majority of 4-MUCT degrading activity was harbored within the *CHIA-oe* secreted protein fraction (Figure 3-28A). Unexpectedly, no differences were seen between the activity in the *chia-kd* and WT or *secGFP* control samples. This raises the question whether the induction of *CHIA* upon treatment with pathogenic fungi or the fungal PAMP chitin could result in differences in the different genotypes (see also chapter 4.2).

The observed chitin-degrading activity of extracts from *CHIA-oe* plants led to the assumption that CHIA could contribute to host immunity. Thus, the *CHIA* overexpression lines might be more resistant and the *CHIA* knock-down lines more susceptible to fungal pathogens. Fungal infection assays with the necrotrophs *Botrytis cinerea* and *Alternaria brassicicola* revealed only insignificant but still interesting tendencies (Figure 3-29 and Figure 3-30). Especially in the case of *Alternaria* infection, the degree of disease symptoms was somewhat lower in the *CHIA-oe* and higher in *chia-kd* plants, but still the differences were not significant (Figure 3-30A and D). It is feasible, that the chitinolytic activity of CHIA supports the fungal resistance in *Arabidopsis*, but that due to redundancy among the chitinase members, the loss of one chitinase is not dramatically weakening the plant immunity towards fungal pathogens. Indeed, up to now only little *in vivo* data is presented for the role of single chitinases in fungal resistance (Benhamou et al., 1990; Broque et al., 1991). Moreover, even the depletion of the sole chitin receptor, CERK1, leads only to a very weak fungal growth phenotype in *Arabidopsis* (Miya et al., 2007; Wan et al., 2008). Further examinations are needed to strengthen the supposition of CHIA being a part of the fungal resistance machinery using *in vitro* antifungal assays and analysis of mutants carrying multiple chitinase gene deletions.

4.2.2 PGN-lytic activity of CHIA and its importance to bacterial immunity

The chitinolytic activity observed in the transgenic plants overexpressing *CHIA*, demonstrated that this enzyme can cleave complex carbohydrate structures. Whether this *Arabidopsis* chitinase also degrades the heteromeric glycan backbone of peptidoglycan and displays a lysozyme-like activity characteristic for some plant chitinases of the classes III and V (Passarinho and De Vries, 2002), was determined in turbidity assays. The reduction of turbidity in a suspension of insoluble substrate, like purified peptidoglycan or bacterial cells containing intact cell walls, is a good indicator for enzymatic degradation of such complex structures into soluble and less turbid fragments. The PGN-hydrolysing activity of lysozyme, the standard PGN hydrolase used as reference in turbidity assays (Brunner et al., 1998; Park et al., 2002), leads to complete lysis of bacteria and clarification of the suspension within

short incubation times. The leaf protein extract of *CHIA-oe* displayed towards the *Micrococcus luteus* cell walls very high hydrolysis activity, whereas the activity of both WT and *chia-kd* extracts was low (Figure 3-27C). In the beginning, the activity of *CHIA-oe* extract was lower than that of lysozyme, reaching however similar reduction in turbidity after 4 hours. Since the approaches to purify CHIA from the leaf extracts by immunoprecipitation (Figure 3-22) or to heterologously express it in a highly active form (Figure 3-24 and Figure 3-25) failed so far, the determination of specific enzymatic properties of CHIA are still to be clarified. Despite the indications for a formation of CHIA dimers *in vivo* (Figure 3-22 and Figure 3-24), the homooligomerisation could not be observed *in vitro* (Figure 3-26). It is also possible that other yet unknown plant proteins present in the crude extract are interacting with and affecting the enzymatic properties of CHIA. Further experiments are needed to show in which functional form CHIA is operating and whether CHIA is interacting with components of the PGN receptor complex. Interestingly, in addition to the Gram-positive *M.luteus* cell walls containing Lys-type PGN, *CHIA-oe* extracts also hydrolysed purified Dap-type PGN from *Bacillus subtilis* (Figure 3-27D). This indicates that CHIA is able to cleave the glycosidic bonds in both PGN subtypes. Also the *Arabidopsis* PGN receptor proteins, LYM3 and CERK1, display similar broad PGN specificity. Not all peptidoglycans are suitable substrates for CHIA or other PGN hydrolases though. The *CHIA-oe* leaf extract was unable to degrade *Staphylococcus aureus* PGN (data not shown). Similar results have also been reported for lysozyme (Bera et al., 2007). The resistance against PGN degradation displayed by *S.aureus* enhances virulence and is due to peptidoglycan modifications including O-acetylation and heavy cross-linking and associated wall teichoic acids. The majority of the PGN-hydrolysing activity in the *CHIA-oe* leaves was harbored in the secreted protein fraction as shown by the protoplast assays (Figure 3-28B). Furthermore, the CHIA protein was detectable in the secretion sample (Figure 3-28C). These observations once more support the earlier indications of CHIA being targeted into the apoplast (see chapter 4.2).

Intriguingly, the PGN-degrading properties of CHIA seem to be linked to bacterial immunity. The infection of *CHIA* knock-down lines with the hypervirulent *Pto* DC3000 resulted in increased bacterial propagation in comparison to WT plants (Figure 3-31A). Even the hypovirulent *P.syringae* mutant strain lacking the effectors *avrPto* and *avrPtoB* (*Pto* DC3000 Δ *avrPto/PtoB*) was able to grow better in the *chia-kd* plants (Figure 3-31B). Thus, CHIA obviously contributes to bacterial resistance in *Arabidopsis* and can be regarded as an innate immunity protein. Similarly, the depletion of lysozyme M and the resulting decrease of PGN hydrolysis and antimicrobial activity led to enhanced susceptibility towards *Streptococcus pneumoniae* infection in mice (Shimada et al., 2008). However, the analysis of the *CHIA* overexpression lines in bacterial infection assays delivered unexpected results. Instead of

being more resistant against *P.syringae*, the *CHIA-oe* lines showed similar susceptibility as the *chia-kd* lines upon infection with either hypervirulent or less-virulent strains (Figure 3-31A-C). Despite the dramatic differences in the PGN hydrolysis properties of *CHIA* overexpression and knock-down lines, both genotypes display a similar output phenotype being less resistant towards the Gram-negative phytopathogen *P.syringae*. One possible role of CHIA in defending *Arabidopsis* plants during bacterial attack is the release of immunogenic PGN fragments with a defined chain length, which upon recognition by a PGN receptor could enhance the activation of downstream responses. In such case, both the complete loss of PGN hydrolase activity but also too strong activity cleaving PGN into fragment lengths, which no longer stimulate the innate immune system, would have devastating effects. This correlates with the precedence of the rice LysM protein, OsCEBiP, to bind chitin chains only with a specific degree of polymerization (Ito et al., 1997; Okada et al., 2002) and might also be true for AtLYM3 regarding PGN binding. Hence, the detailed analysis of the PGN fragments produced by CHIA is crucial for understanding the molecular basis for its action. Another possibility is that CHIA is, like lysozyme, able to directly inhibit bacterial growth by massive lysis. However, this hypothesis would not explain why the *CHIA* overexpression lines are also more susceptible. Although the *CHIA-oe* plants do not show any dramatic phenotypic alterations, the presence of overexpression-derived artefacts cannot be totally excluded. The *in vitro* analysis of antibacterial activity with either highly purified *Arabidopsis* CHIA or recombinantly expressed CHIA could enlighten its mode of action. CHIA gets posttranslationally glycosylated (Figure 3-23), hence expression systems relying on eukaryotic hosts, such as yeast or insect cells, are needed for the production of active CHIA. In addition, it would also be important to test a Gram-positive phytobacterium in the bacterial infection assays to see whether the impact of CHIA, but also CERK1 and LYM3, is similar to that observed upon *Pseudomonas* infection. For example, the Gram-positive phytopathogen *Rhodococcus fascians* (Hogenhout and Loria, 2008) could be tested to see whether the broad PGN specificity observed for all three innate immunity proteins, CHIA, CERK1 and LYM3, also contributes to the formation and maintenance of resistance against both Gram-negative and Gram-positive pathogenic bacteria in *Arabidopsis thaliana*.

4.3 Peptidoglycan perception systems have arisen through convergent evolution in metazoans and plants

The experimental data obtained during this work and in Willmann (2011) revealed novel insights into peptidoglycan perception in plants allowing for the first time a kingdom-wide comparison. Similar to invertebrates and higher animals, also plants possess a peptidoglycan pattern recognition machinery operating in the innate immunity and especially

in the resistance against bacterial pathogens. Whereas the recognition of peptidoglycan structures in metazoans is mainly mediated by proteins containing LRRs or PGRP domains (Royet and Dziarski, 2007), the newly characterised plant PGN receptors are designated by the presence of LysM domains. Also PGN hydrolysing activity that contributes to host immunity is found across the phylae. So far, all identified plant PGN hydrolases belong to glucosaminidases, thus displaying different cleavage specificity than lysozymes (muramidase) or enzymatically active PGRPs (amidase) in animals (Bokma et al., 1997; Dziarski and Gupta, 2010; Park et al., 2002; Royet and Dziarski, 2007). Thus, the proteins involved in the PGN degradation and recognition processes vary not only in their domain features but also in their specificities pointing strongly to convergent evolution of these systems in the different eukaryotic lineages.

5 Summary

Plants as sessile organisms cannot escape, when they are confronted with harmful pathogens. Instead, they are weaponed with sophisticated and highly complex molecular responses that allow them to defend themselves. The innate immunity forms the basis for the self-defense of higher organisms, including mammals, invertebrates and plants. During the basal immune response, conserved microbial signatures are perceived by pattern recognition receptors and trigger a variety of defense reactions leading to protection of the plant tissue and resistance. The bacterial cell wall component peptidoglycan (PGN) is one of such conserved signatures activating the plant defense responses, however the molecular mechanisms of its recognition was until now not understood.

The importance of LysM-domain containing plant proteins in the recognition of carbohydrate ligands, such as chitin and lipochitooligosaccharides, has been elucidated in the last years (Kaku et al., 2006; Limpens et al., 2003; Madsen et al., 2003; Miya et al., 2007). Due to the structural similarities between chitin, lipochitooligosaccharide and peptidoglycan, members of this protein family provide interesting candidates for a putative PGN receptor. The reverse genetics approach performed in this work revealed a LysM receptor kinase, CERK1, to be involved in PGN perception. CERK1 is not only essential for the PGN-mediated activation of defense responses in *Arabidopsis thaliana*, it also contributes to bacterial resistance. Consequently, CERK1 is a dual player within plant immunity, as it is important for both the recognition of carbohydrate signatures derived of both fungi and bacteria. The in parallel identified LysM protein, LYM3, binds PGN and is also essential for PGN-responsiveness and bacterial resistance (Willmann, 2011). As LYM3 lacks a signaling domain the obtained data suggest that CERK1 and LYM3 form a functional receptor complex and are both needed for PGN-triggered immunity towards bacterial infection.

The second focus of this work was to analyse the possible PGN processing properties of *Arabidopsis*. Studies on analogous, complex polymeric ligands, like fungal chitin and oomycete β -glucan and the corresponding perception systems in plants (Fliegmann et al., 2004; Ito et al., 1997), but also peptidoglycan perception in animals (Filipe et al., 2005; Leulier et al., 2003) gave indications for such processing events. In addition, both complex and fragmented peptidoglycans act immunostimulatory in *Arabidopsis*, and are recognised by the same CERK1/LYM3-based receptor system. Therefore, the class III chitinase CHIA, a putative PGN hydrolase, was analysed regarding its role in peptidoglycan degradation and bacterial immunity. CHIA possesses both chitinolytic and peptidoglycan-hydrolysing activity, as observed with *CHIA-oe* leaf protein extracts but also with protein derived from the secreted fraction of *CHIA-oe* protoplasts. Both Gram-positive and Gram-negative

peptidoglycan subtypes can be cleaved by CHIA. The posttranslational glycosylation and apoplastic localisation of CHIA depend on the N-terminal secretion signal. Absence or excess of CHIA-dependent PGN hydrolysis affects the plant defense response towards bacterial pathogens in a negative manner, suggesting that CHIA is a plant innate immunity protein contributing to bacterial resistance.

6 Zusammenfassung

Pflanzen sind sessile Organismen und können daher nicht vor schädigenden Pathogenen flüchten. Stattdessen sind sie mit raffinierten und hochkomplexen zellulären Mechanismen bewaffnet, die es ihnen ermöglichen sich zu wehren. Die angeborene Immunität bildet dabei die Grundlage für die Selbstverteidigung von höheren Organismen, wie Säugetieren, Invertebraten und Pflanzen. Während der basalen Immunantwort werden hochkonservierte mikrobielle Signaturen von Mustererkennungsrezeptoren (PRR, „pattern recognition receptor“) erkannt und eine Reihe von Abwehrreaktionen ausgelöst, die die Pflanze vor Schäden schützen und den Pathogenangriff abwehren. Peptidoglycan (PGN) ist als Bestandteil der bakteriellen Zellwand eine solche konservierte Signatur, die in der Lage ist die pflanzliche Abwehrantwort zu aktivieren. Allerdings sind die molekularen Mechanismen, die zu der Erkennung von PGN führen noch weitgehend unerforscht.

Die Bedeutung von pflanzlichen Proteinen mit LysM-Domänen in der Erkennung von kohlenhydrathaltigen Liganden, wie Chitin und Lipochitooligosacchariden, wurde in den letzten Jahren belegt (Kaku et al., 2006; Limpens et al., 2003; Madsen et al., 2003; Miya et al., 2007). Aufgrund der ähnlichen Struktur von Chitin, Lipochitooligosacchariden und Peptidoglycan liefern die Mitglieder dieser Protein-Familie interessante Kandidaten für einen möglichen PGN-Rezeptor. Während dieser Arbeit konnte mit einem Reversen Genetik-Ansatz der LysM-Rezeptor Kinase, CERK1, eine Rolle in der Peptidoglycan Perzeption zugeschrieben werden. CERK1 ist nicht nur notwendig für die PGN-vermittelte Aktivierung von Abwehrreaktionen in *Arabidopsis thaliana*, sondern auch für die bakterielle Resistenz. Somit ist CERK1 ein dualer Spieler der pflanzlichen Immunität, da es bedeutsam für die Erkennung von Kohlenhydrat-Signaturen sowohl pilzlichen als auch bakteriellen Ursprungs ist. Das zeitgleich identifizierte LysM Protein, LYM3, bindet PGN und ist ebenfalls sowohl für die PGN-Erkennung als auch für die bakterielle Resistenz unabdingbar (Willmann, 2011). Da LYM3 eine Signaltransduktionsdomäne fehlt, deuten die Ergebnisse auf einen funktionellen Komplex aus CERK1 und LYM3, wobei beide für die von PGN ausgelöste Immunität gegen bakterielle Erreger essentiell sind.

Im zweiten Teil dieser Arbeit wurde Fokus auf die PGN Prozessierung in *Arabidopsis* gelegt. Studien an analogen und ähnlich komplexen polymeren Liganden, wie zum Beispiel Chitin aus Pilzen und β -Glucan aus Oomyceten, und den dazugehörigen pflanzlichen Erkennungssystemen (Fliegmann et al., 2004; Ito et al., 1997), aber auch der PGN-Perzeption der Tieren (Filipe et al., 2005; Leulier et al., 2003) lieferten Indizien für solche Prozessierungsvorgänge. Darüber hinaus stimulieren sowohl komplexes als auch fragmentiertes Peptidoglycan die Immunantwort in *Arabidopsis* und beides wird über das

gleiche CERK1/LYM3-Rezeptorsystem erkannt. Deshalb wurde die Klasse III Chitinase CHIA, eine putative PGN Hydrolase, hinsichtlich einer möglichen Rolle in der Peptidoglycan-Degradierung und der bakteriellen Immunität untersucht. CHIA besitzt sowohl chitinolytische als auch PGN-hydrolytische Aktivität. Diese Aktivität wurde in Proteinextrakten aus Blättern und auch der sekretierten Fraktion von Protoplasten von *CHIA* überexprimierenden *Arabidopsis* Pflanzen detektiert. Beide Subtypen von PGN, Gram-positiv und Gram-negativ, können von CHIA hydrolysiert werden. Die posttranslationelle Glykosylierung von CHIA und deren Sekretion in den Apoplasten sind abhängig von der N-terminalen Signalsequenz. Des Weiteren hat die Abwesenheit oder das Übermaß der CHIA-vermittelten PGN-Hydrolyse einen negativen Einfluss auf die pflanzliche Abwehr gegenüber bakteriellen Pathogenen. Infolgedessen gehört auch CHIA zu den Proteinen der angeborenen Immunität und trägt zur bakteriellen Resistenz bei.

7 References

- Abramovitch, R.B., Anderson, J.C., and Martin, G.B.** (2006). Bacterial elicitation and evasion of plant innate immunity. *Nat Rev Mol Cell Biol* 7, 601-611.
- Apel, K., and Hirt, H.** (2004). REACTIVE OXYGEN SPECIES: Metabolism, Oxidative Stress, and Signal Transduction. *Annu Rev Plant Biol* 55, 373-399.
- Arlorio, M., Ludwig, A., Boller, T., and Bonfante, P.** (1992). Inhibition of fungal growth by plant chitinases and -1,3-glucanases. *Protoplasma* 171, 34-43.
- Arrighi, J., Barre, A., Ben Amor, B., Bersoult, A., Soriano, L., Mirabella, R., Carvalho-Niebel, F., Journet, E., Gherardi, M., and Huguet, T.** (2006). The *Medicago truncatula* lysin motif-receptor-like kinase gene family includes NFP and new nodule-expressed genes. *Plant Physiol* 142, 265 - 279.
- Asai, T., Tena, G., Plotnikova, J., Willmann, M.R., Chiu, W.-L., Gomez-Gomez, L., Boller, T., Ausubel, F.M., and Sheen, J.** (2002). MAP kinase signalling cascade in Arabidopsis innate immunity. *Nature* 415, 977-983.
- Ausubel, F.M.** (2005). Are innate immune signaling pathways in plants and animals conserved? *Nat Immunol* 6, 973-979.
- Ausubel, F.M., Brent, R., Kingston, R.E., Moore, D.D., Seidman, J.G., Smith, J.A., Struhl, K.** (1993). *Current protocols in molecular biology* (NY, John Wiley and Sons).
- Basbous, N., Coste, F., Leone, P., Vincentelli, R., Royet, J., Kellenberger, C., and Roussel, A.** (2011). The *Drosophila* peptidoglycan-recognition protein LF interacts with peptidoglycan-recognition protein LC to downregulate the Imd pathway. *EMBO Rep* 12, 327-333.
- Bateman, A., and Bycroft, M.** (2000). The structure of a LysM domain from *E. coli* membrane-bound lytic murein transglycosylase D (MltD). *J Mol Biol* 299, 1113-1119.
- Belvin, M.P., and Anderson, K.V.** (1996). A CONSERVED SIGNALING PATHWAY: The *Drosophila* Toll-Dorsal Pathway. *Annu Rev Cell Dev Biol* 12, 393-416.
- Benhamou, N., Joosten, M., and de Wit, P.** (1990). Subcellular localization of chitinase and of its potential substrate in tomato root tissues infected by *Fusarium oxysporium f.sp. radicis-lycopersici*. *Plant Physiol* 92, 1108-1120.
- Bensadoun, A., and Weinstein, D.** (1976). Assay of proteins in the presence of interfering materials. *Anal Biochem* 70, 241-250.
- Bera, A., Biswas, R., Herbert, S., Kulauzovic, E., Weidenmaier, C., Peschel, A., and Götz, F.** (2007). Influence of Wall Teichoic Acid on Lysozyme Resistance in *Staphylococcus aureus*. *J Bacteriol* 189, 280-283.
- Bera, A., Herbert, S., Jakob, A., Vollmer, W., and Götz, F.** (2005). Why are pathogenic staphylococci so lysozyme resistant? The peptidoglycan O-acetyltransferase OatA is the

major determinant for lysozyme resistance of *Staphylococcus aureus*. *Mol Microbiol* 55, 778-787.

Bergman, L.W. (2001). Growth and maintenance of yeast. *Methods Mol Biol* 177, 9-14.

Bielnicki, J., Devedjiev, Y., Derewenda, U., Dauter, Z., Joachimiak, A., and Derewenda, Z.S. (2006). *B. subtilis* ykuD protein at 2.0 Å resolution: Insights into the structure and function of a novel, ubiquitous family of bacterial enzymes (Wiley Subscription Services, Inc., A Wiley Company), pp. 144-151.

Bischoff, V., Vignal, C., Boneca, I.G., Michel, T., Hoffmann, J.A., and Royet, J. (2004). Function of the drosophila pattern-recognition receptor PGRP-SD in the detection of Gram-positive bacteria. *Nat Immunol* 5, 1175-1180.

Bischoff, V., Vignal, C., Duvic, B., Boneca, I.G., Hoffmann, J.A., and Royet, J. (2006). Downregulation of the *Drosophila* Immune Response by Peptidoglycan-Recognition Proteins SC1 and SC2. *PLoS Pathog* 2, e14.

Biswas, R., Voggu, L., Simon, U.K., Hentschel, P., Thumm, G., and Gotz, F. (2006). Activity of the major staphylococcal autolysin Atl. *FEMS Microbiol Lett* 259, 260-268.

Blume, B., Nürnberger, T., Nass, N., and Scheel, D. (2000). Receptor-Mediated Increase in Cytoplasmic Free Calcium Required for Activation of Pathogen Defense in Parsley. *Plant Cell* 12, 1425-1440.

Boch, J., and Bonas, U. (2001). Gram-negative plant pathogenic bacteria. *Contrib Microbiol* 8, 186-196.

Bokma, E., van Koningsveld, G., Jeronimus-Stratingh, M., and Beintema, J. (1997). Hevamine, a chitinase from the rubber tree *Hevea brasiliensis*, cleaves peptidoglycan between the C-1 of N-acetylglucosamine and C-4 of N-acetylmuramic acid and therefore is not a lysozyme. *FEBS Lett* 411, 161-163.

Boller, T. (1995). Chemoperception of Microbial Signals in Plant Cells. *Annu Rev Plant Physiol Plant Mol Biol* 46, 189-214.

Boller, T., Gehri, A., Mauch, F., and Vögeli, U. (1983). Chitinase in bean leaves: induction by ethylene, purification, properties, and possible function. *Planta* 157, 22-31.

Bolstad, B.M., Irizarry, R.A., Astrand, M., and Speed, T.P. (2003). A comparison of normalization methods for high density oligonucleotide array data based on variance and bias. *Bioinformatics* 19, 185-193.

Bolte, S., Talbot, C., Boutte, Y., Catrice, O., Read, N.D., and Satiat-Jeunemaitre, B. (2004). FM-dyes as experimental probes for dissecting vesicle trafficking in living plant cells. *J Microsc* 214, 159-173.

Boothby, D., Daneo-Moore, L., Higgins, M.L., Coyette, J., and Schockman, G.D. (1973). Turnover of bacterial cell wall peptidoglycans. *J Biol Chem* 248, 2161-2169.

Boudsocq, M., Willmann, M.R., McCormack, M., Lee, H., Shan, L., He, P., Bush, J., Cheng, S.-H., and Sheen, J. (2010). Differential innate immune signalling via Ca²⁺ sensor protein kinases. *Nature* 464, 418-422.

- Bradford, M.M.** (1976). A rapid and sensitive method for the quantitation of microgram quantities of protein utilizing the principle of protein-dye binding. *Anal Biochem* 72, 248-254.
- Brameld, K.A., and Goddard, W.A.** (1998). The role of enzyme distortion in the single displacement mechanism of family 19 chitinases. *PNAS* 95, 4276-4281.
- Broque, K., Chet, I., Holliday, M., Cressman, R., Biddle, P., Knowlton, S., Mauvais, C., and Broglie, R.** (1991). Transgenic Plants with Enhanced Resistance to the Fungal Pathogen *Rhizoctonia solani* *Science* 22, 1194-1197.
- Brunner, F., Rosahl, S., Lee, J., Rudd, J.J., Geiler, C., Kauppinen, S., Rasmussen, G., Scheel, D., and Nürnberger, T.** (2002). Pep-13, a plant defense-inducing pathogen-associated pattern from *Phytophthora* transglutaminases. *Embo J* 21, 6681-6688.
- Brunner, F., Stintzi, A., Fritig, B., and Legrand, M.** (1998). Substrate of tobacco chitinases. *Plant J* 14, 225-234.
- Bubeck Wardenburg, J., Williams, W.A., and Missiakas, D.** (2006). Host defenses against *Staphylococcus aureus* infection require recognition of bacterial lipoproteins. *PNAS* 103, 13831-13836.
- Buist, G., Steen, A., Kok, J., and Kuipers, O.P.** (2008). LysM, a widely distributed protein motif for binding to (peptido)glycans. *Mol Microbiol* 68, 838-847.
- Büttner, D., and Bonas, U.** (2006). Who comes first? How plant pathogenic bacteria orchestrate type III secretion. *Curr Opin Microbiol* 9, 193-200.
- Cabeen, M.T., and Jacobs-Wagner, C.** (2005). Bacterial cell shape. *Nat Rev Micro* 3, 601-610.
- Callewaert, L., and Michiels, C.W.** (2010). Lysozymes in the animal kingdom. *J Biosci* 35, 127-160.
- Caplan, J., Padmanabhan, M., and Dinesh-Kumar, S.P.** (2008). Plant NB-LRR Immune Receptors: From Recognition to Transcriptional Reprogramming. *Cell Host Microbe* 3, 126-135.
- Chamaillard, M., Hashimoto, M., Horie, Y., Masumoto, J., Qiu, S., Saab, L., Ogura, Y., Kawasaki, A., Fukase, K., Kusumoto, S., *et al.*** (2003). An essential role for NOD1 in host recognition of bacterial peptidoglycan containing diaminopimelic acid. *Nat Immunol* 4, 702-707.
- Chaput, C., and Boneca, I.G.** (2007). Peptidoglycan detection by mammals and flies. *Microb Infect* 9, 637-647.
- Chisholm, S.T., Coaker, G., Day, B., and Staskawicz, B.J.** (2006). Host-microbe interactions: shaping the evolution of the plant immune response. *Cell* 124, 803-814.
- Cho, J.H., Fraser, I.P., Fukase, K., Kusumoto, S., Fujimoto, Y., Stahl, G.L., and Ezekowitz, R.A.B.** (2005). Human peptidoglycan recognition protein S is an effector of neutrophil-mediated innate immunity. *Blood* 106, 2551-2558.
- Choe, K.-M., Werner, T., Stöven, S., Hultmark, D., and Anderson, K.V.** (2002). Requirement for a Peptidoglycan Recognition Protein (PGRP) in Relish Activation and Antibacterial Immune Responses in *Drosophila*. *Science* 296, 359-362.

- Chomczynski, P., and Sacchi, N.** (1987). Single-step method of RNA isolation by acid guanidinium thiocyanate-phenol-chloroform extraction. *Anal Biochem* *162*, 156-159.
- Clarke, A., and Dupont, C.** (1992). O-acetylated peptidoglycan: its occurrence, pathobiological significance and biosynthesis. *Can J Microbiol* *38*, 85-91.
- Clough, S.J., and Bent, A.F.** (1998). Floral dip: a simplified method for *Agrobacterium*-mediated transformation of *Arabidopsis thaliana*. *The Plant Journal* *16*, 735-743.
- Cohen-Kupiec, R., and Chet, I.** (1998). The molecular biology of chitin digestion. *Curr Opin Biotechnol* *9*, 270-277.
- Collinge, D.B., Kragh, K.M., Mikkelsen, J.D., Nielsen, K.K., Rasmussen, U., and Vad, K.** (1993). Plant Chitinases. *Plant J* *3*, 31-40.
- Cosio, E.G., Frey, T., Verduyn, R., van Boom, J., and Ebel, J.** (1990). High-affinity binding of a synthetic heptaglucoside and fungal glucan phytoalexin elicitors to soybean membranes. *FEBS Lett* *271*, 223-226.
- D'Ovidio, R., Mattei, B., Roberti, S., and Bellincampi, D.** (2004). Polygalacturonases, polygalacturonase-inhibiting proteins and pectic oligomers in plant-pathogen interactions. *Biochim Biophys Acta* *1696*, 237-244.
- Da Silva, C.A., Hartl, D., Liu, W., Lee, C.G., and Elias, J.A.** (2008). TLR-2 and IL-17A in Chitin-Induced Macrophage Activation and Acute Inflammation. *J Immunol* *181*, 4279-4286.
- de Azambuja, P., Garcia, E.S., Ratcliffe, N.A., and David Warthen Jr, J.** (1991). Immune-depression in *Rhodnius prolixus* induced by the growth inhibitor, azadirachtin. *J Insect Physiol* *37*, 771-777.
- de Jonge, R., Peter van Esse, H., Kombrink, A., Shinya, T., Desaki, Y., Bours, R., van der Krol, S., Shibuya, N., Joosten, M.H.A.J., and Thomma, B.P.H.J.** (2010). Conserved Fungal LysM Effector Ecp6 Prevents Chitin-Triggered Immunity in Plants. *Science* *329*, 953-955.
- Dow, M., Newman, M.-A., and von Roepenack, E.** (2000). The Induction and Modulation of Plant Defense Responses by Bacterial Lipopolysaccharides. *Annu Rev Phytopathol* *38*, 241-261.
- Dziarski, R., and Gupta, D.** (2005a). Peptidoglycan recognition in innate immunity. *J Endotoxin Res* *11*, 304-310.
- Dziarski, R., and Gupta, D.** (2005b). *Staphylococcus aureus* peptidoglycan is a toll-like receptor 2 activator: a reevaluation. *Infect Immun* *73*, 5212-5216.
- Dziarski, R., and Gupta, D.** (2006). Mammalian PGRPs: novel antibacterial proteins. *Cell Microbiol* *8*, 1059-1069.
- Dziarski, R., and Gupta, D.** (2010). Mammalian peptidoglycan recognition proteins (PGRPs) in innate immunity. *Innate Immun* *16*, 168-174.
- Dziarski, R., Tapping, R.I., and Tobias, P.S.** (1998). Binding of Bacterial Peptidoglycan to CD14. *J Biol Chem* *273*, 8680-8690.

- Eckardt, N.A.** (2008). Chitin Signaling in Plants: Insights into the Perception of Fungal Pathogens and Rhizobacterial Symbionts. *Plant Cell* 20, 241-243.
- Edwards, K., Johnstone, C., and Thompson, C.** (1991). A Simple and Rapid Method for the Preparation of Plant Genomic DNA for Pcr Analysis. *Nucleic Acids Res* 19, 1349-1349.
- Erbs, G., Silipo, A., Aslam, S., De Castro, C., Liparoti, V., Flagiello, A., Pucci, P., Lanzetta, R., Parrilli, M., Molinaro, A., et al.** (2008). Peptidoglycan and muropeptides from pathogens *Agrobacterium* and *Xanthomonas* elicit plant innate immunity: structure and activity. *Chem Biol* 15, 438-448.
- Felix, G., Duran, J.D., Volko, S., and Boller, T.** (1999). Plants have a sensitive perception system for the most conserved domain of bacterial flagellin. *Plant J* 18, 265-276.
- Felix, G., Regenass, M., and Boller, T.** (1993). Specific Perception of Subnanomolar Concentrations of Chitin Fragments by Tomato Cells - Induction of Extracellular Alkalinization, Changes in Protein-Phosphorylation, and Establishment of a Refractory State. *Plant J* 4, 307-316.
- Filipe, S.R., Tomasz, A., and Ligoxygakis, P.** (2005). Requirements of peptidoglycan structure that allow detection by the *Drosophila* Toll pathway. *EMBO Rep* 6, 327-333.
- Fliegmann, J., Mithöfer, A., Wanner, G., and Ebel, J.** (2004). An Ancient Enzyme Domain Hidden in the Putative β -Glucan Elicitor Receptor of Soybean May Play an Active Part in the Perception of Pathogen-associated Molecular Patterns during Broad Host Resistance. *J Biol Chem* 279, 1132-1140.
- Flors, V., Ton, J., Jakab, G., and Mauch-Mani, B.** (2005). Abscisic acid and callose: team players in defense against pathogens? In *J Phytopathol* (Berlin, Blackwell Verlag), pp. 377-383.
- Gachon, C., and Saindrenan, P.** (2004). Real-time PCR monitoring of fungal development in *Arabidopsis thaliana* infected by *Alternaria brassicicola* and *Botrytis cinerea*. *Plant Physiol Biochem* 42, 367-371.
- Garver, L.S., Wu, J., and Wu, L.P.** (2006). The peptidoglycan recognition protein PGRP-SC1a is essential for Toll signaling and phagocytosis of *Staphylococcus aureus* in *Drosophila*. *PNAS* 103, 660-665.
- Gelius, E., Persson, C., Karlsson, J., and Steiner, H.** (2003). A mammalian peptidoglycan recognition protein with N-acetylmuramoyl-L-alanine amidase activity. *Biochem Biophys Res Commun* 306, 988-994.
- Gietz, R.D., and Woods, R.A.** (2002). Transformation of yeast by lithium acetate/single-stranded carrier DNA/polyethylene glycol method. *Methods Enzymol* 350, 87-96.
- Gimenez-Ibanez, S., Hann, D.R., Ntoukakis, V., Petutschnig, E., Lipka, V., and Rathjen, J.P.** (2009). AvrPtoB targets the LysM receptor kinase CERK1 to promote bacterial virulence on plants. *Curr Biol* 19, 423-429.
- Girardin, S.E., Boneca, I.G., Carneiro, L.A.M., Antignac, A., Jéhanno, M., Viala, J., Tedin, K., Taha, M.-K., Labigne, A., Zähringer, U., et al.** (2003a). Nod1 Detects a Unique Muropeptide from Gram-Negative Bacterial Peptidoglycan. *Science* 300, 1584-1587.

- Girardin, S.E., Boneca, I.G., Viala, J., Chamaillard, M., Labigne, A., Thomas, G., Philpott, D.J., and Sansonetti, P.J.** (2003b). Nod2 Is a General Sensor of Peptidoglycan through Muramyl Dipeptide (MDP) Detection. *J Biol Chem* 278, 8869-8872.
- Girardin, S.E., and Philpott, D.J.** (2004). Mini-review: The role of peptidoglycan recognition in innate immunity (WILEY-VCH Verlag), pp. 1777-1782.
- Glauner, B.** (1988). Separation and quantification of muropeptides with high-performance liquid chromatography. *Anal Biochem* 172, 451-464.
- Glauner, B., Höltje, J.V., and Schwarz, U.** (1988). The composition of the murein of *Escherichia coli*. *J Biol Chem* 263, 10088-10095.
- Glazebrook, J.** (2005). Contrasting Mechanisms of Defense Against Biotrophic and Necrotrophic Pathogens. *Annu Rev Phytopathol* 43, 205-227.
- Gómez-Gómez, L., and Boller, T.** (2000). FLS2: An LRR Receptor-like Kinase Involved in the Perception of the Bacterial Elicitor Flagellin in *Arabidopsis*. *Mol Cell* 5, 1003-1011.
- Gómez-Gómez, L., Felix, G., and Boller, T.** (1999). A single locus determines sensitivity to bacterial flagellin in *Arabidopsis thaliana*. *Plant J* 18, 277-284.
- Goodell, E.W.** (1985). Recycling of murein by *Escherichia coli*. *J Bacteriol* 163, 305-310.
- Gottar, M., Gobert, V., Michel, T., Belvin, M., Duyk, G., Hoffmann, J.A., Ferrandon, D., and Royet, J.** (2002). The *Drosophila* immune response against Gram-negative bacteria is mediated by a peptidoglycan recognition protein. *Nature* 416, 640-644.
- Guan, R., Roychowdhury, A., Ember, B., Kumar, S., Boons, G.-J., and Mariuzza, R.A.** (2004). Structural basis for peptidoglycan binding by peptidoglycan recognition proteins. *PNAS* 101, 17168-17173.
- Gupta, D., Kirkland, T.N., Viriyakosol, S., and Dziarski, R.** (1996). CD14 Is a Cell-activating Receptor for Bacterial Peptidoglycan. *J Biol Chem* 271, 23310-23316.
- Gust, A.A., Biswas, R., Lenz, H.D., Rauhut, T., Ranf, S., Kemmerling, B., Götz, F., Glawischnig, E., Lee, J., Felix, G., et al.** (2007). Bacteria-derived peptidoglycans constitute pathogen-associated molecular patterns triggering innate immunity in *Arabidopsis*. *J Biol Chem* 282, 32338-32348.
- Hauck, P., Thilmony, R., and He, S.Y.** (2003). A *Pseudomonas syringae* type III effector suppresses cell wall-based extracellular defense in susceptible *Arabidopsis* plants. *PNAS* 100, 8577-8582.
- Hayashi, F., Smith, K.D., Ozinsky, A., Hawn, T.R., Yi, E.C., Goodlett, D.R., Eng, J.K., Akira, S., Underhill, D.M., and Aderem, A.** (2001). The innate immune response to bacterial flagellin is mediated by Toll-like receptor 5. *Nature* 410, 1099-1103.
- He, P., Shan, L., Lin, N.-C., Martin, G.B., Kemmerling, B., Nürnberger, T., and Sheen, J.** (2006). Specific Bacterial Suppressors of MAMP Signaling Upstream of MAPKKK in *Arabidopsis* Innate Immunity. *Cell* 125, 563-575.
- Heitz, T., Segond, S., Kauffmann, S., Geoffroy, P., Prasad, V., Brunner, F., Fritig, B., and Legrand, M.** (1994). Molecular characterization of a novel tobacco pathogenesis-related (PR) protein: a new plant chitinase/lysozyme. *Mol Gen Genet* 245, 246-254.

- Hellens, R.P., Edwards, E.A., Leyland, N.R., Bean, S., and Mullineaux, P.M.** (2000). pGreen: a versatile and flexible binary Ti vector for Agrobacterium-mediated plant transformation. *Plant Mol Biol* 42, 819-832.
- Henrissat, B.** (1991). A classification of glycosyl hydrolases based on amino acid sequence similarities. *Biochem J* 280, 309-316.
- Hogenhout, S.A., and Loria, R.** (2008). Virulence mechanisms of Gram-positive plant pathogenic bacteria. *Curr Opin Plant Biol* 11, 449-456.
- Hojjer, M., Melief, M.-J., Debets, R., and Hazenberg, M.** (1997). Inflammatory properties of peptidoglycan are decreased after degradation with human N-Acetylmuramyl-L-alanine amidase. *Eur Cytokine Network* 8, 375-382.
- Höltje, J.-V.** (1998). Growth of the Stress-Bearing and Shape-Maintaining Murein Sacculus of *Escherichia coli*. *Microbiol Mol Biol Rev* 62, 181-203.
- Hornig, T., and Medzhitov, R.** (2001). Drosophila MyD88 is an adapter in the Toll signaling pathway. *PNAS* 98, 12654-12658.
- Hückelhoven, R.** (2007). Cell Wall Associated Mechanisms of Disease Resistance and Susceptibility. *Annu Rev Phytopathol* 45, 101-127.
- Huffaker, A., and Ryan, C.A.** (2007). Endogenous peptide defense signals in Arabidopsis differentially amplify signaling for the innate immune response. *PNAS* 104, 10732-10736.
- Iizasa, E., Mitsutomi, M., and Nagano, Y.** (2010). Direct binding of a plant LysM receptor-like kinase, LysM RLK1/CERK1, to chitin in vitro. *J Biol Chem* 285, 2996-3004.
- Imler, J.-L., and Hoffmann, J.A.** (2001). Toll receptors in innate immunity. *Trends Cell Biol* 11, 304-311.
- Indrasumunar, A., Kereszt, A., Searle, I., Miyagi, M., Li, D., Nguyen, C.D.T., Men, A., Carroll, B.J., and Gresshoff, P.M.** (2010). Inactivation of Duplicated Nod Factor Receptor 5 (NFR5) Genes in Recessive Loss-of-Function Non-Nodulation Mutants of Allotetraploid Soybean (*Glycine max* L. Merr.). *Plant Cell Physiol* 51, 201-214.
- Inohara, N., Chamillard, M., McDonald, C., and Nuñez, G.** (2005). NOD-LRR PROTEINS: Role in Host-Microbial Interactions and Inflammatory Disease. *Annu Rev Biochem* 74, 355-383.
- Inohara, N., Ogura, Y., Fontalba, A., Gutierrez, O., Pons, F., Crespo, J., Fukase, K., Inamura, S., Kusumoto, S., Hashimoto, M., et al.** (2003). Host Recognition of Bacterial Muramyl Dipeptide Mediated through NOD2. *J Biol Chem* 278, 5509-5512.
- Irizarry, R.A., Hobbs, B., Collin, F., Beazer-Barclay, Y.D., Antonellis, K.J., Scherf, U., and Speed, T.P.** (2003). Exploration, normalization, and summaries of high density oligonucleotide array probe level data. *Biostatistics* 4, 249-264.
- Ito, Y., Kaku, H., and Shibuya, N.** (1997). Identification of a high-affinity binding protein for N-acetylchitooligosaccharide elicitor in the plasma membrane of suspension-cultured rice cells by affinity labeling. *Plant J* 12, 347-356.

- Jayaswal, R.K., Lee, Y.I., and Wilkinson, B.J.** (1990). Cloning and expression of a *Staphylococcus aureus* gene encoding a peptidoglycan hydrolase activity. *J Bacteriol* *172*, 5783-5788.
- Jefferson, R.A., Kavanagh, T.A., and Bevan, M.W.** (1987). GUS fusions: beta-glucuronidase as a sensitive and versatile gene fusion marker in higher plants. *Embo J* *6*, 3901-3907.
- Jollès, P.** (1996). *Lysozymes: Model Enzymes in Biotechnology and Biology* (Basel, Birkhauser).
- Jones, J.D., and Dangl, J.L.** (2006). The plant immune system. *Nature* *444*, 323-329.
- Joshi, M., Rong, X., Moll, S., Kers, J., Franco, C., and Loria, R.** (2007). *Streptomyces turgidiscabies* Secretes a Novel Virulence Protein, Nec1, Which Facilitates Infection. *MPMI* *20*, 599-608.
- Kaiser, C.** (1994). *Methods in Yeast Genetics* (NY, Cold Spring Harbour Laboratories).
- Kaku, H., Nishizawa, Y., Ishii-Minami, N., Akimoto-Tomiyama, C., Dohmae, N., Takio, K., Minami, E., and Shibuya, N.** (2006). Plant cells recognize chitin fragments for defense signaling through a plasma membrane receptor. *PNAS* *103*, 11086-11091.
- Kaneko, T., Goldman, W.E., Mellroth, P., Steiner, H., Fukase, K., Kusumoto, S., Harley, W., Fox, A., Golenbock, D., and Silverman, N.** (2004). Monomeric and Polymeric Gram-Negative Peptidoglycan but Not Purified LPS Stimulate the *Drosophila* IMD Pathway. *Immunity* *20*, 637-649.
- Karimi, M., De Meyer, B., and Hilson, P.** (2005). Modular cloning in plant cells. *Trends Plant Sci* *10*, 103-105.
- Kasprzewska, A.** (2003). Plant chitinases--regulation and function. *Cell Mol Biol Lett* *8*, 809-824.
- Kemmerling, B., Schwedt, A., Rodriguez, P., Mazzotta, S., Frank, M., Qamar, S.A., Mengiste, T., Betsuyaku, S., Parker, J.E., Mussig, C., et al.** (2007). The BRI1-associated kinase 1, BAK1, has a brassinolide-independent role in plant cell-death control. *Curr Biol* *17*, 1116-1122.
- Kim, M.G., da Cunha, L., McFall, A.J., Belkhadir, Y., DebRoy, S., Dangl, J.L., and Mackey, D.** (2005). Two *Pseudomonas syringae* Type III Effectors Inhibit RIN4-Regulated Basal Defense in *Arabidopsis*. *Cell* *121*, 749-759.
- Kopp, E.B., and Medzhitov, R.** (1999). The Toll-receptor family and control of innate immunity. *Curr Opin Immunol* *11*, 13-18.
- Krol, E., Mentzel, T., Chinchilla, D., Boller, T., Felix, G., Kemmerling, B., Postel, S., Arents, M., Jeworutzki, E., Al-Rasheid, K.A.S., et al.** (2010). Perception of the *Arabidopsis* Danger Signal Peptide 1 Involves the Pattern Recognition Receptor AtPEPR1 and Its Close Homologue AtPEPR2. *J Biol Chem* *285*, 13471-13479.
- Kumar, S., Roychowdhury, A., Ember, B., Wang, Q., Guan, R., Mariuzza, R.A., and Boons, G.-J.** (2005). Selective Recognition of Synthetic Lysine and meso-Diaminopimelic Acid-type Peptidoglycan Fragments by Human Peptidoglycan Recognition Proteins Ialpha and S. *J Biol Chem* *280*, 37005-37012.

- Kunze, G., Zipfel, C., Robatzek, S., Niehaus, K., Boller, T., and Felix, G.** (2004). The N Terminus of Bacterial Elongation Factor Tu Elicits Innate Immunity in Arabidopsis Plants. *Plant Cell* 16, 3496-3507.
- Kurata, S.** (2010). Extracellular and intracellular pathogen recognition by *Drosophila* PGRP-LE and PGRP-LC. *Int Immunol* 22, 143-148.
- Kwon, H., Yokoyama, R., and Nishitani, K.** (2005). A proteomic approach to apoplastic proteins involved in cell wall regeneration in protoplasts of Arabidopsis suspension-cultured cells. *Plant Cell Physiol* 46, 843.
- Laemmli, U.K.** (1970). Cleavage of structural proteins during the assembly of the head of bacteriophage T4. *Nature* 227, 680-685.
- Lecourieux, D., Mazars, C., Pauly, N., Ranjeva, R., and Pugin, A.** (2002). Analysis and Effects of Cytosolic Free Calcium Increases in Response to Elicitors in *Nicotiana glauca* Cells. *Plant Cell* 14, 2627-2641.
- Lerouge, P., Cabanes-Macheteau, M., Rayon, C., Fischette-Lainé, A.-C., Gomord, V., and Faye, L.** (1998). N-Glycoprotein biosynthesis in plants: recent developments and future trends. *Plant Mol Biol* 38, 31-48.
- Leulier, F., Parquet, C., Pili-Floury, S., Ryu, J.-H., Caroff, M., Lee, W.-J., Mengin-Lecreulx, D., and Lemaitre, B.** (2003). The *Drosophila* immune system detects bacteria through specific peptidoglycan recognition. *Nat Immunol* 4, 478-484.
- Lim, J.-H., Kim, M.-S., Kim, H.-E., Yano, T., Oshima, Y., Aggarwal, K., Goldman, W.E., Silverman, N., Kurata, S., and Oh, B.-H.** (2006). Structural Basis for Preferential Recognition of Diaminopimelic Acid-type Peptidoglycan by a Subset of Peptidoglycan Recognition Proteins. *J Biol Chem* 281, 8286-8295.
- Limpens, E., Franken, C., Smit, P., Willemse, J., Bisseling, T., and Geurts, R.** (2003). LysM domain receptor kinases regulating rhizobial Nod factor-induced infection. *Science* 302, 630-633.
- Liu, C., Gelius, E., Liu, G., Steiner, H.k., and Dziarski, R.** (2000). Mammalian Peptidoglycan Recognition Protein Binds Peptidoglycan with High Affinity, Is Expressed in Neutrophils, and Inhibits Bacterial Growth. *J Biol Chem* 275, 24490-24499.
- Liu, Z., Jia, L., Mao, Y., and He, Y.** (2010). Classification and quantification of leaf curvature. *J Exp Bot* 61, 2757-2767.
- Livak, K.J., and Schmittgen, T.D.** (2001). Analysis of Relative Gene Expression Data Using Real-Time Quantitative PCR and the 2- $^{-\Delta\Delta CT}$ Method. *Methods* 25, 402-408.
- Lu, X., Wang, M., Qi, J., Wang, H., Li, X., Gupta, D., and Dziarski, R.** (2006). Peptidoglycan Recognition Proteins Are a New Class of Human Bactericidal Proteins. *J Biol Chem* 281, 5895-5907.
- Luna, E., Pastor, V., Robert, J., Flors, V., Mauch-Mani, B., and Ton, J.** (2011). Callose Deposition: A Multifaceted Plant Defense Response. *MPMI* 24, 183-193.

- Macheboeuf, P., Contreras-Martel, C., Job, V., Dideberg, O., and Dessen, A.** (2006). Penicillin Binding Proteins: key players in bacterial cell cycle and drug resistance processes (Blackwell Publishing Ltd), pp. 673-691.
- Madsen, E.B., Madsen, L.H., Radutoiu, S., Olbryt, M., Rakwalska, M., Szczyglowski, K., Sato, S., Kaneko, T., Tabata, S., Sandal, N., et al.** (2003). A receptor kinase gene of the LysM type is involved in legume perception of rhizobial signals. *Nature* **425**, 637-640.
- Majeau, N., Trudel, J., and Asselin, A.** (1990). Diversity of cucumber chitinase isoforms and characterization of one seed basic chitinase with lysozyme activity. *Plant Sci* **68**, 9-16.
- Mauch, F., Mauch-Mani, B., and Boller, T.** (1988). Antifungal Hydrolases in Pea Tissue : II. Inhibition of Fungal Growth by Combinations of Chitinase and Î²-1,3-Glucanase. *Plant Physiol* **88**, 936-942.
- Medzhitov, R., and Janeway, C., Jr.** (2000). Innate immune recognition: mechanisms and pathways. *Immunol Rev* **173**, 89-97.
- Medzhitov, R., Preston-Hurlburt, P., and Janeway, C.A.** (1997). A human homologue of the Drosophila Toll protein signals activation of adaptive immunity. *Nature* **388**, 394-397.
- Mellroth, P., Karlsson, J., Håkansson, J., Schultz, N., Goldman, W.E., and Steiner, H.** (2005). Ligand-induced dimerization of Drosophila peptidoglycan recognition proteins in vitro. *PNAS* **102**, 6455-6460.
- Mellroth, P., Karlsson, J., and Steiner, H.** (2003). A Scavenger Function for a Drosophila Peptidoglycan Recognition Protein. *J Biol Chem* **278**, 7059-7064.
- Melotto, M., Underwood, W., Koczan, J., Nomura, K., and He, S.Y.** (2006). Plant Stomata Function in Innate Immunity against Bacterial Invasion. *Cell* **126**, 969-980.
- Michel, T., Reichhart, J.-M., Hoffmann, J.A., and Royet, J.** (2001). Drosophila Toll is activated by Gram-positive bacteria through a circulating peptidoglycan recognition protein. *Nature* **414**, 756-759.
- Misas-Villamil, J.C., and van der Hoorn, R.A.L.** (2008). Enzyme-inhibitor interactions at the plant-pathogen interface. *Curr Opin Plant Biol* **11**, 380-388.
- Mithöfer, A., Fliegmann, J., Neuhaus-Url, G., Schwarz, H., and Ebel, J.** (2000). The Hepta-beta-Glucoside Elicitor-Binding Proteins from Legumes Represent a Putative Receptor Family. *Biol Chem* **381**, 705-713.
- Miya, A., Albert, P., Shinya, T., Desaki, Y., Ichimura, K., Shirasu, K., Narusaka, Y., Kawakami, N., Kaku, H., and Shibuya, N.** (2007). CERK1, a LysM receptor kinase, is essential for chitin elicitor signaling in Arabidopsis. *PNAS* **104**, 19613-19618.
- Miyauchi, K., Matsumiya, M., and Mochizuki, A.** (2006). Purification and characterization of lysozyme from purple washington clam *Saxidomus purpurata*. *Fisheries Science* **72**, 1300-1305.
- Monchois, V., Abergel, C., Sturgis, J., Jeudy, S., and Claverie, J.-M.** (2001). Escherichia coli ykfE ORF Gene Encodes a Potent Inhibitor of C-type Lysozyme. *J Biol Chem* **276**, 18437-18441.

- Mucyn, T.S., Clemente, A., Andriotis, V.M.E., Balmuth, A.L., Oldroyd, G.E.D., Staskawicz, B.J., and Rathjen, J.P.** (2006). The Tomato NBARC-LRR Protein Prf Interacts with Pto Kinase in Vivo to Regulate Specific Plant Immunity. *Plant Cell* 18, 2792-2806.
- Mulder, L., Lefebvre, B., Cullimore, J., and Imberty, A.** (2006). LysM domains of *Medicago truncatula* NFP protein involved in Nod factor perception. Glycosylation state, molecular modeling and docking of chitooligosaccharides and Nod factors. *Glycobiol* 16, 801-809.
- Müller-Anstett, M.A., Müller, P., Albrecht, T., Nega, M., Wagener, J., Gao, Q., Kaesler, S., Schaller, M., Biedermann, T., and Götz, F.** (2010). Staphylococcal Peptidoglycan Co-Localizes with Nod2 and TLR2 and Activates Innate Immune Response via Both Receptors in Primary Murine Keratinocytes. *PLoS ONE* 5, e13153.
- Müller, P., Müller-Anstett, M., Wagener, J., Gao, Q., Kaesler, S., Schaller, M., Biedermann, T., and Götz, F.** (2010). The *Staphylococcus aureus* Lipoprotein SitC Colocalizes with Toll-Like Receptor 2 (TLR2) in Murine Keratinocytes and Elicits Intracellular TLR2 Accumulation. *Infect Immun* 78, 4243-4250.
- Nakagawa, T., Kaku, H., Shimoda, Y., Sugiyama, A., Shimamura, M., Takanashi, K., Yazaki, K., Aoki, T., Shibuya, N., and Kouchi, H.** (2010). From defense to symbiosis: limited alterations in the kinase domain of LysM receptor-like kinases are crucial for evolution of legume–*Rhizobium* symbiosis. *Plant J* 65, 169-180.
- Nanninga, N.** (1998). Morphogenesis of *Escherichia coli*. *Microbiol Mol Biol Rev* 62, 110-129.
- Navarre, W.W., and Schneewind, O.** (1999). Surface Proteins of Gram-Positive Bacteria and Mechanisms of Their Targeting to the Cell Wall Envelope. *Microbiol Mol Biol Rev* 63, 174-229.
- Nilsen, I.W., Øverbø, K., Sandsdalen, E., Sandaker, E., Sletten, K., and Myrnes, B.** (1999). Protein purification and gene isolation of chlamysin, a cold-active lysozyme-like enzyme with antibacterial activity. *FEBS Lett* 464, 153-158.
- Ntoukakis, V., Mucyn, T.S., Gimenez-Ibanez, S., Chapman, H.C., Gutierrez, J.R., Balmuth, A.L., Jones, A.M.E., and Rathjen, J.P.** (2009). Host Inhibition of a Bacterial Virulence Effector Triggers Immunity to Infection. *Science* 324, 784-787.
- Nürnberger, T., and Brunner, F.** (2002). Innate immunity in plants and animals: emerging parallels between the recognition of general elicitors and pathogen-associated molecular patterns. *Curr Opin Plant Biol* 5, 318-324.
- Nürnberger, T., Brunner, F., Kemmerling, B., and Piater, L.** (2004). Innate immunity in plants and animals: striking similarities and obvious differences. *Immunol Rev* 198, 249-266.
- Nürnberger, T., Nennstiel, D., Jabs, T., Sacks, W.R., Hahlbrock, K., and Scheel, D.** (1994). High affinity binding of a fungal oligopeptide elicitor to parsley plasma membranes triggers multiple defense responses. *Cell* 78, 449-460.
- Okada, M., Matsumura, M., Ito, Y., and Shibuya, N.** (2002). High-Affinity Binding Proteins for N-Acetylchitooligosaccharide Elicitor in the Plasma Membranes from Wheat, Barley and Carrot Cells: Conserved Presence and Correlation with the Responsiveness to the Elicitor. *Plant Cell Physiol* 43, 505-512.

- Onaga, S., and Taira, T.** (2008). A new type of plant chitinase containing LysM domains from a fern (*Pteris ryukyuensis*): roles of LysM domains in chitin binding and antifungal activity. *Glycobiol* 18, 414.
- Ossowski, S., Schwab, R., and Weigel, D.** (2008). Gene silencing in plants using artificial microRNAs and other small RNAs. *Plant J* 53, 674-690.
- Park, S., Kim, D., Truong, N., and Itoh, Y.** (2002). Heterologous expression and characterization of class III chitinases from rice (*Oryza sativa* L.). *Enzyme Microb Technol* 30, 697-702.
- Passarinho, P., and De Vries, S.** (2002). Arabidopsis chitinases: a genomic survey. The Arabidopsis Book Rockville, American Society of Plant Biologists, 1-25.
- Patil, R., Ghormade, V., and Deshpande, M.** (2000). Chitinolytic enzymes: An exploration. *Enzyme Microb Technol* 26, 473-483.
- Petersen, B., Egelund, J., Damager, I., Faber, K., Krüger Jensen, J., Yang, Z., Bennett, E., Scheller, H., and Ulvskov, P.** (2009). Assay and heterologous expression in *Pichia pastoris* of plant cell wall type-II membrane anchored glycosyltransferases. *Glycoconjugate J* 26, 1235-1246.
- Petterson, T., Jendholm, J., Månsson, A., Bjartell, A., Riesbeck, K., and Cardell, L.-O.** (2011). Effects of NOD-like receptors in human B lymphocytes and crosstalk between NOD1/NOD2 and Toll-like receptors. *J Leukocyte Biol* 89, 177-187.
- Petutschnig, E.K., Jones, A.M., Serazetdinova, L., Lipka, U., and Lipka, V.** (2010). The lysin motif receptor-like kinase (LysM-RLK) CERK1 is a major chitin-binding protein in *Arabidopsis thaliana* and subject to chitin-induced phosphorylation. *J Biol Chem* 285, 28902-28911.
- Ponting, C.P., Aravind, L., Schultz, J., Bork, P., and Koonin, E.V.** (1999). Eukaryotic Signalling Domain Homologues in Archaea and Bacteria. *Ancient Ancestry and Horizontal Gene Transfer. J Mol Biol* 289, 729-745.
- Prithviraj, B., Bais, H.P., Jha, A.K., and Vivanco, J.M.** (2005). *Staphylococcus aureus* pathogenicity on *Arabidopsis thaliana* is mediated either by a direct effect of salicylic acid on the pathogen or by SA-dependent, NPR1-independent host responses. *Plant J* 42, 417-432.
- Radutoiu, S., Madsen, L.H., Madsen, E.B., Felle, H.H., Umehara, Y., Gronlund, M., Sato, S., Nakamura, Y., Tabata, S., Sandal, N., et al.** (2003). Plant recognition of symbiotic bacteria requires two LysM receptor-like kinases. *Nature* 425, 585-592.
- Ramet, M., Manfruell, P., Pearson, A., Mathey-Prevot, B., and Ezekowitz, R.A.B.** (2002). Functional genomic analysis of phagocytosis and identification of a *Drosophila* receptor for *E. coli*. *Nature* 416, 644-648.
- Ranf, S., Wünnenberg, P., Lee, J., Becker, D., Dunkel, M., Hedrich, R., Scheel, D., and Dietrich, P.** (2008). Loss of the vacuolar cation channel, AtTPC1, does not impair Ca²⁺ signals induced by abiotic and biotic stresses. *Plant J* 53, 287-299.
- Raymond, J.B., Mahapatra, S., Crick, D.C., and Pavelka, M.S.** (2005). Identification of the namH Gene, Encoding the Hydroxylase Responsible for the N-Glycolylation of the Mycobacterial Peptidoglycan. *J Biol Chem* 280, 326-333.

- Reissig, J.L., Strominger, J.L., and Leloir, L.F.** (1955). A MODIFIED COLORIMETRIC METHOD FOR THE ESTIMATION OF N-ACETYLAMINO SUGARS. *J Biol Chem* 217, 959-966.
- Rodriguez Suarez, M.C., Petersen, M., and Mundy, J.** (2010). Mitogen-Activated Protein Kinase Signaling in Plants. *Annu Rev Plant Biol* 61, 621-649.
- Royet, J., and Dziarski, R.** (2007). Peptidoglycan recognition proteins: pleiotropic sensors and effectors of antimicrobial defences. *Nat Rev Microbiol* 5, 264-277.
- Ryan, C.A., Huffaker, A., and Yamaguchi, Y.** (2007). New insights into innate immunity in Arabidopsis. *Cell Microbiol* 9, 1902-1908.
- Sahai, A.S., and Manocha, M.S.** (1993). Chitinases of fungi and plants: their involvement in morphogenesis and host-parasite interaction (Blackwell Publishing Ltd), pp. 317-338.
- Samac, D., Hironaka, C., Yallaly, P., and Shah, D.** (1990). Isolation and characterization of the genes encoding basic and acidic chitinase in Arabidopsis thaliana. *Plant Physiol* 93, 907.
- Samac, D.A., and Shah, D.M.** (1991). Developmental and pathogen-induced activation of the Arabidopsis acidic chitinase promoter. *Plant Cell* 3, 1063.
- Sambrook, J., and Russell, D.W.** (2001). *Molecular Cloning: a laboratory manual* (New York, Cold Spring Harbor Press).
- Schindler, C., and Schuhardt, V.** (1964). Lysostaphin: a new bacteriolytic agent for the staphylococcus. *PNAS*, 414-421.
- Schleifer, K.H., and Kandler, O.** (1972). Peptidoglycan types of bacterial cell walls and their taxonomic implications. *Bacteriol Rev* 36, 407-477.
- Schlumbaum, A., Mauch, F., Vögeli, U., and Boller, T.** (1986). Plant chitinases are potent inhibitors of fungal growth. *Nature* 324, 365-367.
- Schwab, R., Palatnik, J.F., Riester, M., Schommer, C., Schmid, M., and Weigel, D.** (2005). Specific effects of MicroRNAs on the plant transcriptome. *Dev Cell* 8, 517-527.
- Schwandner, R., Dziarski, R., Wesche, H., Rothe, M., and Kirschning, C.J.** (1999). Peptidoglycan- and Lipoteichoic Acid-induced Cell Activation Is Mediated by Toll-like Receptor 2. *J Biol Chem* 274, 17406-17409.
- Schweizer, P., Felix, G., Buchala, A., Müller, C., and Métraux, J.P.** (1996). Perception of free cutin monomers by plant cells. *Plant J* 10, 331-341.
- Scott, A., Wyatt, S., Tsou, P., Robertson, D., and Allen, N.** (1999). Model system for plant cell biology: GFP imaging in living onion epidermal cells. *Biotechniques* 26, 1128-1132.
- Shapiro, A.D., and Zhang, C.** (2001). The Role of NDR1 in Avirulence Gene-Directed Signaling and Control of Programmed Cell Death in Arabidopsis. *Plant Physiol* 127, 1089-1101.
- Shimada, J., Moon, S., Lee, H.-Y., Takeshita, T., Pan, H., Woo, J.-I., Gellibolian, R., Yamanaka, N., and Lim, D.** (2008). Lysozyme M deficiency leads to an increased susceptibility to Streptococcus pneumoniae-induced otitis media. *BMC Infectious Diseases* 8, 134.

- Shimizu, T., Nakano, T., Takamizawa, D., Desaki, Y., Ishii-Minami, N., Nishizawa, Y., Minami, E., Okada, K., Yamane, H., Kaku, H., et al.** (2010). Two LysM receptor molecules, CEBiP and OsCERK1, cooperatively regulate chitin elicitor signaling in rice. *Plant J* 64, 204-214.
- Shiu, S.-H., and Bleecker, A.B.** (2001). Receptor-like kinases from Arabidopsis form a monophyletic gene family related to animal receptor kinases. *PNAS* 98, 10763-10768.
- Shockman, G.D., and Höltje, J.V.** (1994). Microbial peptidoglycan (murein) hydrolases. In, J.M. Ghuysen, and R. Hakenbeck, eds. (Amsterdam, Elsevier Biomedical Press), pp. 131-166.
- Singh, K.B.** (1998). Transcriptional Regulation in Plants: The Importance of Combinatorial Control. *Plant Physiol* 118, 1111-1120.
- Stenbak, C.R., Ryu, J.-H., Leulier, F., Pili-Floury, S., Parquet, C., Hervé, M., Chaput, C., Boneca, I.G., Lee, W.-J., Lemaitre, B., et al.** (2004). Peptidoglycan Molecular Requirements Allowing Detection by the Drosophila Immune Deficiency Pathway. *J Immunol* 173, 7339-7348.
- Stone, B.A., and Clarke, A.E.** (1992). Chemistry and Biology of higher plant 1,3- β -glucans (Callose). In Chemistry and Biology of (1-3)- β -Glucans (Stone, BA and Clarke, AE, eds), 365-429.
- Storey, J.D., and Tibshirani, R.** (2003). Statistical significance for genomewide studies. *PNAS* 100, 9440-9445.
- Strober, W., Murray, P.J., Kitani, A., and Watanabe, T.** (2006). Signalling pathways and molecular interactions of NOD1 and NOD2. *Nat Rev Immunol* 6, 9-20.
- Swaminathan, C.P., Brown, P.H., Roychowdhury, A., Wang, Q., Guan, R., Silverman, N., Goldman, W.E., Boons, G.-J., and Mariuzza, R.A.** (2006). Dual strategies for peptidoglycan discrimination by peptidoglycan recognition proteins (PGRPs). *PNAS* 103, 684-689.
- Tada, H., Aiba, S., Shibata, K.-I., Ohteki, T., and Takada, H.** (2005). Synergistic Effect of Nod1 and Nod2 Agonists with Toll-Like Receptor Agonists on Human Dendritic Cells To Generate Interleukin-12 and T Helper Type 1 Cells. *Infect Immun* 73, 7967-7976.
- Takehana, A., Yano, T., Mita, S., Kotani, A., Oshima, Y., and Kurata, S.** (2004). Peptidoglycan recognition protein (PGRP)-LE and PGRP-LC act synergistically in Drosophila immunity. *Embo J* 23, 4690-4700.
- Takeuchi, O., Hoshino, K., Kawai, T., Sanjo, H., Takada, H., Ogawa, T., Takeda, K., and Akira, S.** (1999). Differential Roles of TLR2 and TLR4 in Recognition of Gram-Negative and Gram-Positive Bacterial Cell Wall Components. *Immunity* 11, 443-451.
- Tanabe, T., Chamailard, M., Ogura, Y., Zhu, L., Qiu, S., Masumoto, J., Ghosh, P., Moran, A., Predergast, M.M., Tromp, G., et al.** (2004). Regulatory regions and critical residues of NOD2 involved in muramyl dipeptide recognition. *Embo J* 23, 1587-1597.
- Tata, S., Beintema, J., and Balabaskaran, S.** (1983). The lysozyme of *Hevea brasiliensis* latex: isolation, purification, enzyme kinetics and partial amino acid sequence. *J Rubb Res Inst Malaysia* 31, 35-48.

- Teh, O.K., and Moore, I.** (2007). An ARF-GEF acting at the Golgi and in selective endocytosis in polarized plant cells. *Nature* 448, 493-496.
- Tekoah, Y.** (2004). Posttranslational modifications to plants - glycosylation (John Wiley & Sons, Ltd).
- Terwisscha van Scheltinga, A., Hennig, M., and Dijkstra, B.** (1996). The 1.8 Å resolution structure of hevamine, a plant chitinase/lysozyme, and analysis of the conserved sequence and structure motifs of glycosyl hydrolase family 18. *J Mol Biol* 262, 243-257.
- Thomma, B.P.H.J., Eggermont, K., Tierens, K.F.M.-J., and Broekaert, W.F.** (1999a). Requirement of Functional Ethylene-Insensitive 2Gene for Efficient Resistance of Arabidopsis to Infection by Botrytis cinerea. *Plant Physiol* 121, 1093-1101.
- Thomma, B.P.H.J., Nelissen, I., Eggermont, K., and Broekaert, W.F.** (1999b). Deficiency in phytoalexin production causes enhanced susceptibility of Arabidopsis thaliana to the fungus Alternaria brassicicola. *The Plant Journal* 19, 163-171.
- Tipper, D., Strominger, J., and Ghuysen, J.** (1964). Staphylolytic Enzyme from Chalaropsis: Mechanism of Action. *Science*, 781-782.
- Travassos, L.H., Girardin, S.E., Philpott, D.J., Blanot, D., Nahori, M.-A., Werts, C., and Boneca, I.G.** (2004). Toll-like receptor 2-dependent bacterial sensing does not occur via peptidoglycan recognition. *EMBO Rep* 5, 1000-1006.
- Tydell, C.C., Yount, N., Tran, D., Yuan, J., and Selsted, M.E.** (2002). Isolation, Characterization, and Antimicrobial Properties of Bovine Oligosaccharide-binding Protein. *J Biol Chem* 277, 19658-19664.
- Ueda, T., Yamaguchi, M., Uchimiya, H., and Nakano, A.** (2001). Ara6, a plant-unique novel type Rab GTPase, functions in the endocytic pathway of Arabidopsis thaliana. *Embo J* 20, 4730-4741.
- van Aalten, D.M.F., Komander, D., Synstad, B., Gåseidnes, S., Peter, M.G., and Eijsink, V.G.H.** (2001). Structural insights into the catalytic mechanism of a family 18 exo-chitinase. *PNAS* 98, 8979-8984.
- van den Burg, H., Harrison, S., Joosten, M., Vervoort, J., and de Wit, P.** (2006). Cladosporium fulvum Avr4 protects fungal cell walls against hydrolysis by plant chitinases accumulating during infection. *MPMI* 19, 1420-1430.
- van Heijenoort, J.** (2001). Formation of the glycan chains in the synthesis of bacterial peptidoglycan. *Glycobiol* 11, 25-36.
- van Loon, L.C., Rep, M., and Pieterse, C.M.J.** (2006). Significance of Inducible Defense-related Proteins in Infected Plants. *Annu Rev Phytopathol* 44, 135-162.
- Vandepoele, K., and van de Peer, Y.** (2005). Exploring the Plant Transcriptome through Phylogenetic Profiling. *Plant Physiol* 137, 31-42.
- Voinnet, O., Rivas, S., Mestre, P., and Baulcombe, D.** (2003). An enhanced transient expression system in plants based on suppression of gene silencing by the p19 protein of tomato bushy stunt virus. *Plant J* 33, 949-956.

- Wan, J., Zhang, X.C., Neece, D., Ramonell, K.M., Clough, S., Kim, S.Y., Stacey, M.G., and Stacey, G.** (2008). A LysM receptor-like kinase plays a critical role in chitin signaling and fungal resistance in Arabidopsis. *Plant Cell* 20, 471-481.
- Wang, L., Weber, A.N., Atilano, M.L., Filipe, S.R., Gay, N.J., and Ligoxygakis, P.** (2006). Sensing of Gram-positive bacteria in Drosophila: GGBP1 is needed to process and present peptidoglycan to PGRP-SA. *Embo J* 25, 5005-5014.
- Wang, M.H., Liu, L.H., Wang, S.Y., Li, X.N., Lu, X.F., Gupta, D., and Dziarski, R.** (2007). Human peptidoglycan recognition proteins require zinc to kill both Gram-positive and Gram-negative bacteria and are synergistic with antibacterial peptides. *J Immunol* 178, 3116-3125.
- Wang, Z.M., Li, X.N., Cocklin, R.R., Wang, M.H., Wang, M., Fukase, K., Inamura, S., Kusumoto, S., Gupta, D., and Dziarski, R.** (2003). Human peptidoglycan recognition protein-L is an N-acetylmuramoyl-L-alanine amidase. *J Biol Chem* 278, 49044-49052.
- Weber, A.N., Tauszig-Delamasure, S., Hoffmann, J.A., Lelievre, E., Gascan, H., Ray, K.P., Morse, M.A., Imler, J.L., and Gay, N.J.** (2003). Binding of the Drosophila cytokine Spatzle to Toll is direct and establishes signaling. *Nat Immunol* 4, 794-800.
- Wendehenne, D., Lamotte, O., Frachisse, J.-M., Barbier-Brygoo, H., and Pugin, A.** (2002). Nitrate Efflux Is an Essential Component of the Cryptogein Signaling Pathway Leading to Defense Responses and Hypersensitive Cell Death in Tobacco. *Plant Cell* 14, 1937-1951.
- Werner, T., Liu, G., Kang, D., Ekengren, S., Steiner, H.k., and Hultmark, D.** (2000). A family of peptidoglycan recognition proteins in the fruit fly *Drosophila melanogaster*. *PNAS* 97, 13772-13777.
- Willmann, R.** (2011). Charakterisierung von Proteinen mit Lysin-Motiven und ihre Rolle in der Peptidoglycanperzeption und der angeborenen Immunität in *Arabidopsis thaliana*. In Institut für Pflanzenbiochemie (Tübingen, Eberhard-Karls Universität).
- Xue, Q.-G., Schey, K.L., Volety, A.K., Chu, F.-L.E., and La Peyre, J.F.** (2004). Purification and characterization of lysozyme from plasma of the eastern oyster (*Crassostrea virginica*). *Biochem Mol Biol* 139, 11-25.
- Yamaguchi, Y., Pearce, G., and Ryan, C.A.** (2006). The cell surface leucine-rich repeat receptor for AtPep1, an endogenous peptide elicitor in Arabidopsis, is functional in transgenic tobacco cells. *PNAS* 103, 10104-10109.
- Yano, T., Mita, S., Ohmori, H., Oshima, Y., Fujimoto, Y., Ueda, R., Takada, H., Goldman, W.E., Fukase, K., Silverman, N., et al.** (2008). Autophagic control of listeria through intracellular innate immune recognition in drosophila. *Nat Immunol* 9, 908-916.
- Yoo, S.D., Cho, Y.H., and Sheen, J.** (2007). Arabidopsis mesophyll protoplasts: a versatile cell system for transient gene expression analysis. *Nat Protoc* 2, 1565-1572.
- Yoshimura, A., Lien, E., Ingalls, R.R., Tuomanen, E., Dziarski, R., and Golenbock, D.** (1999). Cutting Edge: Recognition of Gram-Positive Bacterial Cell Wall Components by the Innate Immune System Occurs Via Toll-Like Receptor 2. *J Immunol* 163, 1-5.
- Zähringer, U., Lindner, B., Inamura, S., Heine, H., and Alexander, C.** (2008). TLR2 - promiscuous or specific? A critical re-evaluation of a receptor expressing apparent broad specificity. *Immunobiol* 213, 205-224.

Zaidman-Rémy, A., Hervé, M., Poidevin, M., Pili-Floury, S., Kim, M.-S., Blanot, D., Oh, B.-H., Ueda, R., Mengin-Lecreulx, D., and Lemaitre, B. (2006). The *Drosophila* Amidase PGRP-LB Modulates the Immune Response to Bacterial Infection. *Immunity* *24*, 463-473.

Zhang, X.-C., Wu, X., Findley, S., Wan, J., Libault, M., Nguyen, H.T., Cannon, S.B., and Stacey, G. (2007). Molecular Evolution of Lysin Motif-Type Receptor-Like Kinases in Plants. *Plant Physiol* *144*, 623-636.

Zipfel, C. (2009). Early molecular events in PAMP-triggered immunity. *Curr Opin Plant Biol* *12*, 414-420.

Zipfel, C., Kunze, G., Chinchilla, D., Caniard, A., Jones, J.D.G., Boller, T., and Felix, G. (2006). Perception of the Bacterial PAMP EF-Tu by the Receptor EFR Restricts *Agrobacterium*-Mediated Transformation. *Cell* *125*, 749-760.

Zipfel, C., Robatzek, S., Navarro, L., Oakeley, E.J., Jones, J.D.G., Felix, G., and Boller, T. (2004). Bacterial disease resistance in *Arabidopsis* through flagellin perception. *Nature* *428*, 764-767.

8 Appendix

Table 8-1 summarizes the primers used in the frame of this work.

Primer name	Sequence	T _{mel} /°C	AGI
At5g24090gatF	AAAAAGCAGGCTACatgaccaacatgactctcg	68.3	<i>At5g24090</i>
At5g24090gatR	AGAAAGCTGGGTAcacactagccaatatagatg	67	<i>At5g24090</i>
At5g24090gatR-STOP	AGAAAGCTGGGTAtcacactagccaatatag	67	<i>At5g24090</i>
FP_5g24090d(2-22)gat	aaaaagcaggcttcATGAAACCCTCCGATGCATCCAGAG GTG	74.3	<i>At5g24090</i>
RP_5g24090-STOPgat	agaaagctgggtcCACACTAGCCAATATAGATGAACTG	70.5	<i>At5g24090</i>
At5g24090_gatF	aaaaagcaggctatgccgtaggcgagtgttc	69.5	<i>At5g24090</i>
At5g24090_gatR	agaaagctgggtgttttggttaaagatgttg	64.7	<i>At5g24090</i>
At5g24090miR-s	gaTTTGACGTAAGCATACCGCCctctctttgtattcc	70.5	<i>At5g24090</i>
At5g24090miR-a	gaGGGCGGTATGCTTACGTCAAAtcaaagagaatcaatga	72.5	<i>At5g24090</i>
At5g24090miR*s	gaGGACGGTATGCTTTCGTCAATtcacaggctgatgatg	68.4	<i>At5g24090</i>
At5g24090miR*s	gaATTGACGAAAGCATACCGTCCtctacatatattctct	59.4	<i>At5g24090</i>
5g24090EcoRIF	gatgaattcaatgaccaacatgac	57.6	<i>At5g24090</i>
5g24090NotI_ostopR	ctggcggccgccacactagccaa	69.6	<i>At5g24090</i>
5g24090NotI_mstopR	ctggcggccgctcacacactagcc	71.3	<i>At5g24090</i>
FP_EcoRI_pPIC9K	gtagaattcatgaccaacatgac	57.1	<i>At5g24090</i>
RP_20bp_tag_stop_NotI	gcggccgctcaatgatgatg	61.4	<i>At5g24090</i>
EF1a-s	TCA CAT CAA CAT TGT GGT CAT TGG	59.3	<i>At1g07920/30/40</i>
EF1a-as	TTG ATC TGG TCA AGA GCC TAC AG	60.6	<i>At1g07920/30/40</i>
At5g24090F	atgaccaacatgactctcg	53.2	<i>At5g24090</i>
At5g24090R	tcacacactagccaatatag	53.2	<i>At5g24090</i>
At5g24090F1	ccagaggtggcatagccatc	61.4	<i>At5g24090</i>
At5g24090R1	catctggtgggatatagccac	59.8	<i>At5g24090</i>

LP_N853931	tgacgaacctgataaatggg	55.9	<i>At5g24090</i>
RP_N853931	cataacctcacactgtgctcg	59.8	<i>At5g24090</i>
LP_N595362	tagtgcacatgtaaacgg	55.9	<i>At5g24090</i>
RP_N595362	agctcctcaatgccaattcc	57.9	<i>At5g24090</i>
580H03LP	TACATTTGGTTACATGGCAC	53.2	<i>At3g21630</i>
580H03RP	TAAGACTGACTAAATCTTCG	51.2	<i>At3g21630</i>
640374LP	ATATCTAAGCGACGGTCTTG	53.2	<i>At1g51940</i>
640374RP	ATCTTCCTTGGACTAGACCAC	51.2	<i>At1g51940</i>
N654015F2	CCCCAACATGATGGATTTATAC	56.5	<i>At1g51940</i>
N660797R2	TACATCTCTTCATTGATTCTCC	55.3	<i>At1g51940</i>
GT7089LP	TTCCCACAACAACAACGACTC	57.3	<i>At2g33580</i>
GT7089RP2	TTCTCCACATACTCTGGAGC	57.3	<i>At2g33580</i>
631911LP	ATCTCCTGACTTACTTAGTC	53.2	<i>At2g33580</i>
631911RP	ATCACTTTCACAGCGGCATC	51.2	<i>At2g33580</i>
2g23770F2	atcgaagaagaaaacatggg	53.2	<i>At2g23770</i>
2g23770R1	ttagtacgacgattctccc	59.3	<i>At2g23770</i>
512441LP	AAGTGGCAGTCATGTGTGTG	57.3	<i>At3g01840</i>
512441RP	TATGTGGATTCTTCTCTCTG	53.2	<i>At3g01840</i>
ef1a-100-f	gaggcagactgttcagctcg	61.4	<i>At1g07920/30/40</i>
ef1a-100-r	tcacttcgaccctcttga	57.3	<i>At1g07920/30/40</i>
At5g24090Fq	cacttcacccatttggc	56	<i>At5g24090</i>
At5g24090Rq	cctcgaccaatcgagta	56.7	<i>At5g24090</i>
FRK1-100-f	agcggtcagattcaacagt	55.3	<i>At2g19190</i>
FRK1-100-f	aagactataaacatcactct	49.1	<i>At2g19190</i>
AT2G39200MLO12_F	ACGGTGGTTGTCGGTATAAGCC	62.1	<i>At2g39200</i>
AT2G39200MLO12_R	AGGGCAGCCAAAGATATGAGTCC	62.4	<i>At2g39200</i>
AT3G26830PAD3_F	CTTTAAGCTCGTGGTCAAGGAGAC	62.7	<i>At3g26830</i>
AT3G26830PAD3_R	TGGGAGCAAGAGTGGAGTTGTTG	62.4	<i>At3g26830</i>

attB1	GGGGACAAC TTTGTACAAAAAGCAGGCT	66	Gateway adaptor
attB2	GGG GAC CAC TTT GTA CAA GAA AGC TGG GT	68.9	Gateway adaptor
Oligo-dT	TTT TTT TTT TTT TTT TT(AGC)	38.3	RT-PCR
Salk-Lba	TGG TTC ACG TAG TGG GCC ATC G	64	T-DNA/SALK line
Gabi-Kat-Lba	cccattggacgtgaatgtagacac	55.3	T-DNA/Gabi-Kat line
Ds3-1	ACC CGA CCG GAT CGT ATC GGT	63.7	T-DNA 3'-end/CSHL line
Ds5-1	GAA ACG GTC GGG AAA CTA GCT CTA C	64.6	T-DNA5'-end /CSHL line
Wisc-Lba (p745)	AACGTCCGCAATGTGTTATTAAGTTGTC	60	T-DNA/WiscDsLox line
GC248	gacgcacaatcccactatcctcg	64.4	P35S
A-PRS300	ctg caa ggc gat taa gtt ggg taa c	63	amiRNA
B-PRS300	gcg gat aac aat ttc aca cag gaa aca g	63.7	amiRNA

Table 8-1: Used oligonucleotides

```

1  H T N M T L R K H V I Y F L F F I S C S - L S K P S D A S R G G I A I Y W G Q N G N E G N L S A T C A T G R Y at5g24090
1  M A K - - - R T Q A I L L L L - L A I S L I M S S S H V D G G G I A I Y W G Q N G N E G T L T Q T C S T R K Y hevamineA
1  M T - - - - - - I N L L L P S I L F L A L I Q T S I A R S G I A I Y W G Q N G N E A T L M D T C A S G M Y Capsicum annuum chit I
1  M - K M A L K S T I S F T F F - S L V I L A L A N D S M A G K I S I Y W G Q N G N E G T L A E A C A T G M Y Medicago truncatula ch
1  M - - - - - I R Y S F L L T A L V L F L R A L K L E A G D I V I Y W G Q N G N E G S L A D T C A T M M Y Nicotiana tabacum chit
1  M M T S R M F S - A M Q M L I M V V U A L A G L A S A G A R A G D I A I Y W G Q N G N E G T L A Q T C A T G M Y Oryza sativa chit III
1  M A R - - - T P Q S T P L L I S L S U A L L L Q T S Y - - A G G I A I Y W G Q N G N E G T L T Q T C M T G K Y Vitis vinifera chit II

55  A Y V N V A F L V K F G N G Q T P E L N L A G H C N P A A N T C T H F G S Q V K D C Q S R G I K V M L S L G G at5g24090
52  S Y V N I A F L M K F G N G Q T P Q I N L A G H C N P A A G G C T I U S M G I R S C Q I Q G I K V M L S L G G hevamineA
48  A Y V N L S F L M K F G N G Q T P E I N L A G H C N P A V N G C T I L G P Q I K F C Q K L G U K V M L S M G G Capsicum annuum chit I
53  E Y V I I A F L P T F G D G Q T P M I N L A G H C D P Y S N E C T G L S S D I K S C Q A K G I K V L L S L G G Medicago truncatula ch
48  A I V N I A F L V V F G N G Q M P U L N L A G H C D P N A G A C T G L S M D I R A C Q M Q G I K V M L S L G G Nicotiana tabacum chit
55  R F V I V A F L P V F G K G Q T P U L N L A G H C D P A S N G C T G U G A D I K S C Q S L G I K V M P S I G G Oryza sativa chit III
51  S Y V N I A F L M K F G N G Q T P E I N L A G H C N P A S N G C T S U S T G I R M C Q M R G I K V M L S I G G Vitis vinifera chit II

110  G I G N Y S I G S R E D A K V I A D Y L W M N F L G G K S S S R P L G D A V L D G I D F N I E L G S P Q H W D at5g24090
107  G I G S Y T L A S Q A D A K M V A D Y L W M N F L G G K S S S R P L G D A V L D G I D F D I E H C S T L Y W D hevamineA
103  G V G N Y S L A S K K D A K D V A R Y L Y M N F L G G R S S F R P L G M A R L D G I D F D I E L G S S L Y Y E Capsicum annuum chit I
108  G A G S Y S I A S T Q D A K S V A T Y L W M N F L G G Q S S S R P L G P A V L D G I D F D I E G S W Q H W G Medicago truncatula ch
103  G A G S Y F L S A D D A R M V A M Y L W M M V L G G Q S M T R P L G D A V L D G I D F D I E G T T Q H W D Nicotiana tabacum chit
110  G V G N Y G L S R D D A K Q V A A Y L W M V L G G T S P S R P L G D A V M D G I D F D I E S G G M V W D Oryza sativa chit III
106  G V G S Y S L S S S M D A Q M V A M Y L W M N F L G G Q S S S R P L G D A V L D G I D F D I E L G S T L H W D Vitis vinifera chit II

165  D L A R T L S K F S H R G - - - R K I Y L T G A P Q C P F P D R L M G S A L N T K R F D Y V W I Q F Y N N P P at5g24090
162  D L A R Y L S A Y S K Q G - - - K K V Y L T A A P Q C P F P D R Y L G T A L N T G L F D Y V W U Q F Y N N P P hevamineA
158  D L A Q Y L K R Y S K L G - - - R K M Y L T A A P Q C P F P D R L D G T A L N T G L F D M W I Q F Y N N P S Capsicum annuum chit I
163  D L A K Y L K G Y M G - - - - K K U Y I T A A P Q C P F P D A W I G M A L T T G L F D Y V W U Q F Y N N P P Medicago truncatula ch
158  E L A K T L S Q F S Q Q - - - R K U Y L T A A P Q C P F P D T M L M G A L S T G L F D Y V W U Q F Y N N P P Nicotiana tabacum chit
165  D L A R Y L K A Y S R Q G S S K K P U Y L T A A P Q C P F P D A S L G V A L S T G L F D Y V W U Q F Y N N P P Oryza sativa chit III
161  D L A R A L S G F S K R G - - - R K U Y L T A A P Q C P F P D K F L G T A L N T G L F D Y V W U Q F Y N N P Q Vitis vinifera chit II

217  C S Y S S G M - T Q N L F D S W N K W T T S I A A Q K F F L G L P A A P E A A G S G Y I P P D U L T S Q I L P at5g24090
214  C Q Y S S G N - I M N I I M S W N R W T T S I M A G K I F L G L P A A P E A A G S G Y U P P D U L T S R I L P hevamineA
210  C Q Y T T M N - V D D L K M S W T R W T T S V W A R R I F L G L P A A P Q A A G S G F I P A D U L T G G I L P Capsicum annuum chit I
213  C Q Y M P F G E - I S N L E D A W K Q W T S G I P A N K I F L G L P A A S P E A A G S G F I P A T D L T S T V L P Medicago truncatula ch
209  C Q Y S G G S - A D N L K N Y W N Q W - M A I Q A G K I F L G L P A A Q G A A G S G F I P S D V L W S Q V L P Nicotiana tabacum chit
220  C Q Y S S S M G V G N L A S A W K Q W T S - I F A G R U F L G L P A A A E A A G S G F V E T S D L W S K V L P Oryza sativa chit III
213  C Q Y S S G N - T M N L L N S W N R W T S S I M S - Q I F M G L P A S S A A A G S G F I P A M V L T S Q I L P Vitis vinifera chit II

271  T L K K S R K Y G G V H L W S K F W D D K N G Y S S S I L A S V at5g24090
268  E I K K S P K Y G G V H L W S K F Y D D K N G Y S S S I L D S V L F L H S E E C M T V L hevamineA
264  V I K K S R K Y G G V H L W S K F W D E Q T G Y S S I V K S V Capsicum annuum chit I
267  A I K G S A K Y G G V H L W S R Y D D V Q S G Y S S S I K S H V Medicago truncatula ch
262  L I M G S P K Y G G V H L W S K F Y D - N G Y S S I K A M V Nicotiana tabacum chit
274  V V K K S P K Y G G I H L W S R Y Y D G L T G Y S D K V K S S V Oryza sativa chit III
266  V I K R S P K Y G G V H L W S K Y Y D D Q S G Y S S S I K S S V Vitis vinifera chit II

```

Figure 8-1: ClustalW2 protein sequence alignment of CHIA (*At5g24090*) and selected plant class chitinases

A multiple sequence alignment of the full-length protein sequences of *Arabidopsis thaliana* CHIA, *Hevea brasiliensis* HevamineA, *Capsicum annuum* chitinase I, *Medicago truncatula* chitinase, *Nicotiana tabacum* chitinase, *Oryza sativum* chitinase III and *Vitis vinifera* chitinase II using the ClustalW2 algorithm. Black boxes indicate differences in the amino acid residues.

Danksagung

Diese Arbeit wurde vom November 2007 bis August 2011 am Institut für Pflanzenbiochemie des Zentrums der Molekularbiologie der Pflanzen der Eberhard-Karls-Universität in Tübingen angefertigt.

Als erstes möchte ich meinen Doktorvater, Herrn Prof. Dr. Thorsten Nürnberger, für die Bereitstellung meines Projektes, sowie für die ausgezeichneten Arbeitsbedingungen und seine fachlichen Ratschläge danken.

Ich danke ebenfalls Herrn Prof. Dr. Georg Felix dafür, dass er das Zweitgutachten übernommen hat.

Frau Dr. Andrea Gust möchte ich ganz herzlich danken für die Betreuung und Mitkorrektur meiner Arbeit sowie für ihre Unterstützung und ihren unermüdlichen Optimismus, der mich über manche steinigen Wegabschnitte getragen hat.

Ein ganz besonderer Dank gilt für die einzigartige N1-Truppe (Roland Willmann, Eva Haller, Dagmar Kolb, Dr. Heike Lenz, Dr. Anita Brock, Dr. Stefan Engelhardt, Weiguo Zhang und Dr. Yoshitake Desaki) für die tolle Arbeitsatmosphäre, die tiefgründigen Diskussionsrunden und die lustigen Pausenaktivitäten während meiner Doktorarbeit.

Roland möchte ich auch ganz besonders für die gemeinsamen PGN-Abenteuer danken – die *Pseudomonas*-Ernte und die PGN-Isolation haben es in sich gehabt!

Ich bin dankbar für die vielen Kooperationen innerhalb unseres Sonderforschungsbereiches SFB 766 (Die bakterielle Zellhülle: Struktur, Funktion und Schnittstelle bei der Infektion). Auch alle Kollegen des gesamten Pflanzenbiochemie-Instituts, das Gärtner-Team des ZMBP und unseren Computerspezialisten Dieter Steinmetz möchte ich für ihre Hilfsbereitschaft danken.

Vielen lieben Dank auch an meinen Eltern, denn ohne sie wäre ich nicht soweit gekommen. Und zu guter Letzt danke ich meine bessere Hälfte, Robert, von ganzem Herzen für seinen liebevollen Rückhalt in den letzten zehn Jahren, sowie meinen winzigen inneren Motivator der letzten Monate.

Lebenslauf

Heini Marjatta Grabherr

Geburtsdatum und -ort	15.12.1981 in Helsinki, Finnland
Staatsangehörigkeit	finnisch
Familienstand	verheiratet

Schulbildung

1988 – 1991	Grundschule in Kitee, Finnland
1991 – 1997	Grundschule in Savonlinna, Finnland
1997 – 2000	Gymnasium in Savonlinna, Finnland
	Abschluss der allgemeinen Hochschulreife

Hochschulbildung

2002 – 2007	Studium der Biologie an der Johann Wolfgang Goethe-Universität Frankfurt am Main mit den Schwerpunkten Genetik, Mikrobiologie und Zell- und Entwicklungsbiologie Mündliche Diplomprüfungen in allen Schwerpunktfächern
11/2006 – 07/2007	Diplomarbeit bei Jun. Prof. P. von Kosküll-Döring am Lehrstuhl für Molekulare Biowissenschaften an der Johann Wolfgang Goethe-Universität Frankfurt am Main Titel der Arbeit: „Functional characterization of HsfC1 in <i>Arabidopsis thaliana</i> “
Seit 11/2007	Promotion bei Prof. Dr. T. Nürnberger am Institut für Pflanzenbiochemie des Zentrums für Molekulare Biologie der Pflanzen an der Eberhard Karls-Universität Tübingen Titel der Arbeit: „Characterisation of the role of LysM-receptor-like kinases and the CHIA chitinase in the perception of peptidoglycan and in the innate immunity of <i>Arabidopsis thaliana</i> “

